Climate Change Impacts in a River Basin having Flow Regulating Structures

Thesis submitted for the partial fulfilment of the requirements
for the award of the degree of

Doctor of Philosophy

by

Jeffrey Denzil K. Marak

Department of Civil Engineering
Indian Institute of Technology Guwahati
Guwahati – 781039, India

March 2022

Department of Civil Engineering
Indian Institute of Technology Guwahati
Guwahati-781039, Assam, India

Certificate

This is to certify that this thesis entitled **"Climate Change Impacts in a River Basin having Flow Regulating Structures"** submitted by Jeffrey Denzil K. Marak, Roll Number 166104105, a student in the Department of Civil Engineering, Indian Institute of Technology Guwahati for the award of the degree of Doctor of Philosophy has been carried out under our supervision and that this work has not been submitted elsewhere for a degree.

Prof. Arup Kumar Sarma
Professor
Department of Civil Engineering
Indian Institute of Technology
Guwahati-781039

Date:

Place:

Prof. Rajib Kumar Bhattacharjya
Professor
Department of Civil Engineering
Indian Institute of Technology
Guwahati-781039

Date:

Place:

Declaration of Authorship

I, Jeffrey Denzil K. Marak, declare that this thesis titled **"Climate Change Impacts in a River Basin having Flow Regulating Structures"** and the work presented in it has been carried out by me under the supervision of Prof. Arup Kumar Sarma and Prof. Rajib Kumar Bhattacharjya, Department of Civil Engineering, Indian Institute of Technology Guwahati. This work has not been submitted for the award of any other degree.

Place:

Date:

Jeffrey Denzil K. Marak
Department of Civil Engineering
Indian Institute of Technology, Guwahati
Guwahati-781039, Assam, India

Dedicated to my parents

Brelitha K. Marak

&

Perendro K. Sangma

Acknowledgements

In these years of academic learning and research I have always relied upon God, the Heavenly Father for his unending grace. I am thankful to Him for all his blessings and for keeping me and my family in good health throughout my PhD.

My source of inspiration is my mother, Brelitha K. Marak and my father, Perendro K. Sangma. They have always been by my side from the very beginning and supported me to pursue PhD. I cannot thank them enough for all that they have done for me. I also thank my sister, nono Nokmera K. Marak for her support and making me feel less far from home during my stay in Guwahati.

I'm extremely grateful to my supervisors Prof. Arup Kumar Sarma and Prof. Rajib Kumar Bhattacharjya whose unwavering guidance and unparalleled support has made this thesis a reality. They always showed a profound belief in my work and provided insightful suggestions for my research work.

I would like to express my deepest appreciation to my Doctoral Committee members, Prof. Sajal K. Deb (Chairman), Dr. Sreeja P, Prof. Ujjwal K. Saha for their valuable suggestions and kind support during my research work.

I would like to extend my sincere thanks to Smt. Parijat Gogoi and Juran Ali Ahmed from Assam Water Resources Department for helping me in obtaining discharge data for my work. I am also grateful to Central Water Commission (CWC) Shillong, and Meghalaya Power Generation Corporation Limited, Shillong for providing me the discharge data.

Special thanks to my friend Tufa Feyissa Negewo and Anurag Gogoi who helped me during my bathymetric survey.

I am also thankful to my friend Agatha, for her support and encouragement during my thesis work.

I am thankful to my lab mates Dr. Gilbert, Anupal, Dipsikha, Mamta, Prajna, Gaurav, Dr. Pulendra, Bhaswati, Amit, Priyam, Bhruba, and many others who were always there for me during the entire phase of my PhD. Our discussions during uncountable tea breaks will always be my cheerful moments to look back.

I would also like to extend my gratitude to my friends Vikavi, Regulus, Riju, Ato, Rajesh and many others who were always there to lend their support during my stay in campus and made my PhD life a delightful and a memorable one.

Jeffrey Denzil K. Marak

Abstract

The hydraulic structures constructed for the benefits of society can cause perturbations in the streamflow. Such perturbations to natural conditions may affect the river ecosystem. The assessment of the changes in the hydrological regime due to man-made structures requires a comparison between the existing and the counterfactual scenario. It is a challenging task to carry out such assessments when pre-impact condition data do not exist. In this paper, a methodological framework is proposed and applied to Umiam watershed to generate natural streamflow by using the post-impact data when pre-impact data is not available. The Soil and Water Assessment Tool (SWAT) model is applied for simulating streamflow under the presence of reservoir and water transfer out of the watershed. The Indicators of Hydrologic Alteration (IHA) method was used for the analysis of changes in streamflow. The results reveal a reduction in the monthly median flow rate by at least 21% in all the months during the five-decade period. The large floods and small floods are found to be reduced in the presence of the reservoir, whereas it also causes more frequent low flows which last for longer durations. The extreme annual minimum flow conditions (1-day, 3-day, 7-day, 30-day, 90-day minima) shows low alteration while the corresponding annual maximum flow conditions show medium alteration. The frequency and duration of high and low pulses are greatly affected by the reservoir. The rising-rate, falling-rate, and the number of reversals show a significantly decreasing trend. The results indicate a high overall degree of alteration in streamflow. The analysis of individual reservoir effects revealed increase in monthly flows due to Kyrdemkulai, Nongmahir, Umiam Stage IV and Umtru Reservoirs. The individual effect of Umtru Reservoir was found to be highest among the four. The second highest effect was due to Nongmahir Reservoir. The cumulative effect of all reservoirs could increase the yearly median flows by 38.49% as compared to unaltered flow without IBWT and reservoirs. The change in yearly median flows were 95.43% in Umtru Basin if no water was transferred from Umiam Basin. Since rainfall plays a significant role in hydrologic response of a watershed, the spatial and temporal trends in rainfall over Umiam and Umtru watersheds were analyzed. The analysis used the gridded rainfall data from the Indian Meteorological Department from 1901 to 2018. The Innovative Trend Analysis (ITA) method was used to identify the trends in low, medium, and high-intensity rainfall. The results indicated a decreasing trend in low and medium intensity rainfall while high-intensity rainfall is increasing across annual and seasonal time scales. For the assessment of climate and landuse change CORDEX data of IITM_RegCM4, MPI-CSC-

REMO2009 and SMHI-RCA4 were considered. Under dammed condition, highest flow in January to March occurs in S3 and S4 (RCP 8.5). In April, June highest flow occurs in S3 and S4 (RCP 4.5). Under undammed scenario, the timing of highest flow shifts to September for S3 and S4 scenarios under RCP 8.5. In all the scenarios, sub-basin 4 is found to have the highest change in flow due to climate and landuse change.

Keywords: Hydrological modeling, climate change, SWAT model, Hydrological Alteration

Contents

List of Figures

List of Tables

List of symbols

Symbols	Description
SW_t	Final soil water content (mm)
SW_0	The initial soil water content (mm)
R_i	Precipitation amount on i^{th} day
Q_i	Surface runoff on i^{th} day
ET_i	Evapotranspiration (ET) amount on i^{th} day
P_i	Percolated water on i^{th} day
QR_i	The amount of return flow on i^{th} day.
V	Water volume in the reservoir at the end of the day (m^3)
V_{stored}	Water volume stored in the reservoir at the beginning of the day (m^3)
V_{flowin}	Water volume entering the reservoir during the day (m^3)
$V_{flowout}$	Water volume flowing out of the reservoir during the day (m^3)
V_{pcp}	Vpcp is the volume of precipitation falling into the reservoir during the day (m^3)
V_{evap}	Water volume evaporated from the reservoir during the day (m^3),
V_{seep}	Volume of water seepage from the reservoir during the day (m^3).
D	Degree of alteration of flow regime

CHAPTER 1

Introduction

1.1 Background

Climate change is one of the biggest environmental threats facing the world, potentially impacting food production and security, sustained water supply, biodiversity of forests and other natural ecosystems, human health and settlements. In studies conducted by (Ravindranath et al. 2011a) Climate change modelling studies for India show that the Indian sub-continent is likely to experience a warming of over 3–5°C and significant changes (in- creases and decreases) in flood and drought frequency and intensity. Dash et. al. also found that the annual mean surface temperature by about 0.64 °C in the 30 years from 2011 to 2040 and by 5.15 °C at the end of the century (2071–2100). It also projects increase in annual mean precipitation by about 0.09 mm/day in the near future and by 0.48 mm/day at the end of the century (Priyadarshini 2018).

The development of hydrologic and watershed models has been the direct outcome of the need to integrate our knowledge on existing theories on real world flow behaviour with all physical and measured data. However, largescale and complex environmental systems such as the global hydrological cycle cannot be investigated directly through experimentation, but instead must be generalized into their component processes through modelling. Watershed scale study is necessary and useful for the designers/planers/administrators to evaluate the influence of local dams/sluices on water quantity/quality in other parts or the entire watershed (Wang and Xia 2010).

Different catchments respond differently to the same change in climate drivers, depending largely on watershed physio-geographical and hydrogeological characteristics and the amount of lake or groundwater storage in the catchment (IPCC, 2007). Climate changes are undergoing globally, however, mitigation policies are expected at local scale.

1.2 **Problem Statement**

As the global climate changes, it is likely to affect ecology and hydrology, and socio-economic lives of the people. With the increase in extreme events of precipitation natural hazards such as floods will occur more frequently(Rahmstorf et al. 2017). Climate change also represents a key driver in power markets given electricity is linked to weather variables. The measured trend of higher surface average temperatures implies risks as well as opportunities for the electricity sector. Opportunities for the electricity sector arise from the expansion of the market due to increasing electricity needs, e.g. because of cooling systems and delivery rates of water pumps.

Urbanization and climate change induced alterations in catchment hydrology can lead to increased risk of flooding on a local scale. The role of manmade flow control infrastructure to enhance resilience in ecosystem and as a climate change adaptation strategy in coping with climate change is an emerging research area. The social role of these structures in serving the population and integrating ecological design with community planning needs to be studied. It is necessary to understand the interaction between society and ecology, the hydrological functions in the urban system and the livelihood of residents in relation to flooding hazards that can be potentially aggravated by climate change. Evaluation of the effect of planning interventions in the social ecological systems in order to better plan for climate change towards resilience and sustainability.

1.3 **Research Objectives**

Considering the above discussion, the objectives of this thesis are as follows:

- To analyze the temporal and spatial variability of rainfall in the Umiam and Umtru Watershed.
- To model the rainfall runoff process using SWAT model for the study area.
- To quantify the effects of under inter basin water transfer reservoir on streamflow.
- To assess the changes in flow regime due to cascading reservoirs and water transfer.
- Impact of projected climate and human activities on streamflow.

1.4 **Organization of the Thesis**

Chapter 2 Presents a literature review of the works related to the thesis objective. It briefly describes about the climate change and its impacts on water resources, climate models, effect of reservoirs and hydrological models.

Chapter 3 Deals with the hydrological modeling of Umiam Watershed.

Chapter 4 Presents the impacts of inter-basin water transfer on streamflow.

Chapter 5 Explores the effect of inter-basin water transfer and cascading reservoirs on recipient watershed.

Chapter 6 Analyses the spatial and temporal variation of rainfall using the Innovative Trend Analysis Method and Mann-Kendall Method.

Chapter 7 Presents the impacts of climate change and landuse change on streamflow.

Chapter 8 Summarizes all the chapters and discusses the entire research work done.

CHAPTER 2

Review of Literature

2.1 Climate change

The Intergovernmental Panel on Climate Change (IPCC) Special Report on Emissions Scenarios (SRES) published projections of future greenhouse gas emissions in 2000 (IPCC, 2000). According to this report, "a set of scenarios was developed to represent the range of driving forces and emissions in the scenario literature so as to reflect current understanding and knowledge about underlying uncertainties". Four narrative storylines represent different demographic, economic, social, environmental and technological developments.

Emission scenarios are important components and tools for the modeling of climate change(Werner and Gerstengarbe 1997). They are based on an extensive assessment of driving forces and possible future evolving emissions, assuming a wide range of main demographic, economic, and technological driving forces of GHG and sulfur emissions (Nakicenovic *et al*., 2000). The IPCC Special Report on Emissions Scenarios (SRES) groups the latter into four scenario families or storylines that explore alternative development pathways as shown in (IPCC, 2007). A full description of the SRES can be found on the IPCC-homepage.

In IPCC fifth Assessment Report (AR5) in 2014, SRES Emission scenarios were superseded by four different 21st century pathways of greenhouse gas (GHG) emissions and atmospheric concentrations, air pollutant emissions and land use called Representative Concentration Pathways (RCPs). The pathways are used for climate modeling and research. They describe four possible climate futures, all of which are considered possible depending on how much greenhouse gases are emitted in the years to come.

2.1.1 Climate Change Impact Studies

Dimri et al., (2018) carried out an assessment of the projection of near surface air temperature over the Himalayan region from the Coordinated Regional Climate Downscaling EXperiment-South Asia (hereafter, CORDEX-SA) regional climate model (RCM) experiments for different Representative Concentration Pathway (RCP) scenarios. Their purpose was to assess the probable future changes in the mean temperature climatology and its long term trend for different seasons under greenhouse gas forcing scenarios for different seasons till the end of 21st century. climatology from present climate to far future. They observed a general pattern of increase is in the regionally averaged T_{mean} climatology from present climate to far future. The magnitude of warming increases with intensification of GHG emissions with respect to different RCPs. Further, the rate of warming is found to be least for RCP 2.6 (0.3 °C/decade) and highest for RCP8.5 (0.3–0.9 °C/decade).

Although RCMs have been frequently used in recent years to provide hydrologists with fine-scale climate parameter for runoff predictions, this is still a relatively new field of research. Clear rules are missing, and there is no such thing as 'common practice' in terms of how to best apply RCM simulations for impact studies(Teutschbein and Seibert 2010).

Hussen *et al.*, 2018 studied the impact of climate change on surface water availability and its allocation system within Bilate watershed in the Abaya-Chamo sub-basin of Rift Valley Lakes Basin in Ethiopia using outputs of Coordinated Regional Climate Downscaling Experiment (CORDEX)-Africa. SWAT and WEAP models were used for this study. Four scenarios were developed based on different set of assumptions in the basin up to 2035. This study also determines the environmental flow requirements (25% of the mean annual flow volume) to maintain the basic ecological functioning in the basin and regulate flow for downstream uses. This study found that integrated water resources management strategy in the basin could utilize water resources potential effectively in the future.

Ahmadaali *et al.*, 2018 performed modeling of hydrologic behavior of Urmia Lake Basin, Iran using WEAP model. The model was analyzed for three future emission scenarios (A2, A1B, and B1), for the period of 2015–2040 and five water management scenarios: (1) keeping the existing situation; (2) crop pattern change; (3) improving the conveyance and distribution efficiency; (4) combining the improvement of conveyance and distribution efficiency with improving the application efficiency using modern technology; and (5) the combination of crop pattern change with the improvement of total irrigation efficiency. The results show that the highest values of indices of environmental sustainability and agricultural sustainability are related to the scenario

of combining the crop pattern change with improving the total irrigation efficiency under the B1 emission scenario (B1S4).

2.1.2 Climate Change Studies in the North East India

The regional climate model simulation has been used from the COordinated Regional climate Downscaling EXperiment (CORDEX) South Asia framework by Kumar and Dimri, 2017. It was found that there has been a consistent warming during the present for the winter (December, January, and February (DJF)) and post-monsoon (October and November (ON)) especially in the northern and eastern parts of the region. During the present climate (1970–2005), an increasing trend of the daily mean precipitation has been observed for the pre-monsoon season followed by a decrease in the monsoonal precipitation in many parts over NEI region.

The future climate vulnerability for the near-term (2020–2035) A1B scenario was assessed for the three vulnerability indices; agricultural, water and forest using vulnerability indices (Ravindranath et al. 2011a). Tirap, West Siang, Nalbari, Changlang and Dibrugarh were found to be the most vulnerable districts to current climate vulnerability. Kolasib, N.C. Hills, Cachar, Ukhrul and Morigaon are the districts with least vulnerability. Overall in the North East region, higher agricultural vulnerability was observed in the northern parts and vulnerability declines towards the south. The impact of climate change on water resources of the two river basins was simulated using hydrological model SWAT. The results show both spatial and temporal variability. State-wise analysis shows that in Tripura, Mizoram, Manipur, parts of Meghalaya and Nagaland, the flood magnitude is likely to increase by about 25% in the future compared to the present. In forest vulnerability, Bishnupur and Tirap have very high vulnerability, while Tuensang, Lohit and West Garo hills have moderate to high vulnerability.

Shivam *et al.*, 2017 performed analysis of the change in temperature trends in Subansiri River basin for RCP scenarios using CMIP5 datasets. Statistical downscaling technique was used to generate Long-term (2011–2100) maximum temperature (T max) and minimum temperature (Tmin) time series. The comparison by magnitude shows an overall increase in T max by 0.47 °C over the period 2011–2100 and 0.72 °C for RCP8.5. The analysis of diurnal temperature range shows a significant decreasing trend with the magnitude of 0.001 °C/year in diurnal variation at annual temperature scale for RCP6.0.

Bal *et al.*, 2016 used RCM called Providing REgional Climates for Impacts Studies (PRECIS) and applied to all India. For the whole India, the projections of maximum temperature from all

the six models showed an increase within the range 2.5°C to 4.4° C by end of the century with respect to the present day climate simulations. It was found that Max Temperature in Meghalaya will increase by 3.6°C by 2080s and Min temperature will raise by 3.4°C. Meanwhile rainfall is expected to increase by 9.1% in 2080s. Similar changes were predicted for other northeastern states as well.

Das *et al.*, 2009 reported that for a part of the region that the meteorologists of the country officially refer to as the 'South Assam Meteorological Subdivision'(that covers mainly the hill states of Nagaland, Manipur, Mizoram and Tripura and parts of the Barail Hills in southern Assam), a significant change in seasonal rainfall has been observed. Besides scientific evidences, which are however few, he pointed out that individual and collective opinions in various parts of the region bear references to what may be construed as increased variability or changes in local climates. Such anecdotal references talk of irregular rainfall pattern with rainfall starting quite early in the region (say in January), heavy rainfall events (extreme rainfall) and flash floods becoming more frequent and dry periods becoming longer in various parts of the region. Northeast India is vulnerable to water induced disasters because of its location in the eastern Himalayan periphery, fragile geo-environmental setting and economic underdevelopment.

2.2 **Impact of climate change on water resources**

Global changes are undergoing at a larger scale, however, mitigation policies are expected to be applied locally. The impact studies related to surface water resources could be assessed through river flow and environmental requirement (Gul *et al*., 2010), water supply availability (Frederick and Major 1997) and (Bekele and Knapp 2010) regional water management, or flood frequency analysis (Prudhomme et al. 2002). Moreover, it was reported that the changes are variable from one geographic location to another (Kulshreshtha 1998). As such this effect could be pronounced through alteration of regional precipitation and evapotranspiration that have direct consequences on hydrologic processes and water resources (rivers, lakes, aquifers, and springs) through their possible shifts of basin-wide water balances (Loaiciga, 2009). For example, in Europe, climate change will pose two major water management challenges: increasing water stress mainly in south eastern part and increasing risk of floods throughout most of the continent (Alcamo et al. 2007). The mean annual temperatures are likely to increase more than the global mean, with the largest warming in summer for the Mediterranean area, and in particular the highest summer temperatures are expected to increase more than the average for central and southern Europe (Christensen and Lettenmaier 2007). In the Mediterranean area, annual precipitation and annual

number of precipitation days are very likely to decrease. Consequently, significant hydrological changes are expected for southern Europe. In this region, there is a likely decrease in annual runoff, by 0 to 23% up to 2020s and by 6 to 36% up to 2070s; accompanied with a decrease by up to 80% of low summer flows, making the risk of drought particularly important. Projected increase of water withdrawals in Southern Europe would amplify the risks associated to climate change, being the Mediterranean region more exposed to drought risk (Alcamo and Henrichs 2002). This global climatic changes caused by increases in the atmospheric concentration of carbon dioxide and other trace gases may continue to appear in the next few decades where it is expected to change future regional water availability (Xu 1999a).

The impact studies related to surface water resources are more concentrated to the regions in Europe, North America and Australia (Bates et al. 2008), and majority of these use hydrological model driven by scenarios based on climate model simulations (Hamlet and Lettenmaier 2000; Middelkoop et al. 2001; Xu 2000). However, only a few studies focused on African and Asian regions (Kundzewicz and Döll 2009). In surface water, the impact studies related to inland reservoirs are limited in number where the priority is given to the streamflow river runoff. After IPCC's third assessment report, studies at basin scale are also becoming common practice. Nohara *et al.*, (2006) investigated the projections of river discharges for 24 major rivers in the world during the 21st century simulated by 19 coupled AOGCMs based on the SRES A1B scenario. Using weighted ensemble mean, they have shown that at the end of the 21st century, the annual mean precipitation, evapotranspiration, and runoff increase in high latitudes of the northern hemisphere, southern to eastern Asia, and central Africa. In contrast, these variables decrease in the Mediterranean region, southern Africa, southern North America, and Central America. In the same study, they have also shown that for rivers in high-latitude (Amur, Lena, MacKenzie, Ob, Yenisei, and Yukon), the discharge increases, and the peak timing shifts earlier because of an earlier snowmelt caused by global warming. And discharge tends to decrease for the rivers in Europe to the Mediterranean region (Danube, Euphrates, and Rhine), and southern United Sates (Rio Grande). Elshamy *et al.* (2009) have used 17 GCMs from the IPCCs AR4 to evaluate the upper Nile flow at Diem. Their assessment showed that there is poor agreement between the different GCMs used in terms of evaluating change in precipitation. However, their overall result showed that the water balance of the upper Blue Nile basin might become more moisture constrained for moderate change in precipitation in the future. A more comprehensive study for the same basin by Kim and Kaluarachchi (2009) showed that there would be mild increases in

hydrologic variables (precipitation, temperature, potential evapotranspiration and runoff) over the entire area for a weighted scenario from six GCMs. Their finding also indicated low-flow statistics and reliability of stream flows are increased, and severe drought events are decreased due to the increment of precipitation.

In small-size catchments, the study catchments may be approximately captured by only one grid cell in the RCMs. One might argue that using simulations from only one RCM grid cell could be the cause for biases in precipitation as it might be doubtful to what extent RCMs are able to accurately simulate local climate information. To address this issue, Teutschbein and Seibert, 2010, compared observed temperature and precipitation to the values averaged over the central grid cell and its eight neighboring cells. However, using precipitation and temperature values averaged over nine grid cells instead of applying only the center cell did not result in significantly different results.

Asefa *et al.*, 2014 used RRV method for Tampa Bay Water's Enhanced Surface Water System. In their study, for each scenario, a thousand ensembles of 300-years of monthly stream flow traces were first generated by a multi-site rainfall/runoff model. Second, a novel nonlinear disaggregation algorithm was developed to translate monthly outputs into daily values. This may be useful for areas with daily rainfall data scarcity. Several mitigation scenarios such as treatment and reservoir capacity expansion, as well as adaptation through operational changes were considered to evaluate system performance under varying climatic conditions.

Carvalho-Santos *et al.*, 2017, analysed whether or not the shortage of water supply can be effectively addressed through the construction of a new reservoir (two-reservoir system) in the Alto Sabor watershed, northeast Portugal by considering future climate projections. SWAT model was used to simulate river discharge. Outputs from four General Circulation Models (GCM) for two scenarios (RCP 4.5 and 8.5) were statistically downscaled and bias-corrected with ground observations. It was found that temperature is expected to increase in the future while the change in precipitation is more uncertain as per the differences among climatic models. Seasonal changes would be more significant than annual changes, with more precipitation in winter and much less in spring and summer. SWAT simulations suggest that the existence of a two-reservoir will better solve the water supply problems under current climate conditions compared to a single reservoir system.

2.3 Climate Models in Water Resources Studies

2.3.1 GCM for Water Resources Studies

Global Atmospheric General Circulation Models (GCMs) have been developed to simulate the present climate and used to predict future climatic changes. In water resources impact assessment there are varieties of such GCMs' and RCMs' outputs at different spatial and temporal resolutions. It is also obvious that GCMs are the only tools that are nowadays providing datasets in water resources impact studies.

The GCMs simulation skills decrease from climate variables to hydrological variables while the hydrological importance increases along the same direction (Xu, 1999a). Further, Xu (1999a) has identified three different gaps in using the GCMs for water resources studies. These are: (i) The spatial and temporal scale mismatches, (ii) The vertical level mismatches, and (iii) The accuracy mismatch. As an additional gap (Loaiciga et al., 1996) has mentioned the issue of feedback as hydrologic models are used in offline process modelling, and GCMs do not consider lateral transfer of water within the land phase. Despite all the above drawbacks, there are numerous studies conducted using the available GCMs in a different part of the world.

Bergstrom et al. (2001) have used two GCMs: UKMO HadCM2 of the Hadley Centre in Reading and the ECHAM4/OPYC3 of the Max Planck Institute for Meteorology in Hamburg to show the impact of climate change on runoff in Sweden. Their result shows a change in extreme values of runoff can be more critical than mean values.

Lotsari et al.(2010) have used two GCMs (HadCM3 and ECHAM5) to evaluate the impact of climate change on future discharges and flow characteristics of the Tana river in sub-arctic northern Fennoscandia under three different emission scenarios: A1B, A2 and B1.

2.3.2 RCM for Water Resources Studies

Regional Climate Models (RCMs) are developed based on the same representations of atmospheric dynamical and physical processes as GCMs. They have a higher spatial resolution in the order of 10-50km that can cover a sub-global domain. As a result of the higher spatial domain, RCMs provide a better description of orographic effects, land-sea surface contrast and land-surface characteristics (Christensen and Christensen, 2007a). There are many different RCMs currently available for various regions, developed at different modelling centres of the world. However, the uncertainty issues remain another drawback in the use of RCM. Due to this

fact, several international efforts have been taken to quantify uncertainties through model intercomparison. Some of these include the project work in the European region: PRUDENCE [Prediction of Regional scenarios and Uncertainties for Defining EuropeaN Climate change risks and Effects] (Christensen and Christensen, 2007a) and ENSEMBLES; and in North America, the NARCCAP (North American Regional Climate Change Assessment Program). More recently, a new project called CORDEX (Coordinated Regional Climate Downscaling Experiment) has been initiated by the world climate research program simulations at 50km resolution for multiple regions.

Teutschbein et al., (2011), and Teutschbein and Seibert, (2012) provided a recent review on the use of RCMs for hydrological models. They recommend that a bias correction is necessary for using the outputs in any hydrological models as RCMs are susceptible to systematic model errors caused by imperfect conceptualization, discretization and spatial averaging within grid cells. Bias correction is also recommended by Wilby et al.(2000) and Wood et al., (2004) as a minimum requirement when using RCM outputs in hydrological impact studies.

The uses of RCMs are most often applied in European river basins. Some of the examples are the studies of the effects of climate change on groundwater assessment (Roosmalen et al., 2007), run-off estimation (Rigon et al., 2007), flood risk assessment (Fowler and Wilby, 2010), precipitation, potential evapotranspiration estimation (Baguis et al., 2010), overall catchment-scale hydrologic processes (Senatore et al., 2011). All these assessments are conducted through further downscaling (bias correction) of RCMs.

2.4 **Known Methodologies for Climate Change Impact Assessment**

One of the earliest review of techniques used for assessing the effect of climate change on water resources is provided by (Leavesley 1994). Their review showed a clear image of the types of models used in impact studies and problem areas related to a number of modelling issues. The issues could be parameter estimation, temporal and spatial scale of application, validation, climate scenario generation, data and modelling tools. Future solutions to such issues are recommended to bring a way for the quantitative determination of climate impacts.

2.4.1 The direct use of GCM outputs in hydrological models

The approach is to directly use the GCM-derived hydrological output since the GCM is the only available tool for detailed modelling of a future climate (Xu et al. 2005). However, direct

representations of hydrological quantities are highly simplified large-scale averages with little spatial reliability or relevance to specific regions as GCMs were not originally designed for climate change impact studies in hydrology. They thus reflect inherent GCM shortcomings such as runoff being calculated as a secondary variable and not a first-order GCM variable such as P, T, wind or vapor pressure.

2.4.2 Coupling GCMs and Macro-Scale Hydrologic Models

Some of the research work done in different parts of the world were reviewed by (Xu 1999b). The results of the studies showed that coupling the hydrological model (macroscale or global) with GCM produces a better representation of the recorded flow regime than GCM predictions of runoff for very large river basin. The examples of such models are: MacPDM(Arnell 2004), WBM (Vörösmarty et al. 2000) and WaterGAP (Alcamo and Henrichs 2002).

2.4.3 Downscaling GCM to Force Hydrological Models

Hydrological models require input data (such as precipitation and temperature) at smaller sub-grid scale, which has to be provided by converting the GCM outputs into a reliable time scale for the study area under consideration. However, due to the limitations of GCMs related to the scale issue, an alternate way of using direct GCM-derived hydrological outputs is to downscale the GCM climate outputs for use in hydrological models.

To date, there are different techniques for downscaling large-scale GCM outputs to small-scale resolutions in order to use in impact models. All the available techniques of downscaling are categorized under two broad groups namely: dynamic downscaling and statistical downscaling techniques (Wilby et al. 1998; Xu 2000) are among other reviews).

1. **Dynamic Downscaling**

   It refers to the use and extraction of local-scale information from large-scale GCM data using regional climate model (RCM) or limited-area models (LAMs) at 0.5°X 0.5° or even higher resolutions that parameterize the atmospheric processes. They utilize large-scale and lateral boundary conditions from GCMs to produce higher resolution outputs required by hydrologic models. However, the computational expensiveness of the dynamical downscaling method limits its applicability. Some of the popular RCMs are PRECIS, CoRDEX, PRUDENCE etc.

2. **Statistical Downscaling**

   In this method, the large-scale atmospheric variables eg. Sea-level pressure and geopotential heights) are empirically related to the local or station-scale atmospheric variables (eg. average precipitation or temperature). The large-scale atmospheric variable is commonly referred to as the predictors, whereas the local scale climate variables are the predictands. The key assumptions (Fowler et al. 2007) of this method include: (a) the predictors are variables of relevance and are realistically modeled by the GCM, (b) the transfer function is valid also under changing climate conditions (may not be provable) and, (c) the predictors employed fully represent the climate change signal.

2.5 Effect of Reservoirs on Streamflow

A large number of water conservation projects have been built in recent years, and water resource that humans must depend on has been under control to a certain degree. However, the runoff process and sediment transport in rivers have also changed greatly (Zhang et al. 2017). Reservoirs improve water availability and provides numerous benefits to people. By storing and redistributing water, reservoirs significantly increase water availability for irrigation. Reservoirs are necessary for sustaining irrigated agriculture (Biemans et al. 2011).

Long-term effects of small dams on stream flow and water quality were studied by Liu *et al.*, 2014 at a watershed scale in South Tobacco Creek, Canada.. They used SWAT hydrologic model with reservoir routine incorporating the concepts of equivalent reservoir storage and equivalent reservoir discharge to characterize small storage and short retention time in small reservoirs. It was observed that the combined effect of small dams can reduce daily peak flow by 0–14%. They concluded that small dams are also effective in reducing nutrient and sediment loading from agricultural runoff.

Zhang *et al.*, 2010, applied SWAT model to study the effect of dams and flood gates on stream flow and water quality in Huai River Basin. Since there was no observed flow data for period before the construction of dam, the SWAT model was calibrated based on present conditions. Then simulation was done for no dam scenario based on the calibrated model. The results showed that in the wet year (1991), the impact of water projects was not obvious because the dams & floodgates were open for flood control, whereas, flow decreased remarkably compared with the flow without dams in dry years.

A hydrology-routing-reservoir was applied by Adam *et al.*, 2007, to simulate the influences of reservoirs on annual and seasonal streamflow changes. Runoff process was simulated using Variable Infiltration Capacity (VIC) model, then a reservoir model was run. Reservoir releases and all other flows were routed to the reservoir outlet. The coupled modeling system was run with and without the reservoir model. The result of this study obtained a reconstructed streamflow before reservoir construction. Due to reservoirs there was an increase in winter low flow and a decrease in summer peak flow, thereby diminishing streamflow seasonality. On the other hand, there was no significant effect on annual flow.

Effects of cascade reservoir dams on the streamflow and sediment transport was investigated by Wu *et al.*, 2018 using nearly 60 years of hydrologic data. They used Mann-Kendal test to explore abrupt changes. It was observed that mean annual rainfall and runoff series did not change significantly; however, the sediment discharge decreased significantly due to cascade dam construction. The cascade dams, modified the flow regimes, trapping sediment in the reservoirs and disrupting the sediment transport downstream. The dams constructed downstream of existing reservoir had lesser effect on sediment transport than the initial dams.

2.6 **Hydrological models**

Hydrological models are valuable tools of study in this kind of research (e.g. climate change, water resources). Many studies show the ability of hydrological models to estimate water balance components and climate change assessment (Arnold and Fohrer 2005; Schuol et al. 2008). Hydrological models can be classified into deterministic and stochastic approaches. In the deterministic approach, a hydrologic model can be divided into empirical (black box), conceptual (grey box) or physical (white box) based. It can also be grouped into lumped or distributed based models. Stochastic approaches are derived from a time series analysis. Figure 1-8 shows the summary of hydrological classifications.

Empirical models are based on mathematical equations. Constrained Linear Systems (CLS) models (Todini 1988) and the Antecedent Precipitation Index (API) model (WMO, 1994) are examples of empirical models. In Lumped models, for the whole modeled area, the parameters are spatially averaged to one value. The Stanford modeling system (Crawford & Linsley, 1966) and HEC-HMS (U.S. Army Corps of Engineers) are lumped models for instance. In a distributed model, the parameters vary spatially. MIKE-SHE model (Refsgaard & Storm, 1995), Precipitation runoff modeling system (PRMS) model (Leavesley et al.,1983), and soil and water assessment tools (SWAT) (Arnold et al., 1998) are some examples of these models.

2.7 Conclusions from the Literature Review

From the literature, it is seen that LULC and climate change can have a huge impact on hydrological processes. Evapotranspiration, soil moisture content is changed when vegetation is altered. Changes in vegetative cover also affects surface runoff. Urbanization may lead to increase in impervious areas due to construction of buildings, roads and pavements. This leads to decline in area for infiltration and affect groundwater levels as well. In watersheds which has rapidly growing population, LULC changes are bound to happen over time. It will be of great value to the management authorities if the change can be predicted for the future.

Various GCMs are available nowadays for obtaining climate data for future timescales. However, the resolution of GCMs are too coarse to be applied directly on hydrological studies at catchment scale. With the advancement in climate modeling, RCMs have provided climatological data at finer resolution (50 Km x 50 Km). However, this resolution may still be large for smaller catchments. RCM outputs may be further downscaled to fit into catchment scale climate parameters and to use as inputs for hydrological models. There is limited number of studies done in Northeast India using RCMs for modeling the effects of climate change at catchment scale. Thus, the applicability of CoRDEX RCM can be explored for small catchment at high altitudes receiving high rainfall with high spatial variation.

According to the study done by Palmer *et al.,* 2008 on world's river basins, it was reported that climate change will have more of an impact on basins dominated by dams. The Umiam-Umtru basin surely comes under this category as it as multiple number of dams within the same basin. Thus, it needs our attention to assess the implications of changing climate on its smooth functioning. From the literature review above it is seen that traditional approaches to climate change impact assessment at the basin scale rely on a modelling chain that usually includes the generation of future emission scenarios, the simulation of GCM to build global climate scenarios, the use of RCM and statistical downscaling to estimate climate scenarios at the basin scale, and the projection of climatic scenarios into discharge scenarios via simulation of hydrological models. The modelling chain often stops here, while further evaluation of hydrological scenarios is committed to experts. Thus, there is a scope to extend quantitative assessment also to impacts on water resources like hydropower generation. To this end, the modelling chain must be extended to include the simulation of the water system management and the evaluation of the impacts by means of performance indicators.

In North East India, the climate change studies have illustrated the future trends of temperature and precipitation in the region (Kumar and Dimri, 2017). However, this future climate projection needs to be confirmed using a process-based study like a hydrologic model. This, will also help in assessment of accuracy of the climate model to simulate climate in catchment scale. Also the vulnerability assessments have been carried out for water, forest and agriculture (Ravindranath et al. 2011a). But, not much of research is found to exist focusing on the consequences of changing climate at catchment scale in this region.

The depth of the literature reviewed shows that human-induced climate change and variability and related impacts are real, ongoing and is expected to increase in the next several years. Global temperature increases, change in precipitation intensity trends, and increases in extreme weather events are expected to have negative impact on water and natural resources and agricultural production. Climate change research and adaptation options are critical for human sustainably managing natural resources and harnessing potential climate change impacts to their advantage. On the other hand, anthropogenic factors are also increasingly contributing to the changes in natural streamflow. Reservoirs are being increasingly constructed to store water for hydropower generation and irrigation. While it might bring economic benefits, it may also change natural ecology in the area. The Umiam-Umtru basin is of utmost importance to the state of Meghalaya, as a source of hydroelectric power generation. A lot of changes have taken place in the catchment due to the construction of multiple reservoirs thus changing the streamflow of Umiam and Umtru Rivers. Climate change is another factor which needs to be taken into account for smooth functioning of reservoirs. It is also seen from the literature that Hydropower is very sensitive to changes in climate as factors such as precipitation, temperature and humidity are likely to impact the production as well as consumption of electricity. Study on climate change and its probable impact on hydropower will help to get insight into the future power scenario in the region and also help the authorities to prepare for alternatives considering climate change in their planning and operations of hydropower stations.

2.8 **Research problem**

Fresh water is one of the most valuable assets for any human civilization. The dependency of a country's overall economy on this resource is due to inevitable demand for water from all sectors of human activities. Dams and reservoirs have served mankind as storage of fresh water for thousands of years. To date, there are over 50000 large dams (structure height higher than 15 m) throughout the world that are used for hydropower, irrigation and drinking purposes (Berga, 2008;

Caston et al., 2009). Reservoirs are even more important for communities living in arid and semi-arid regions, because of scarcity of water resources. The North Eastern Region of India is blessed with the highest hydro power potential in the country. According to Central Electricity Authority, potential sites from North Eastern(NE) states amounts to 44.43 % of total hydro power potential of the country. Among the NE states, Meghalaya ranks third in hydropower potential after Arunachal Pradesh and Sikkim. The series of power generation units in Umiam and Umtru Rivers of Meghalaya has capacity to produce 216 MW of power. Besides power generation and domestic use, the Umiam Reservoir is a popular tourist attraction and watersports point. The reservoirs Umiam, Kyrdemkulai and Nongmahir are also used for reservoir fisheries development. Thus, Umiam-Umtru Basins are vital for the people of the area and for Meghalaya state as a whole. Since the area is comparatively small for climate change studies using General Circulation Models (GCM), the impacts of climate change on regions like northeast India in general and Meghalaya in particular are less explored and less known till now making the future scenarios more uncertain for vulnerability assessment and risk management. However, certain indicators point to impacts being already visible in the region (Das et al. 2009).

This work will envisage to study the individual and combined effects of climate change on streamflow in a watershed having controlled flow. To assess the effect of climate change on natural streamflow it is important to know the flow behaviour before the construction of dams. In watersheds containing dams/sluices a lumped hydrological model is incapable of expressing the spatially distributed features. This study implements a hydrological model to simulate rainfall runoff processes, thus enabling to quantify the hydrologic regime at present and future timelines. The research problem has thus been identified with the following objectives.

- To model the rainfall-runoff process using SWAT model for the study area.
- Reconstruction of natural streamflow before the dam construction.
- To simulate the streamflow after dam construction.
- To identify any spatial and temporal climate change trend of temperature and precipitation in the basin.
- To assess streamflow under future climatic conditions.

With respect to the above objectives the main contributions of this thesis are:

- A semi-distributed hydrological model of the Umiam and Umtru watersheds were developed. This study also incorporated Inter-Basin Water Transfer in the hydrological model.
- Natural streamflow was successfully reconstructed to assess the impact of reservoir on streamflow.
- This study quantified the Effects of Inter-Basin Water Transfer and Cascading Reservoirs on Streamflow of Recipient Watershed.
- The analysis of the effect of Cascading Reservoirs and Inter-Basin Water Transfer was done.
- The spatial and temporal trends in rainfall over Umiam and Umtru Watersheds were identified. In addition to the monthly trends, it also identified trends in different magnitudes of rainfall.
- This study also identified the possible effect of landuse and climate change on streamflow in future.

CHAPTER 3

Hydrological Modeling of Umiam Watershed

3.1 SWAT Hydrological Model

The hydrological model of the Umiam watershed was set up using the Soil and Water Assessment Tool (SWAT) for generating the streamflow. SWAT is a hydrological simulation model developed by the United States Department of Agriculture (USDA). The SWAT model was developed with an aim to predict runoff, sediment yield, and agricultural chemical yields in large ungauged basins (Arnold et al. 1998; Neitsch et al. 2011). SWAT uses the water balance equation for simulation of hydrological processes (3.1).

$$SW_t = SW_0 + \sum_{t=1}^{t} (R_i - Q_i - ET_i - P_i - QR_i) \quad (3.1)$$

where SW_t (mm) is the final soil water content, SW_0 (mm) is the initial soil water content on i^{th} day, t (days) is time, R_i (mm) is the precipitation amount on i^{th} day, Q_i (mm) is the amount of surface runoff on i^{th} day, ET_i (mm) is the evapotranspiration (ET) amount on i^{th} day, P_i (mm) is the amount percolated water on i^{th} day, and QR_i (mm) is the amount of return flow on i^{th} day.

SWAT also comes with a reservoir routing module to account for the presence of reservoirs in the watershed. The reservoir water balance equation used by SWAT is given by the following equation (3.2).

$$V = V_{stored} + V_{flowin} - V_{flowout} + V_{pcp} - V_{evap} - V_{seep} \quad (3.2)$$

where V is the water volume in the reservoir at the end of the day (m^3), V_{stored} is the water volume stored in the reservoir at the beginning of the day (m^3), V_{flowin} is the water volume entering the reservoir during the day (m^3), $V_{flowout}$ is the water volume flowing out of the reservoir during the day (m^3), V_{pcp} is the volume of precipitation falling into the reservoir during the day (m^3), V_{evap} is the water volume evaporated from the reservoir during the day (m^3), and V_{seep} is the volume of water seepage from the reservoir during the day (m^3).

SWAT facilitates estimation reservoir outflow using four different methods: (1) average annual release rate (an uncontrolled reservoir), (2) measured daily flow, (3) measured monthly flow, and (4) controlled outflow with target release. In this study, there was no release through the spillways except when the water level reaches the maximum level. Thus, the outflow takes place only through the headrace tunnel to Umtru watershed. For the simulation of water transfer from Umiam Reservoir to Umtru Watershed, the consumptive water use management tool inbuilt in SWAT is used (Neitsch et al. 2011). Consumptive water use management tool can account for monthly variations in water transfer. An average daily volume of water that is removed from the reservoir is given as input to the model. For the water transfer, the reservoir simulation must be set to operational mode by initiating the year of operation.

3.2 **Study Area**

The Umiam River, located in the Meghalaya, India (Figure 3.1), is of great significance as it serves as an important source of water for hydropower generation. It flows from Sohiong region in Meghalaya and joins the Kapili River in Assam, which empties into the Brahmaputra River. The flow length of the mainstream of Umiam River is 118 km and covers an area of 1410.27 Km^2. The elevation ranges from 1723 m above the mean sea level (MSL) in the upper reach to 60 m above MSL at the watershed outlet. Compared to the high elevation Shillong region with annual precipitation of 2140.3 mm, the downstream plains in Assam region receives annual precipitation of 1709.5 mm (Das et al. 2015). The mean maximum temperature in Umiam is 24.81°C, and the mean minimum temperature is 15.75°C (Choudhury et al. 2012). The Umiam

Reservoir was built across Umiam River to divert water for hydropower generation. The reservoir became operational in 1965 and had a storage capacity of 185 million cubic meters. The water from the Umiam river is being stored and diverted for power generation to another watershed drained by Umtru River through a headrace tunnel, with a design capacity of 28.12 m3/s. The cascade of reservoirs comprising of Umiam Reservoir, Kyrdemkulai Reservoir, Nongmahir Reservoir, Umiam Stage-4 Reservoir and New Umtru Hydropower project together produce about 196 MW of electricity. The Umiam Stage-1 power station located at Sumer village generates electricity from the diverted water from the Umiam Reservoir. The Stage-2 power house uses the tailwater of Stage-1 power house to generate electricity. The tailwater from the Stage-2 then joins Umtru River and flows to Kyrdemkulai Reservoir and continues to flow through the cascade of reservoirs shown in Figure 3.1.

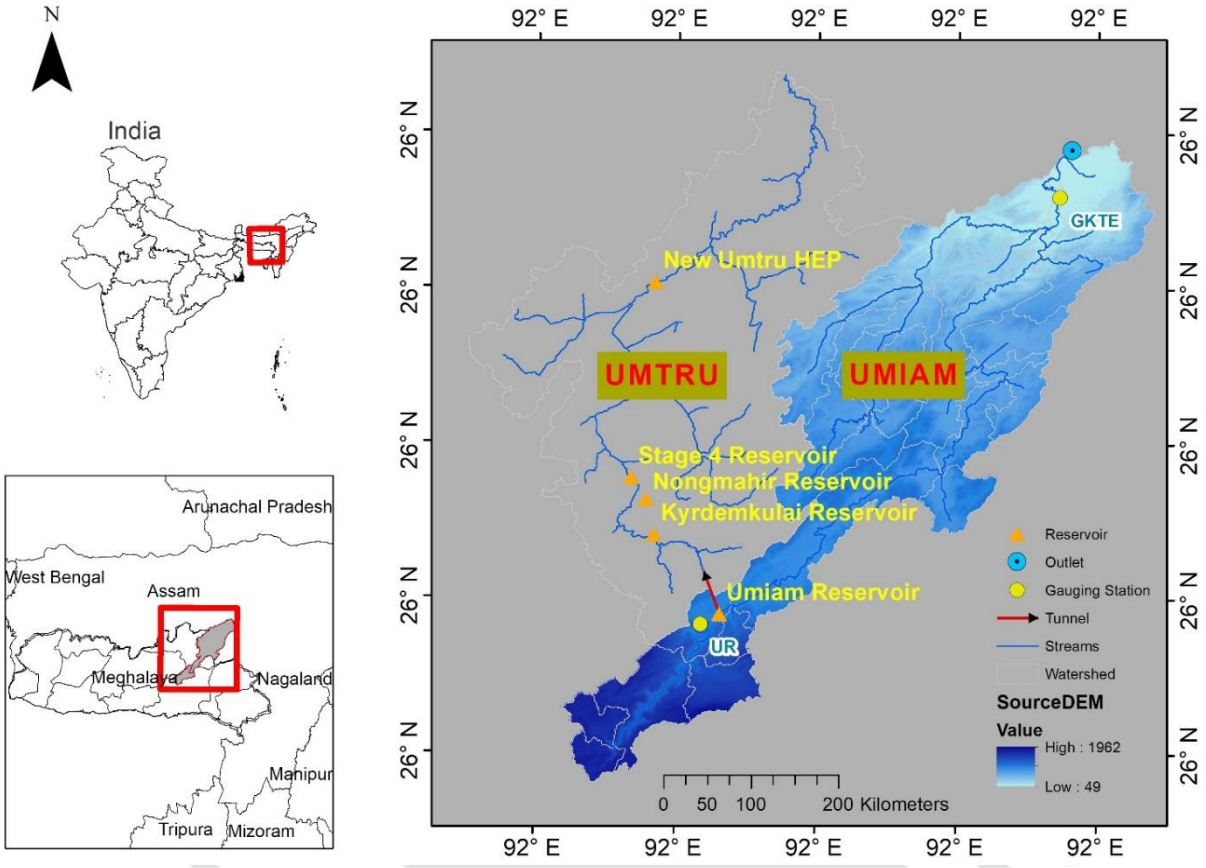

Figure 3.1 Umiam Watershed

3.3 **Model Parameterization**

SWAT uses Digital Elevation Model (DEM) to delineate the watershed and to generate stream networks. The SRTM (Shuttle Radar Topographic Mission) 30 m resolution DEM was downloaded from https://earthexplorer.usgs.gov/ website and projected to UTM (Universal Transverse Mercator) Zone 46N. Watershed delineation with sub-basin threshold area of 2000 ha resulted in thirty-seven sub-basins.

Land use and land cover (LULC) data used in this study were obtained from the National Remote Sensing Centre (NRSC) (available on request at https://bhuvan-app1.nrsc.gov.in/thematic/thematic/index.php). The NRSC-LULC data is prepared from multi-

temporal Advanced Wide Field Sensor (AWiFS) imagery and is available for the whole of India. This dataset contained 17 different land use classes for Umiam watershed, which were reclassified into 7 classes according to SWAT LULC database. The LULC of Umiam watershed consisted of 2.59% built-up area, 5.3% agricultural area, 10.26% rangeland, 1.17% orchard/plantation area. Most of the area was under evergreen forest (47.32%) and deciduous forest (32.22%) while water bodies accounted for 1.13% of the watershed area. The soil map required for SWAT model was extracted for Umiam Watershed from Harmonized World Soil Database (HWSD) (http://www.fao.org/soils-portal/soil-survey/soil-maps-and-databases/harmonized-world-soil-database-v12/en/).

In order to drive the SWAT hydrological model, the basic meteorological data required are precipitation and temperature. The precipitation data used was 0.25° X 0.25° latitude by longitude, gridded data from the Indian Meteorological Department (IMD) (Pai et al. 2015). This dataset is prepared from observed rainfall data at IMD stations and is available for all regions of India from 1901 to 2015. The gridded temperature data of 0.25° X 0.25° resolution (Sheffield et al. 2006) was obtained from http://hydrology.princeton.edu/home.php website. Other weather parameters like solar radiation, wind speed, and relative humidity were generated using inbuilt weather generator in SWAT due to lack of available data.

The reservoir data were obtained from Meghalaya Energy Corporation Limited (MeECL). The required inputs such as reservoir surface area when the reservoir is filled to the normal operating level and emergency level etc. were fed to SWAT reservoir module. The water transfer to Umtru watershed through the head race tunnel was also defined for each month as daily average values under WURESN (consumptive water use).

Using the above-mentioned data as inputs the SWAT model was run. While SWAT offers several methods for computing evapotranspiration and runoff (Neitsch et al. 2011), we chose Penman-Monteith method and the SCS Curve Number Method as per the availability of data.

3.4 **Calibration and validation**

To analyse how a parameter may affect the model output, a sensitivity analysis was performed using global sensitivity analysis in SWAT Calibration and Uncertainty Programs (SWAT-CUP) (Atkinson et al. 2010) software. The results of global sensitivity also gave an idea about how to adjust the range of each parameter during calibration. The model calibration was carried out using the SUFI-2 algorithm. In SUFI-2, all the uncertainties arising due to input data, conceptual assumptions, model parameters are mapped to the parameters and the algorithm aims to attain smallest parameter uncertainty (ranges). The parameter uncertainty is quantified by the 95% prediction uncertainty (95PPU). More details about the SUFI-2 algorithm can be found in Abbaspour (2015a).

The SWAT model was set up for the Umiam watershed which had an area of 1410.27 Km^2. The discharge data of Umiam River at the inlet of UR was collected from Meghalaya Power Generation Corporation Limited (MePGCL). The data was available as inflow to the reservoir and is obtained from the mass balance equation based on inflow, outflow and storage of the reservoir. Up to the Umiam Reservoir, five sub-basins (33-37) were covered in the model and were selected using the regionalization scheme in SWAT-CUP. Fourteen parameters (Table 3.1) and their initial ranges were chosen based on literature (Arnold et al. 2012; Poméon et al. 2018; Rahbeh et al. 2011; Shrestha et al. 2016; Zhang et al. 2008) for initial calibration and sensitivity analysis. The input data required for SWAT reservoir simulation such as reservoir surface area and volume when the reservoir is filled to the emergency spillway (RES_ESA, RES_EVOL) and those for principal spillway (RES_PSA, RES_PVOL, etc) were defined (Table 3.2). The reservoir

was set to operational mode during calibration so as to represent the present scenario. The most sensitive parameters identified by sensitivity analysis for UR were: RCHRG_DP.gw, GW_DELAY.gw, CN2.mgt, SOL_K().sol, SOL_AWC(..).sol, and ALPHA_BF.gw (Descriptions in Table 3.1). Whereas for second gauging station at Gopal Krishna Tea Estate (GKTE), the most sensitive parameters were CN2.mgt, RCHRG_DP.gw, GWQMN.gw, GW_REVAP.gw, and GW_DELAY.gw. The Sub-basins calibrated under GKTE are Sub-basin 1-32. Parameterization protocol of Abbaspour *et al.* (2015) was used for the calibration process. Step by step calibration technique was followed, beginning from upstream and working towards the downstream. After obtaining satisfactory results, these calibrated parameters were fixed for UR (Sub-basin 33-37) and parameter Set-A was obtained. Next, calibration of parameters for sub-basin 1-32 (downstream) was carried out at GKTE station and parameter Set-B was obtained.

Table 3.1 Parameters used in SWAT model calibration

Sl. No	**Parameter**	**Description of Parameter**
1.	R__CN2.mgt	SCS runoff curve number
2.	V__GWQMN.gw	Threshold depth of water in the shallow aquifer required for return flow to occur (mm)
3.	V__GW_REVAP.gw	Groundwater "revap" coefficient
4.	V__REVAPMN.gw	Threshold depth of water in the shallow aquifer for "revap" to occur (mm)
5.	V__ESCO.hru	Soil evaporation compensation factor
6.	V__EPCO.hru	Plant uptake compensation factor
7.	R__OV_N.hru	Manning's "n" value for overland flow
8.	V__ALPHA_BF.gw	Baseflow alpha factor (days)
9.	V__GW_DELAY.gw	Groundwater delay (days)
10.	R__SOL_AWC(..).sol	Available water capacity of the soil layer (mm H2O /mm soil)
11.	R__SURLAG.bsn	Surface runoff lag time (days)

12.	R__RCHRG_DP.gw	Deep aquifer percolation fraction
13.	R__SOL_K(..).sol	Saturated hydraulic conductivity (mm/h)
14.	R__HRU_SLP.hru	Average slope steepness (m/m)

Table 3.2 Reservoir data used

Sl. No	Parameter	Value	Description
1.	IYRES	1965	Year of the simulation the reservoir became operational
2.	RES_ESA	980	Reservoir surface area when the reservoir is filled to the emergency spillway (ha)
3.	RES_EVOL	14800	Volume of water needed to fill the reservoir to the emergency spillway (10^4 m^3)
4.	RES_PSA	307	Reservoir surface area when the reservoir is filled to the principal spillway (ha)
5.	RES_PVOL	2280	Volume of water needed to fill the reservoir to the principal spillway (10^4 m3)
6.	RES_VOL	14400	Initial reservoir volume (10^4 m^3)
7.	WURESN	Varies	Consumptive water use (Water Transfer)

3.5 **Performance evaluation**

The performance of the SWAT model was assessed using commonly used statistics such as: **Coefficient of determination (R^2):** It describes the proportion of the variation in the observed data explained by the model prediction. R2 ranges from 0 to 1, with higher values indicating less error variance, and typically values greater than 0.5 are considered acceptable.

$$R^2 = \left(\frac{\sum_{i=1}^{n}(O_i - \bar{O})(P_i - \bar{P})}{\sqrt{\sum_{i=1}^{n}(O_i - \bar{O})^2} \sqrt{\sum_{i=1}^{n}(P_i - \bar{P})^2}} \right)^2 \quad (3.3)$$

where, O_i is the i[th] observed data, $\bar{O}$ is the mean of observed data, P_i is the i[th] predicted value and $\bar{P}$ is the mean of predicted values.

Nash-Sutcliffe efficiency (NSE): It is a widely used statistic to evaluate the goodness of fit of hydrological models. The denominator describes the total variation of the observed values about the mean, while the numerator measures the variation in the observed data that has not been captured by the model.

$$NSE = 1 - \left[\frac{\sum_{i=1}^{n}\left(Y_i^{obs} - Y_i^{sim}\right)^2}{\sum_{i=1}^{n}\left(Y_i^{obs} - Y_i^{mean}\right)^2}\right] \quad (3.4)$$

where, Y_i^{obs} is the i[th] observed value, Y_i^{sim} is the i[th] simulated value and Y_i^{mean} is the mean of the observed values. NSE ranges between -∞ and 1.0 and the optimal value is 1.

Percentage Bias (PBIAS): Percent bias (PBIAS) measures the systematic error variation known as bias. The positive values denote underestimation bias, and negative values indicate overestimation bias. PBIAS is expressed in terms of percentage (%) and has an optimal value at zero. The lower magnitude of PBIAS signifies more accurate model simulation.

$$NSE = 1 - \left[\frac{\sum_{i=1}^{n}\left(Y_i^{obs} - Y_i^{sim}\right)^2}{\sum_{i=1}^{n}\left(Y_i^{obs} - Y_i^{mean}\right)^2}\right] \quad (3.5)$$

where, Y_i^{obs} is the i[th] observed value, Y_i^{sim} is the i[th] simulated value and Y_i^{mean} is the mean of the observed values.

RMSE-observations standard deviation ratio (RSR): RSR is calculated as the ratio of the RMSE (Root mean squared error) and the standard deviation of measured data. Lower RSR value signifies lower RMSE and better model simulation performance.

$$RSR = \frac{RMSE}{STDEV_{obs}} = \frac{\left[\sqrt{\sum_{i=1}^{n}\left(Y_i^{obs} - Y_i^{sim}\right)^2}\right]}{\left[\sqrt{\sum_{i=1}^{n}\left(Y_i^{obs} - Y_i^{mean}\right)^2}\right]} \quad (3.6)$$

The above methods are suggested for SWAT model evaluation in Moriasi et al. (2007).

The above statistical measures are not applicable when the output is given in terms of uncertainty bands as they can only compare two signals. To compare the uncertainty band given by 95PPU in SUFI-2, the measures given by Abbaspour (2015) termed as p-factor and r-factor were used. The p-factor is the observed data in percentage enclosed by the 95PPU band, and r-factor is the thickness of the 95PPU band. The p-factor of 1 indicates 100 % enveloping of observed data by the model simulation, whereas r-factor of zero means the observed and simulated values overlap each other, in other words, observed and simulated values are exactly equal.

3.6 **Results and Discussion**

The multi-site calibration was adopted for capturing the spatial variations in topography, land use, and soil. The SWAT model was calibrated with a stepwise calibration technique using the discharge data available at two locations. Monthly average discharge was available at UR from 1979 to 2004 from MePGCL. The data was split into two sets for calibration (1979-1993) and validation (1994-2004). The regionalization at the sub-basin level was done using the regionalization scheme of SWAT-CUP (Abbaspour et al. 2017). The SWAT model was calibrated first at UR using SUFI-2 algorithm. The model performance was evaluated based on Moriasi et al. (2007) using the coefficient of determination (R^2), Nash Sutcliffe Efficiency (NS), Percent bias (PBIAS), RMSE-observations standard deviation ratio (RSR). For comparison of the uncertainty band, p-factor and r-factor were used. The calibration at UR in monthly timescale (Figure 3.2) achieved an R^2 value of 0.97 and NS value of 0.94, which shows very good model

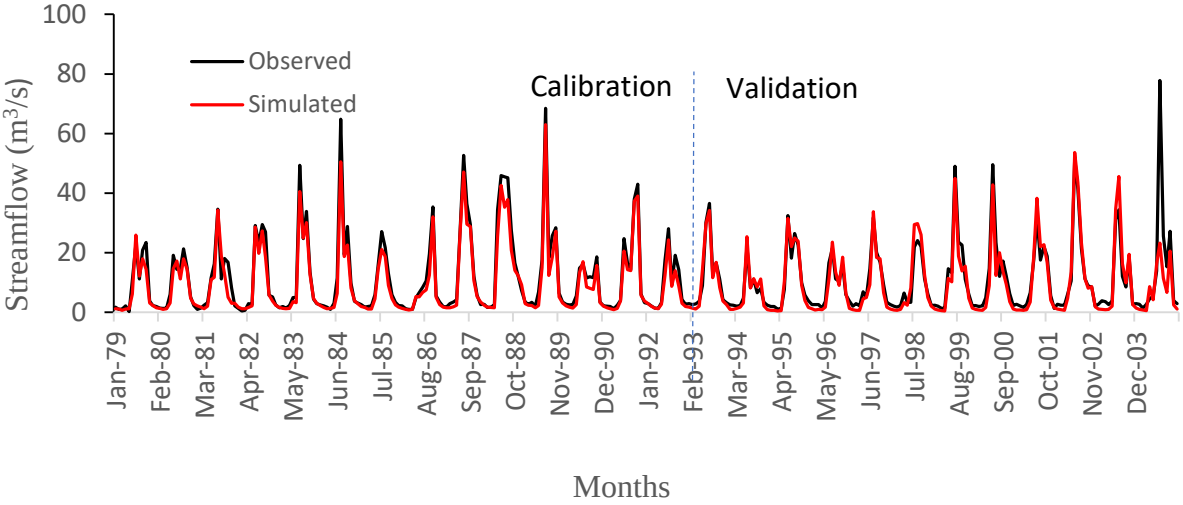

Figure 3.2 Monthly calibration and validation at Umiam Reservoir.

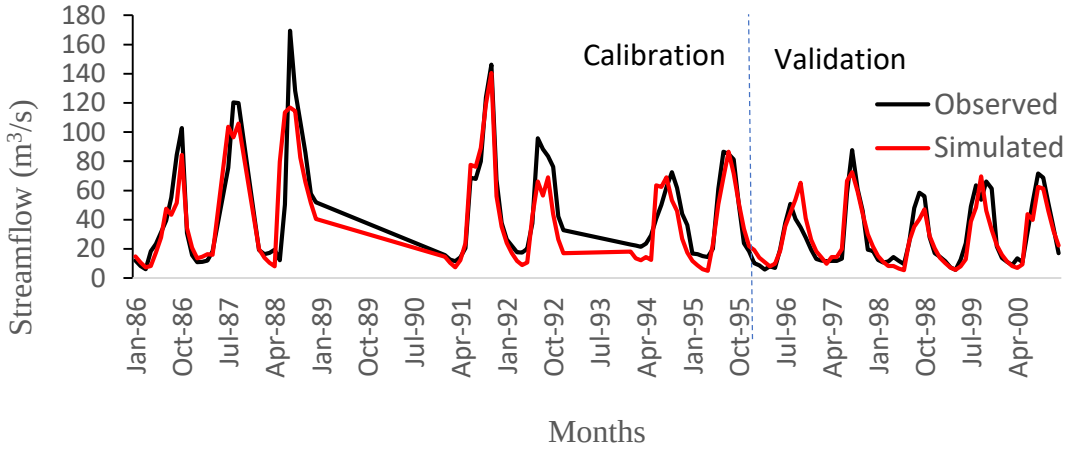

Figure 3.3 Monthly calibration and validation at GKTE

Table 3.3. Calibration and validation statistics on monthly scale

	Gauging site	Model Performance on monthly time scale					
		R^2	NSE	P-Bias	RSR	p-factor	r-factor
Calibration	UR (1979-1993)	0.97	0.94	14.7	0.25	0.79	0.34
	GKTE (1986-1995)	0.79	0.78	10.1	0.47	0.68	0.70
Validation	UR (1994-2004)	0.79	0.77	10.4	0.48	0.80	0.38
	GKTE (1996-2000)	0.81	0.81	3.1	0.44	0.82	0.88

Table 3.4. Calibration and validation statistics on daily scale

	Gauging site	Model Performance on daily time scale					
		R^2	NS	P-Bias	RSR	p-factor	r-factor
Calibration	UR (2005,2009,2010,2012)	0.69	0.64	18.3	0.60	0.58	0.62
	GKTE (1991-1992)	0.71	0.62	18.0	0.61	0.61	0.57
Validation	UR (2014-2015)	0.58	0.54	11.9	0.68	0.57	0.45
	GKTE (1994)	0.75	0.60	11.8	0.63	0.64	0.95

performance in monthly time scale. The PBIAS range for streamflow to be considered good is $\pm 10 \leq PBIAS \leq \pm 15$ (Moriasi et al. 2007), with positive values indicating under estimation and negative values indicating over-estimation. Here, we obtained PBIAS of 14.7% , which shows slight under-prediction but can be considered as good. The RSR obtained gets a very good ($0 \leq$

$RSR \leq 0.5$) rating with a value of 0.25. During the validation period, the model was able to capture 80% of observed data in 95PPU band given by p-factor value. The R^2 and NSE values for the validation period were 0.79 and 0.77. The PBIAS and RSR values also indicate good model performance with values of 10.4 and 0.48 respectively. After calibration at UR, the first set of model parameters were fixed for the sub-basins coming under UR. The next calibration was done at GKTE by regionalizing sub-basins 1 to 32. Larger number of sub-basins falls under GKTE and this part of the watershed lies in the lower elevation areas. Monthly average flow of 1986, 1987, 1991, 1992, 1994 and 1995 to 2000 were used for calibration at GKTE. The model results and the observed data show good agreement (Figure 3.3). The R^2, NSE were also good at GKTE with values of 0.79 and 0.78 respectively but slightly less than that obtained for UR. The PBIAS was 10.1 % and RSR was 0.47. The uncertainty measures p-factor and r-factor were 0.68 and 0.70 respectively (Table 3.3).

The monthly-calibrated model was further refined to simulate daily flows. At UR the daily flow data were available only for six years, i.e. 2005, 2009, 2010, 2012, 2014 and 2015. At GKTE daily data was available for 1991, 1992 and 1994. These data were used to test the performance of the monthly calibrated model on a daily scale and also for further refinement the parameters. Calibration at UR was done using flow data of 2005, 2009 and 2010; remaining data of 2012 and 2014 were used for validation. The results of calibration and validation are given in Table 3.4.

The calibration and validation at UR obtained satisfactory results with NSE and R^2 values of 0.64 and 0.69 during calibration and 0.54 and 0.58 during validation. The PBIAS value of 0.18 and RSR value of 0.61 was under satisfactory range. The uncertainty measures show a significant decrease on daily scale during calibration and validation with p-factor of 0.58, r-factor of 0.62 during calibration and p-factor of 0.57, r-factor of 0.45 during validation. At GKTE site, calibration was performed using 1991-1992 discharge data and validation was done for 1994. The

NSE and R^2 values of 0.62 and 0.71 were obtained during calibration. For the validation period, the NSE and R^2 values were 0.60 and 0.75, respectively. The PBIAS was 18 and 11.8 during calibration and validation. The RSR was 0.61 and 0.63 during calibration and validation, respectively. The p-factor at GKTE was better during validation (0.64) than during calibration (0.61). The r-factor was significantly improved from 0.57 during calibration to 0.95 during the validation period. The statistics show that the model performance is satisfactory in simulating daily flows for the Umiam watershed.

Upon successful calibration, the uncertainties in model prediction is mapped to model parameters using SUFI-2 (Atkinson et al. 2010). The model parameter ranges in both the scenarios are kept exactly the same which implies that similar uncertainty ranges must exist in both the scenarios. The calibrated model was used to simulate streamflow under two scenarios: (1) with reservoir present and (2) without the reservoir. The simulation without the reservoir represents the natural flow that would have existed, had there been no reservoir in Umiam. This gives the baseline streamflow to compare any changes in streamflow due to the reservoir.

CHAPTER 4

Impacts of Inter-Basin Water Transfer Reservoir on Streamflow

4.1 Introduction

Augmentation of flow has been practiced since early civilizations for the benefit of mankind (McCully 1996). However, it is becoming a matter of concern as more and more dams are constructed and the rivers are exploited. At the same time, we cannot deny the role of dams in shaping the developmental needs of society. A reservoir constructed for one purpose may aid in reducing floods downstream, while it may also cause flash floods due to the sudden release of water. As such, it is necessary to develop natural and altered flow scenarios quantitatively to assess the impact of such structures on streamflow. The scenario analysis of natural and altered flow becomes more challenging when the observed streamflow data before dam construction are not available. Obtaining past streamflow data is often extremely hard, particularly in developing countries. Therefore, a methodological framework is proposed in this paper to generate natural streamflow and to carry out the analysis of the changes in the flow regime due to the reservoir. The proposed methodology is applied to Umiam watershed located in the data-scarce yet ecological hotspot region in north-east India (Khan et al. 1997). The perturbations in streamflow due to the presence of the reservoir were quantified using the Indicators of Hydrological Alteration (IHA) (Richter et al. 1997). The north-eastern region of India, with its perennial rivers, has a huge potential for hydropower generation. Due to the richness in water resources, numerous

dams have been constructed in many of its rivers, and many more are planned (Saikia 2012). Although dams may provide benefits for the development of the region, there are apprehensions among the people due to the changes brought about by dams in terms of loss of fisheries, ecology, agriculture, and displacement (Sharma 2018). While it is found in many studies that dams can alter the natural flow of a river (Lajoie et al. 2007; Ouyang et al. 2011; Zhang et al. 2017), to the best of the authors knowledge, there has been no research done to quantify the effects of dams in northeast India.

To analyze the hydrological changes that can be brought about due to man-made structures, an in-depth scientific analysis is required. A study conducted by Brunner *et al*. 2019 in Switzerland found that the reservoirs and natural lakes helped to reduce summer water shortage at the catchment scale. The effect of cascading reservoirs in the Wujiang watershed was studied by Wu et al. (2018) using 60 years of observed flow and sediment data. They reported no significant change in runoff while the sediment discharge reduced. Lu *et al.* (2014) studied the impacts of dam operations in the Mekong River. They found lowered discharge in the dry seasons due to damming, and in the wet seasons, the discharge was marginally lower in the post-dam period. A study on changes in streamflow characteristics due to flood retarding structures using the SWAT model was put forward by Van Liew (2003). The flood retarding structures was found to reduce the annual maximum daily discharges. The studies in the area of hydrological alterations are mostly regional and require site-specific data (Arthington et al. 2006). In the remote northeast region of India, the scarcity of data is a major issue faced in hydrological studies. Thus, the objective of this study is to devise a methodological framework to assess hydrological alterations due to reservoir and water diversion under a lack of pre-impact data. The second objective is to quantify the hydrological alterations in the Umiam watershed in Meghalaya, India, using the Indicators of Hydrologic Alteration(IHA) method (Richter et al. 1996).

4.2 **Study Area**

The Umiam River, located in Meghalaya, India (Figure 4.1), is of great significance as it serves as an important source of water for hydropower generation. It flows from Sohiong region in Meghalaya and joins the Kapili River in Assam, which empties into the Brahmaputra River. The flow length of the mainstream of Umiam River is 118 km and covers an area of 1410.27 Km^2. The elevation ranges from 1723 m above the mean sea level (MSL) in the upper reach to 60 m above MSL at the watershed outlet. Compared to the high elevation Shillong region with annual precipitation of 2140.3 mm, the downstream plains in the Assam region receive annual precipitation of 1709.5 mm (Das et al. 2015). The mean maximum temperature in Umiam is 24.81°C, and the mean minimum temperature is 15.75°C (Choudhury et al. 2012). The Umiam Reservoir was built across the Umiam River to divert water for hydropower generation. The reservoir became operational in 1965 and had a storage capacity of 185 million cubic meters. The water from Umiam river is being stored and diverted for power generation to another watershed drained by Umtru River through a headrace tunnel, with a design capacity of 28.12 m^3/s. The cascade of reservoirs comprising of Umiam Reservoir, Kyrdemkulai Reservoir, Nongmahir Reservoir, Umiam Stage-4 Reservoir and New Umtru Hydropower project together produce about 196 MW of electricity. The Umiam Stage-1 power station located at Sumer village generates electricity from the diverted water from the Umiam Reservoir. The Stage-2 power house uses the tailwater of Stage-1 power house to generate electricity. The tailwater from the Stage-2 then joins Umtru River and flows to Kyrdemkulai Reservoir and continues to flow through the cascade of reservoirs shown in Figure 4.1.

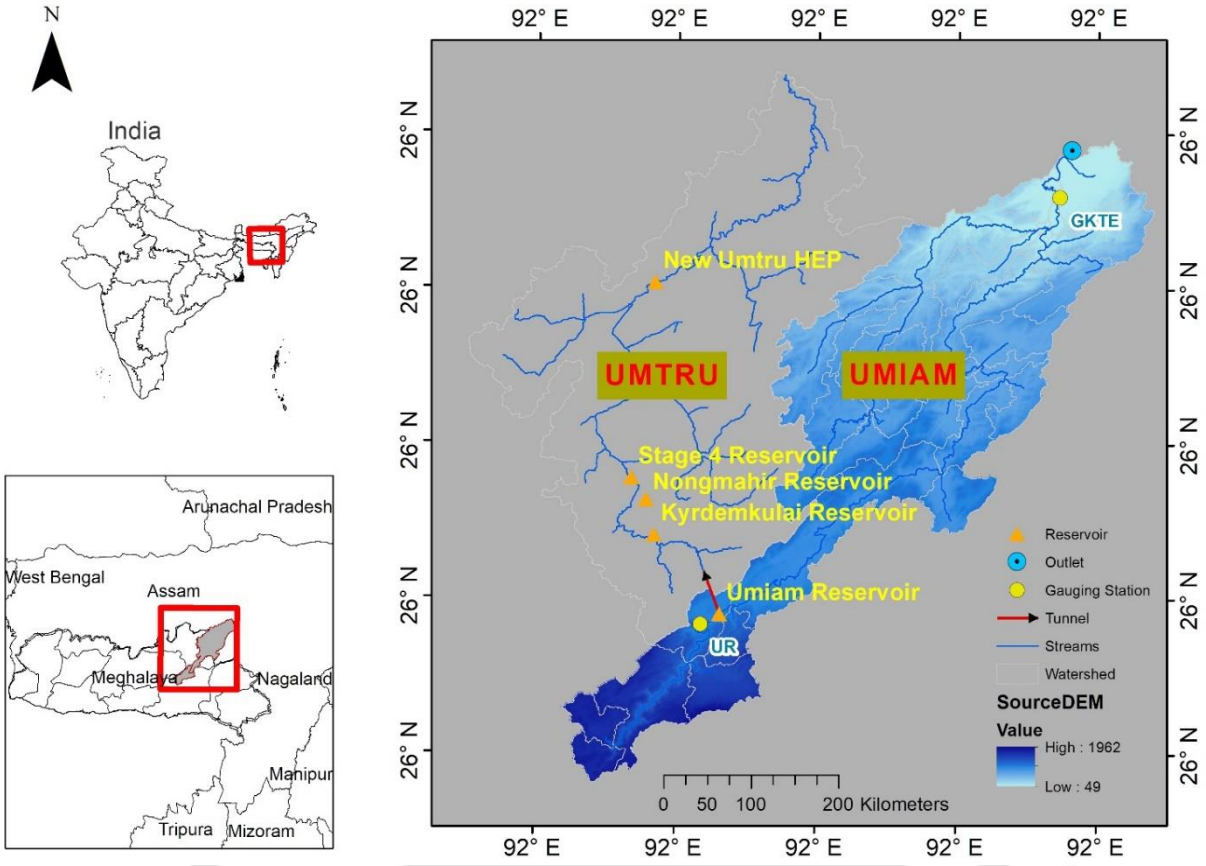

Figure 4.1 Map of the study area.

4.3 **Hydrological Modeling**

The calibrated and validated SWAT model discussed in Chapter 3 of this thesis was used in the assessment done in this chapter.

4.3.1 Simulation of the natural flow

Assessment of changes in streamflow due to damming requires flow data of the pre-dam period. However, in this study, since the pre-dam condition data were not available, we calibrated the SWAT model under the present condition i.e. considering the dam. It is to be noted that the term natural flow in this paper means the streamflow under the present LULC without the reservoir. The calibrated model has parameters that govern the streamflow (CN2, GWQMN, OV_N, etc.) and reservoir parameters (RES_ESA, RES_EVOL, RES_PSA, RES_PVOL, WURESN, RES_K.res, etc.). When the model performance was satisfactory in simulating flow under the

present conditions, the reservoir component in the calibrated model was deactivated to simulate the natural flow. Deactivation of the reservoir can be done by editing the .res file in SWAT output folder. This can be achieved by setting the beginning year of operation of the reservoir (IYRES) to greater than the end of the simulation year or by setting the reservoir attributes such as RES_ESA, RES_EVOL, etc., and water transfer (WURESN) to zeros. Deactivating the reservoir only affects the reservoir parameters without affecting the streamflow parameters. The calibrated model was run after deactivating the reservoir to simulate the natural flow.

4.4 **Assessment of Hydrological Alteration**

The changes in the hydrological regime due to the reservoir are examined using the Indicators of Hydrologic Alteration (IHA) software (The Nature Conservancy 2009). 32 IHA parameters divided into 5 groups of IHA parameters (Richter et al. 1996) were used in this study (Table 4.1). The IHA software applies the RVA (Range of Variability Approach) to IHA parameter values and quantifies the extent of alteration (Richter et al. 1997). The pre-impact natural range of IHA parameter values is considered as the reference for defining the extent of alteration of flow.

In this study, the non-parametric RVA analysis is carried out in which the full range of pre-impact (natural flow) data is divided into three categories: (1) The values less than or equal to the 33rd percentile (lowest category), (2) The values falling between the 34^{th} to 67^{th} percentiles (middle category), and (3) The values greater than the 67^{th} percentile (highest category). More details of the significance of each IHA parameters can be found in Richter *et al.* (1996).

Table 4.1 Indicators of hydrologic alteration (The Nature Conservancy 2009)

IHA statistics group	**Regime characteristics**	**Hydrologic parameters**
1. Magnitude of monthly water conditions	Magnitude Timing	Mean or median value for each calendar month
2. Magnitude and duration of annual extreme water conditions	Magnitude Duration	1-day mean Annual minima, 3-day means Annual minima, 7-day means Annual minima, 30-day means Annual minima, 90-day means Annual maxima, 1-day mean Annual maxima, 3-day means Annual maxima, 7-day means Annual maxima, 30-day means Annual maxima, 90-day means Number of zero-flow days[a] Base flow index: 7-day minimum flow/mean flow for year
3. Timing of annual extreme water conditions	Timing	Julian date of each annual 1-day maximum Julian date of each annual 1-day minimum
4. Frequency and duration of high and low pulse	Frequency Duration	Number of low pulses within each water year Mean or median duration of low pulses (days) Number of high pulses within each water year Mean or median duration of high pulses (days)
5. Rate and frequency of water condition changes	Rates of change Frequency	Rise rates: Mean or median of all positive differences between consecutive daily values Fall rates: Mean or median of all negative differences between consecutive daily values Number of hydrologic reversals

[a]This parameter is not used in this study.

Each IHA is examined based on median value, degree of deviation, and degree of hydrologic alteration. The degree of deviation (Xue et al. 2017) of an IHA is calculated using (4.1) as:

$$P_i = \frac{M_e - M_o}{M_o} \times 100 \quad (4.1)$$

where M_e and M_o are the median values for natural and altered flows respectively. The positive or negative values of P_i indicates the increment or decrement of the median value under the two scenarios. The degree of non-attainment of the RVA target is measured as the hydrologic alteration in terms of percentage (Richter et al. 1998) and is calculated as:

$$D_i = \frac{Observed - Expected}{Expected} \times 100 \quad (4.2)$$

where 'observed' is the number of years in which the observed value of the hydrologic parameter was within the RVA target range of 25th to 75th percentile and 'Expected' is the number of years for which the value is expected to be within the targeted range. According to Richter et al. (1998), $D_i \leq 33\%$ represents little or no alteration, $33\% < D_i < 67\%$ represents moderate alteration and $D_i > 67\%$ represents a high degree of alteration.

The overall degree of hydrological alteration (ODHA) can be quantified by the average degree of hydrological alteration given by Equation 4.3 (Richter et al. 1998).

$$D = \frac{1}{N}\sum_{k=1}^{N} D_k \quad (4.3)$$

where, D is the overall degree of alteration of flow regime, and N is the number of hydrologic indicators. However, Equation(4.3 tends to underestimate an indicator having a high degree of alteration when most of the indicators have low or moderate degrees of alteration. Therefore, Xue

et al. (2017) proposed an equation for an improved overall degree of hydrologic alteration (IODHA) calculated as:

$$D = \sqrt{\left(\frac{D_{jmax}^2 + D_w^2}{2}\right)} \quad (4.4)$$

where, D_{jmax} is the maximum and D_w is the average values of degree of hydrologic alterations for each group of indicators. The improved overall degree of hydrologic alterations is classified into 5 categories as: slight alteration (D < 20%), low alteration (20 ≤ D ≤ 40%), moderate alteration (40 ≤ D ≤ 60%) high alteration (60 ≤ D ≤80%) and severe alteration (D > 80%) (Xue et al. 2017).

4.5 **Results and Discussion**

4.5.1 Changes in the magnitude of monthly flows

The daily flows were simulated with the calibrated SWAT model under two settings, i.e. with reservoir and without reservoir to represent the altered and natural flow. The model was calibrated under present condition (with dam) which represented the altered flow. Based on the calibrated model the natural flow was simulated by deactivating the reservoir. Therefore, parameter ranges governing streamflow were based on the calibrated model on both the scenarios. The reservoir module was disabled to run the simulation for natural flow. The daily flows were analysed using the IHA software based on monthly median flows. For analysis, the point of change, i.e. the year 1965 from which the reservoir became operational is taken as the starting point for both scenarios.

The monthly median flows (Figure 4.2) during the 1965-2015 simulations show reduced flows in the presence of the reservoir. As a result, the RVA targets were achieved in the months of June, March, and April only. This reduction can be attributed to the water impounded in the reservoir and the diversion to the power station. The monthly IHA values are given in Table 4.2. The magnitude of decrease in flow was highest in December (18.64 m^3/s in natural to 12.6 m^3/s in

altered flow). The degree of deviation (P) was negative in all the months indicating a decrease in monthly median flows. The degree of hydrological alteration (D) was found to be moderate (33% <D<67%) in 3 months (December,January,October) while the other 9 months were within the low alteration category.

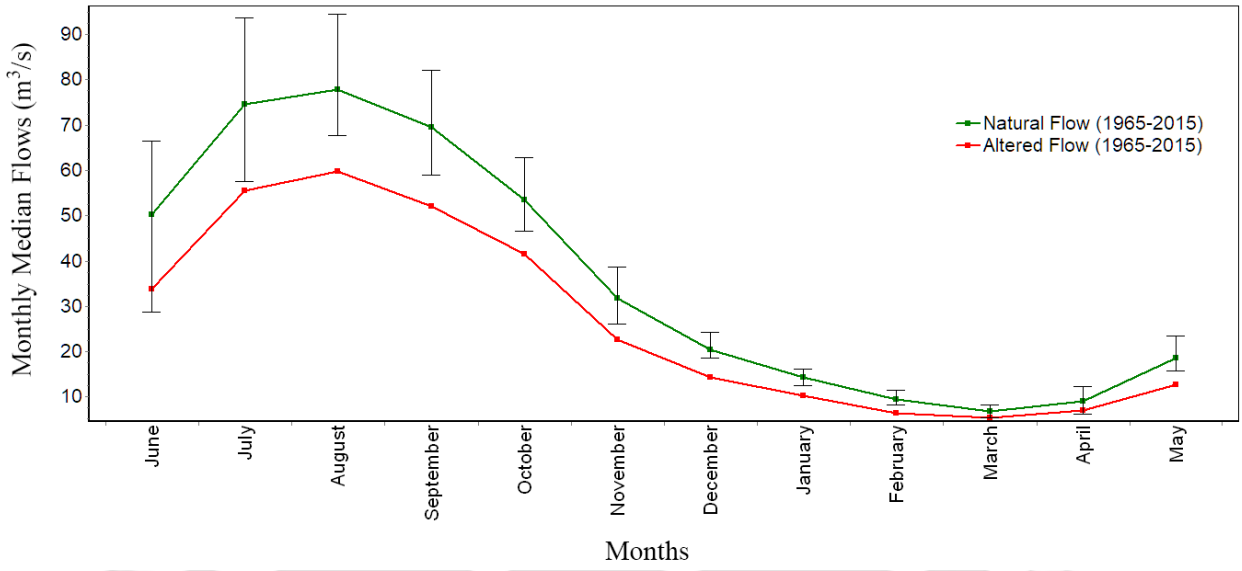

Figure 4.2 Monthly median flows. The vertical lines denote the RVA targets.

4.5.2 Daily flows and hydrologic extremes

The changes in daily flows under natural flow and altered flow conditions is shown in Figure 4.3. It can be observed that the presence of the reservoir has led to a reduction in the number of large floods (10-year return period flow) and small floods (2-year return period flow). Large floods are found to occur more frequently under natural flow scenario as seen in Figure 4.3. The large hydrographs peaks occur in years 1966, 1978, 1988, 1991; whereas with the reservoir present, the large peaks occur in 1966 and 1978 only. However, in recent years, i.e. 2006 to 2015, there are more frequent low flows in the presence of the reservoir than in natural flow. This may be due to rainfall variability and non-release of water to downstream during drought periods. Thus, the

presence of the reservoir may be beneficial in reducing floods in the downstream areas but also

Table 4.2 Hydrologic alterations of group-1 parameters under two flow conditions

Indicators	Natural flow	Altered flow	Degree of deviation	Degree of hydrologic alteration
Parameter Group 1	**Medians**	**Medians**	**P (%)**	**D (%)**
January	50.43	34.74	-31.11	-34.62 (M)
February	77.50	56.41	-27.22	-32.14 (L)
March	77.81	60.65	-22.05	-7.69 (L)
April	69.63	52.70	-24.32	20.83 (L)
May	53.58	41.94	-21.72	-10.53 (L)
June	31.88	22.80	-28.51	22.22 (L)
July	20.48	14.28	-30.27	-8.70 (L)
August	14.11	9.70	-31.25	-4.55 (L)
September	9.30	6.39	-31.35	-19.23 (L)
October	6.76	5.23	-22.69	-40.00 (M)
November	8.97	6.74	-24.86	-32.00 (L)
December	18.64	12.60	-32.38	-38.46 (M)

Note: L = Low, M = Medium and H = High

may reduce streamflow in drought years, which may disturb the health of the downstream ecosystem.

The flow duration curve (FDC) was constructed from daily flow simulations under natural and altered flow conditions (Figure 4.4). An FDC illustrates the percentage of time that a given flow was equal to or exceeded in a given period (Vogel and Fennessey 1994). The probability of

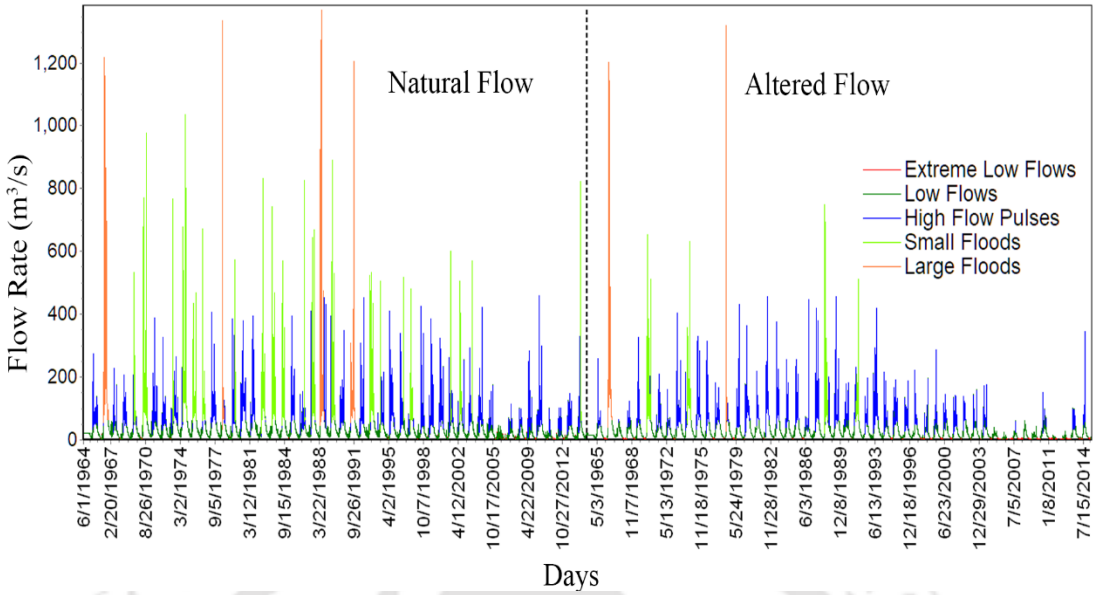

Figure 4.3 Daily flows showing environmental flow components under natural and altered flow conditions in Umiam Watershed.

exceedance is calculated by sorting the daily flows and ranking them with the largest value being ranked as 1. The exceedance probability is then computed as P = 100 * [M / (n + 1)], where, P is the probability that a given flow will be equaled or exceeded (as percentage of time), M is the ranked position on the list, n is the number of events for the period of record.

The high flow rate corresponding to 0.5% exceedance probability was 1368 m^3/s for simulated natural flow, whereas for altered flow, the corresponding flow rate was 1318 m^3/s, indicating a decrease of 3.65 %. At 10% exceedance probability, the flow rates were 98.9 m^3/s and 77.6 m^3/s under natural and altered flow scenarios, respectively (21.5% decrease). At 50% exceedance probability, the flow rates for natural and altered flow were 25.5 m^3/s and 17.2 m^3/s (32.5% decrease).

4.5.3 Hydrological alteration of extreme conditions

The hydrologic alterations for annual extreme flow conditions under group-2 IHA parameters are given in Table 4.3. The 1-day minimum flow was decreased by 16.5 % due to flow alterations by

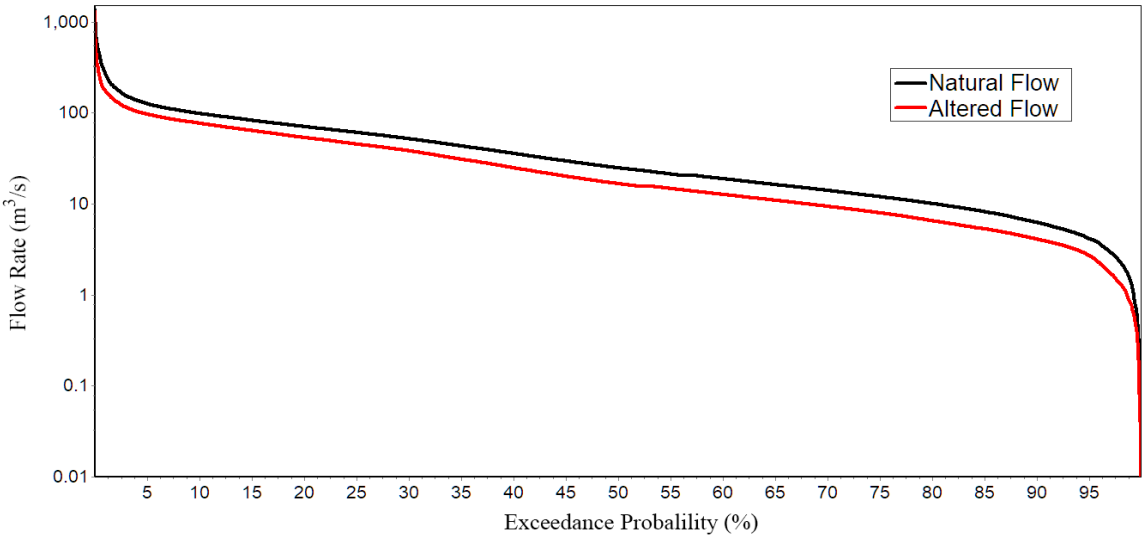

Figure 4.4 Flow duration curve.

the reservoir (Figure 4.5a). The degree of hydrological alteration was still low at 3.85%. However, the 1-day maximum flows (Figure 4.5b) showed decrement by 54% with medium hydrologic alteration (38.5%). A delay of 9 days occurred in 1-day maximum whereas a delay in 1-day minimum was only 1 day. The highest alteration among group-2 and group-3 parameters was observed in 3-day maximum (D=61.54%), whereas the lowest alterations were for 3-day minimum and base flow. In a study by Yang et al. (2012), the 1-day 3-day, 7-day, 30-day and 90 day minimum and maximum flows were found to be lowered due to Sanmenxia Dam. Here, the negative alterations were shown by 9 parameters i.e. the RVA targets were not achieved and the positive alterations were found only in 2 parameters which are, 1-day minimum and date of maximum.

4.5.4 Hydrologic alteration of high and low pulses

Table 8 lists the medians, degree of deviation, and the degree of hydrologic alteration of group 4 and 5 IHA parameters. The low pulse count (D = -87.5%), as well as its duration (D = -81.82%), exhibit a high degree of alteration (Table 8). The alterations to high pulse count (D = -6.67%) and high pulse duration (D = -30.77) were under low category. These findings are similar to Shiau

Table 4.3 Hydrologic alterations of group-2 and 3 parameters under two flow conditions

Indicators	Natural flow	Altered flow	Degree of deviation	Degree of hydrologic alteration
Parameter Group 2	**Medians**	**Medians**	**P (%)**	**D(%)**
1-day minimum	4.13	3.45	-16.53	3.85 (L)
3-day minimum	4.51	3.52	-21.91	0.00 (L)
7-day minimum	5.11	3.65	-28.51	-3.85 (L)
30-day minimum	6.67	4.75	-28.72	-7.69 (L)
90-day minimum	9.53	6.09	-36.08	-11.54 (L)
1-day maximum	474.02	217.36	-54.15	-38.46 (M)
3-day maximum	268.36	144.25	-46.25	-61.54 (M)
7-day maximum	179.44	112.70	-37.19	-53.85 (M)
30-day maximum	114.68	81.50	-28.94	-38.46 (M)
90-day maximum	88.49	65.78	-25.66	-38.46 (M)
Number of zero-days	-	-	-	-
Base flow index	0.00294	0.00344	16.83	0.00 (L)
Parameter Group 3				
Date of minimum	99.00	100.50	1.52	-18.52 (L)
Date of maximum	199.50	208.50	4.51	15.38 (L)

Note: L = Low, M = Medium and H = High

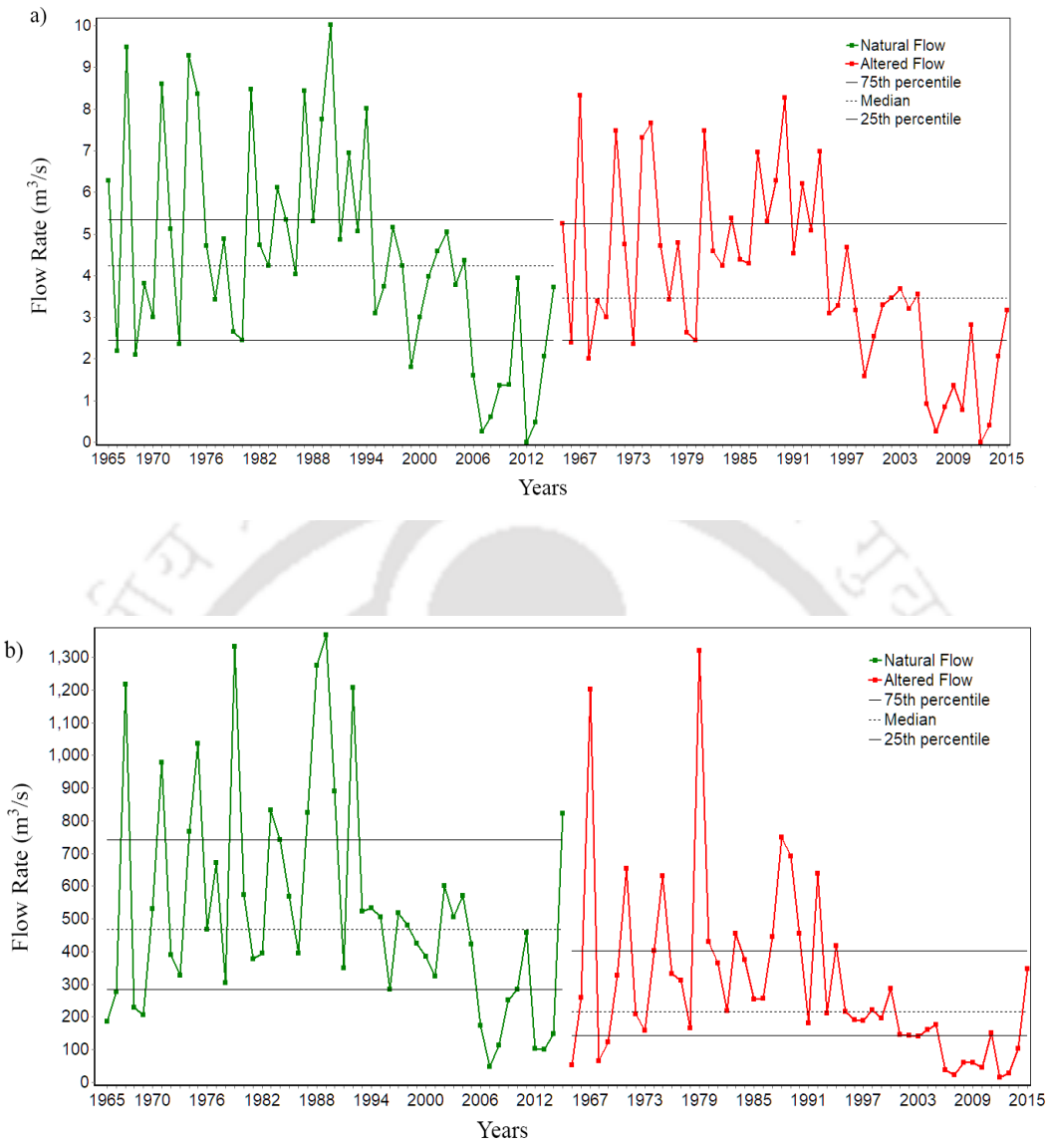

Figure 4.5 Plot of (a) 1-day minimum flow and (b) 1-day maximum flow.

and Wu (2004). They reported that flow diversion can greatly affect the low regime more than the high flow regime. While the decrease in low pulse count in Umiam River may be beneficial for the riverine ecosystem, the increased duration in low pulses and reduction in duration of high pulses may be unfavourable to the aquatic life and also affect bedload transport.

4.5.5 Hydrologic alteration of rate and frequency of flow conditions change

The parameters in group 5 listed in Table 4.4 gives a measure of the number and median rate of positive and negative changes in flow regime from one day to the next. They are a measure of

magnitude and frequency of intra-annual flow changes. The negative degree of deviation in the rising rate (Figure 4.6a), fall rate (Figure 4.6b), and the number of reversals (Figure 4.7) indicate a reduction in their values due to the reservoir. The highest alteration in group 5 parameters is observed in the number of reversals (-96.3) followed by the rise rate (-92.31) and fall rate (-46.15). All the parameters in group 5 did not fall in the expected flow range. The number of reversals was found to be the most altered parameter in a similar study conducted by Pfeiffer and Ionita (2017) in Elbe and Rhine Rivers in Germany. Gao et al. (2018) in their study on the effects of reservoir operations in Yangtze River reported a decrease in rise rate and increase in the number of reversals. They found that the number of reversals was higher in the steep terrains due to the flashy nature of the river. In this study, the contribution of hilly areas with higher rainfall variability was cut off by the reservoir which may be the reason for such a dramatic decrease in the number of reversals.

Table 4.4 Hydrologic alterations of group-4 and 5 parameters under two flow conditions

Indicators	**Natural flow**	**Altered flow**	**Degree of deviation**	**Degree of hydrologic alteration**
Parameter Group 4	**Medians**	**Medians**	**P (%)**	**D(%)**
Low pulse count	9.00	3.00	-66.67	-87.50 (H)
Low pulse duration	3.00	20.00	566.67	-81.82 (H)
High pulse count	8.00	6.00	-25.00	-6.67 (L)
High pulse duration	1.50	2.00	33.33	-30.77 (L)
Parameter Group 5				
Rise rate	151.70	58.27	-61.59	-92.31 (H)
Fall rate	-32.84	-17.22	-47.56	-46.15 (M)
Number of reversals	153.00	96.00	-37.25	-96.30 (H)

Note: L = Low, M = Medium and H = High

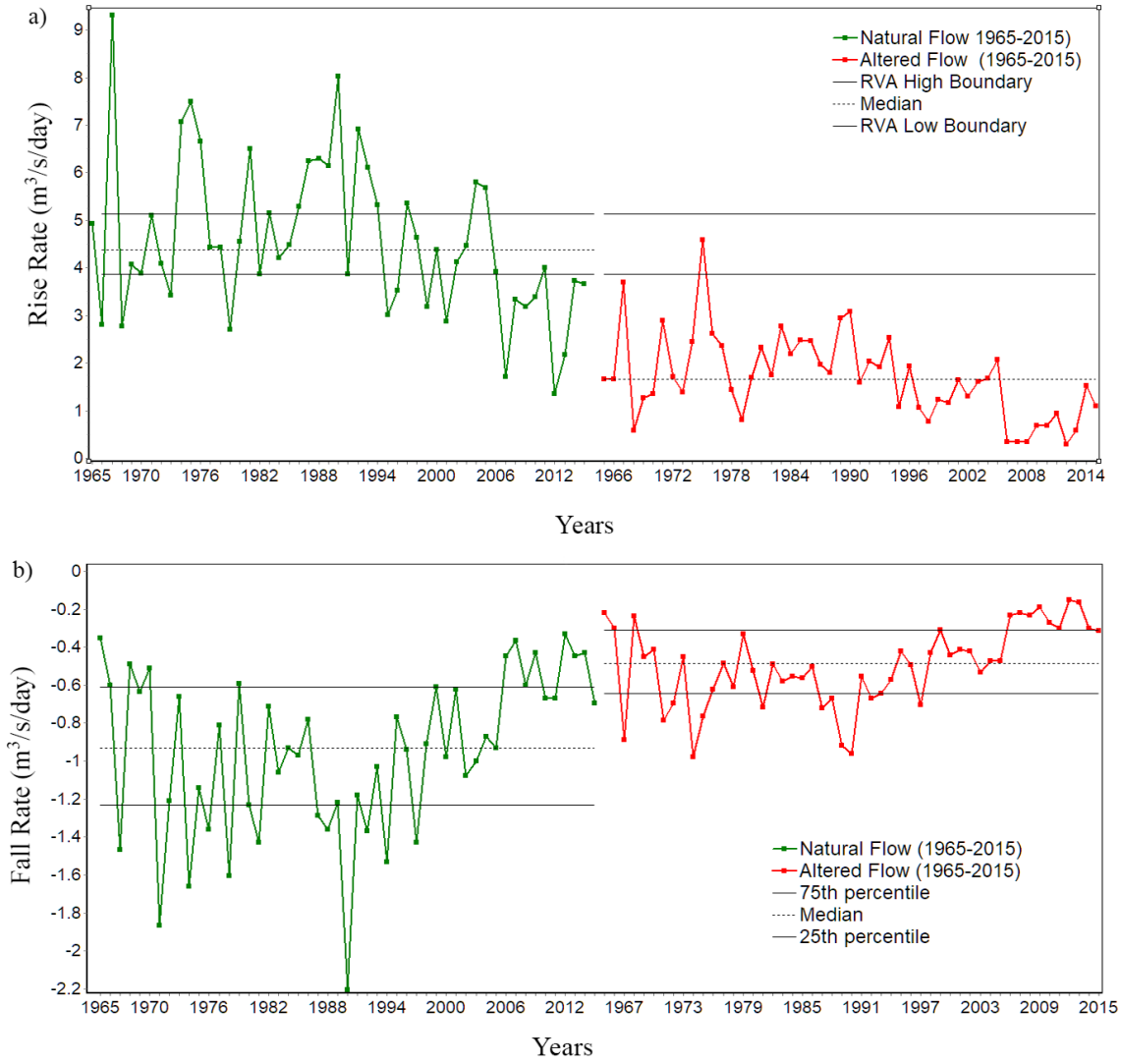

Figure 4.6 (a) Rise rate and (b) Fall rate.

4.5.6 The overall degree of hydrological alteration

The degree of hydrologic alteration for each group of indicators as well as the overall degree of hydrologic alterations (ODHA) is calculated using(4.3 and improved the overall degree of hydrologic alterations calculated using (4.4. (Figure 4.8). The IODHA quantifies the overall degree of hydrologic alteration in Umiam watershed as highly altered whereas, ODHA quantifies it as a low alteration. These differences in quantification may be due to the limitation of Eq. 9 which was reported by Xue *et al.* (2017) that it tends to underestimate some groups with a high

degree of alteration when there are a greater number of groups showing low or medium alterations.

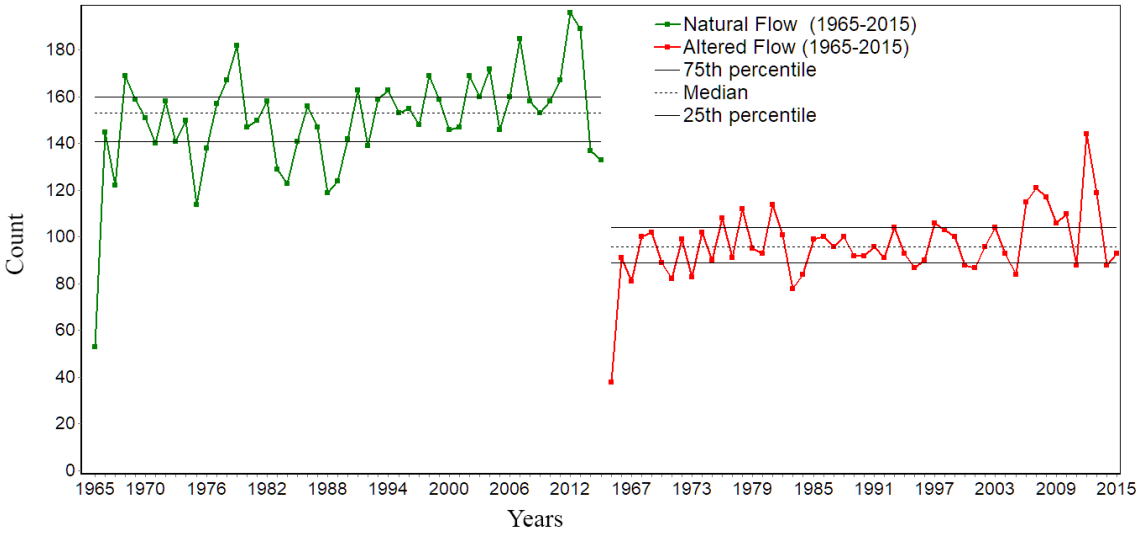

Figure 4.7 Number of reversals.

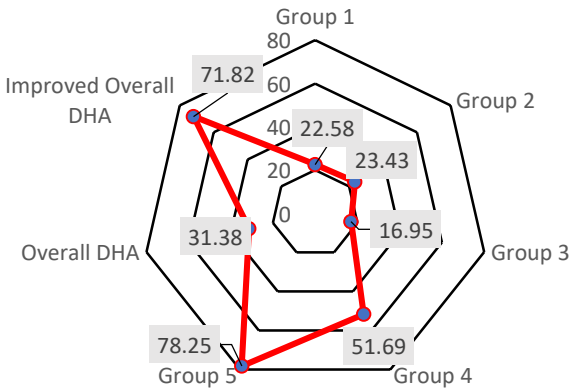

Figure 4.8 Hydrologic alteration for 5 groups calculated using (4.2. Overall DHA was calculated using (4.3 and improved overall DHA was calculated using (4.4.

4.6 **Conclusions**

This study has sought to quantify the hydrologic alterations in a river due to reservoir storage and water diversion. It is important to understand the direct human influence on the flow regime for

the maintenance of ecohydrological balance, but oftentimes, researchers face the problem of data scarcity for assessment of hydrological changes. This study attempted to address this problem by introducing a method for hindcasting streamflow in the absence of flow records before the alteration took place. Reconstruction of natural streamflow was achieved using the SWAT model and applied the methodological framework to Umiam watershed with a water transfer. The widely used IHA analysis was carried out after simulations of natural and altered flow for five decades. The analysis shows that monthly flows have decreased significantly at the downstream. The reservoir reduces the magnitude of high flows and thus acts as flood cushion even though its actual purpose was to generate electricity by diverting water. The hydrologic alterations in hydrologic extremes show low to medium alteration, whereas the hydrological pulses and rate and frequency of flow conditions show high alterations. The reservoir may reduce high flows in the wet months and reduce flood risk, but the prolonged duration of low pulses in dry months may have a negative effect on aquatic habitat. The analysis found an overall alteration of 71.82%, which is high. The findings of this study may be helpful in reservoir operations considering environmental flow requirements and the methodological framework may be followed in data scarce regions. The limitation of this study is that only direct human-induced stress on streamflow was considered. The assessment was done based on hydrological model simulations and is subject to uncertainties inherent in the model and input data. Future studies may include the effect of climate change and reservoir optimization in streamflow alteration.

CHAPTER 5

Effects of Inter-Basin Water Transfer and Cascading Reservoirs on Streamflow of Recipient Watershed

5.1 Introduction

The effects of inter-basin water transfer (IBWT) on streamflow of a donor watershed has been presented in the previous chapter. This chapter focuses on the effects of IBWT on the recipient watershed. IBWT is a common practice all over the world for solving problems arising due to water deficit. But while IBWT may be beneficial for solving human water demands, it can also lead to socio-ecological implications (Sinha et al. 2020). For instance, a study conducted by Tien Bui et al., (2020) found that the IBWT from Zab River could increase the discharge of Gadar River by three times and rise the water level by up to 1 metre from the normal levels. China's ambitious South-to-North Water Transfer Project to transfer water from Yangtze River Basin to the water deficit north and northwest regions of China also faces several criticism as it can lead to environmental impacts such as water shortage and saltwater intrusion (Zhuang 2016).

In the present study, the water from Umiam Basin is diverted to Umtru Basin for hydropower generation. The diversion point is located at Umiam Reservoir (Umiam Stage-I) and the diverted water is used to run the turbines that generate electricity. Along the downstream four more cascading reservoirs are constructed which are, Kyrdemkulai Reservoir, Nongmahir Reservoir, Umiam Stage-IV Reservoir and Umtru Reservoir. The New Umtru Reservoir which was operational from July 2017 is not considered in this analysis due to lack of data.

5.2 Study Area

The Umiam and Umtru Basins are spread over East Khasi Hills and Ri-Bhoi Districts of Meghalaya, India. The two watersheds share their boundaries and drains to Kapili river in the

neighbouring state of Assam. The Umiam Basin (donor basin) has an area of 1410.27 Km^2 and the Umtru Basin (recipient basin) has an area of 1553.75 Km^2 (Figure 5.1). The average annual rainfall in the area is around 1951 mm. The Umtru Basin has Nongkhyllem Wildlife Sanctuary which is known to be the best protected wildlife sanctuaries in North East India.

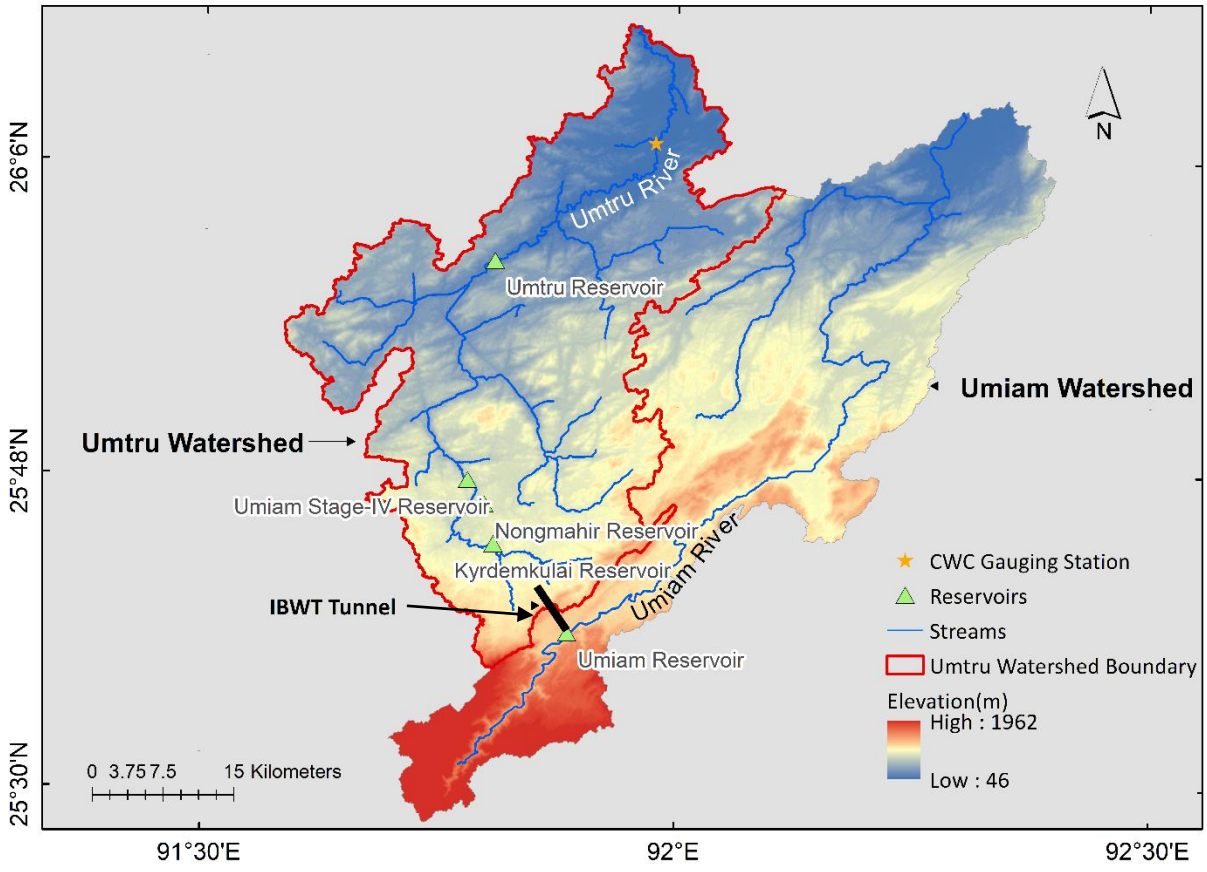

Figure 5.1 Study Area

5.3 **Hydrological Model Set-Up**

The Umtru Watershed was delineated using the SRTM (Shuttle Radar Topographic Mission) 30 metre resolution. Watershed delineation resulted in forty-nine (49) sub-basins. Land use and land cover (LULC) data of National Remote Sensing Centre (NRSC) was used in this study. The landuse types were reclassified into 8 classes according to SWAT LULC database as shown in **Error! Reference source not found.** LULC types in Umtru Basin

The soil data was extracted for Umtru Watershed from Harmonized World Soil Database (HWSD) which is a global scale dataset available free of cost. The gridded precipitation data of 0.25° X 0.25° latitude by longitude, from the Indian Meteorological Department (IMD) (Pai et al. 2015) was used for running SWAT. This dataset is prepared from observed rainfall data at IMD stations and is available for all regions of India from 1901 to 2015. The gridded temperature data of 0.25° X 0.25° resolution (Sheffield et al. 2006) was obtained from http://hydrology.princeton.edu/home.php website. Other weather parameters like solar radiation, wind speed, and relative humidity were generated using inbuilt weather generator in SWAT due to lack of available data.

The reservoir data were obtained from Meghalaya Energy Corporation Limited (MeECL). The required inputs such as reservoir surface area when the reservoir is filled to the normal operating level and emergency level etc. were fed to SWAT reservoir module for each reservoir. The diverted water from Umiam Reservoir which becomes an inflow to the Umtru Watershed was available from the year 1990 to 2015. This data was fed to the SWAT model as “Point Source” inflow on daily scale.

5.4 **Calibration and validation**

The model calibration was carried out using the SUFI-2 algorithm in SWAT-CUP program. The SUFI-2, takes account of the uncertainties arising due to input data, conceptual assumptions, model parameters are mapped to the parameters and the algorithm aims to attain smallest parameter uncertainty (ranges). The parameter uncertainty is quantified by the 95% prediction

uncertainty (95PPU). More details about the SUFI-2 algorithm can be found in Abbaspour (2015a).

The calibration was done on daily scale and the observed daily discharge data from Central Water Commission (CWC) gauging station at Sonapur was used for calibration and validation. The calibration period is from 01-01-1990 to 31-12-2007 and validation period is from 01-01-2008 to 31-12-2015.

5.5 Effect of Cascading Reservoirs

The effect of cascading reservoirs was analysed using the IHA Software under the scenarios as given below.

- **Individual dams scenario**: Under this scenario, the effect of each reservoir is analysed by considering each reservoir separately during simulation. The streamflow before and after the existence of reservoir were compared using the IHA Software.

Table 5.1 Reservoir details

Reservoir Name	**Full Reservoir Volume (Million cubic meters)**	**Pre-Impact**	**Post-impact**
Kyrdemkulai Reservoir	6.17	1953-1979	1980-2015
Nongmahir Reservoir	8.32	1953-1979	1980-2015
Umiam Stage-IV Reservoir	1.81	1953-1993	1994-2015
Umtru Reservoir	3.98	1953-1957	1958-2015

- **All dams scenario** : Under this scenario the stream flow was first simulated for unaltered condition which does not consider inter-basin water transfer (IBWT) from the Umiam Dam and the dams in Umtru Watershed which is the current watershed under consideration. The second simulation was done by considering IBWT from the Umiam Watershed and all the dams in Umtru Watershed in operational condition. The comparison of these two scenarios were done using the IHA software to give an insight into how much the IBWT and cascading reservoirs have an effect on flow.

Thirdly, in order to assess how much impact would have occurred only due to IBWT from the Umiam Watershed, the flow was simulated by considering only the IBWT and ignoring the cascade of reservoirs in Umtru Watershed.

5.6 **Results and Discussion**

There were 15 parameters considered for calibration and the most sensitive parameters were GW_DELAY, RCHRG_DP, GWQMN, CN2, REVAPMN and ESCO. The results of calibration and validation are presented in Figure 5.2 and Figure 5.3. The calibration obtained R^2 value of 0.72, NSE value of 0.71, p-bias of 6.3, p-factor and r-factor of 0.76 and 0.83 respectively. Similarly, the model performance was satisfactory during validation period as well. The validation obtained R^2 , NSE, p-bias, p-factor, and r-factor of 0.65, 0.58, 18.2, 0.62 and 0.74 respectively Table 5.2.

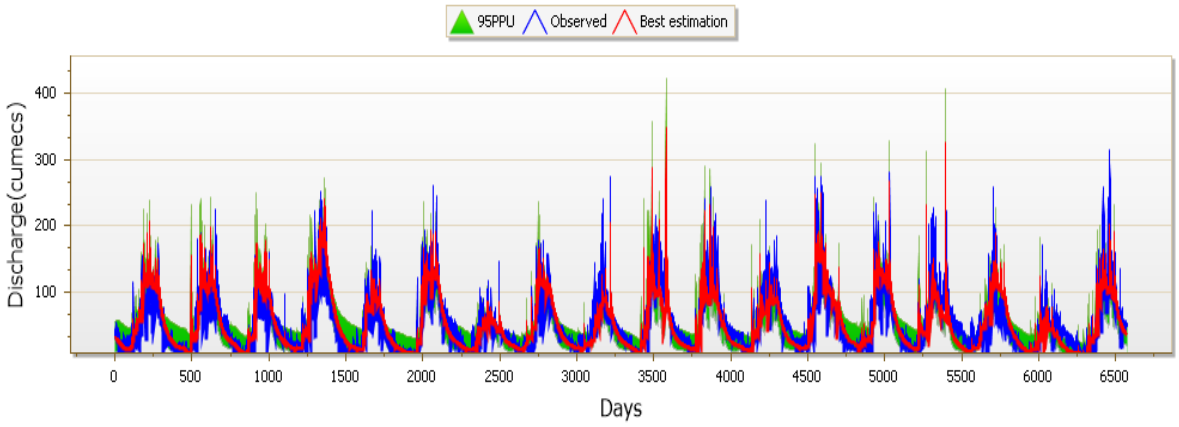

Figure 5.2 Calibration of SWAT model for Umtru Basin

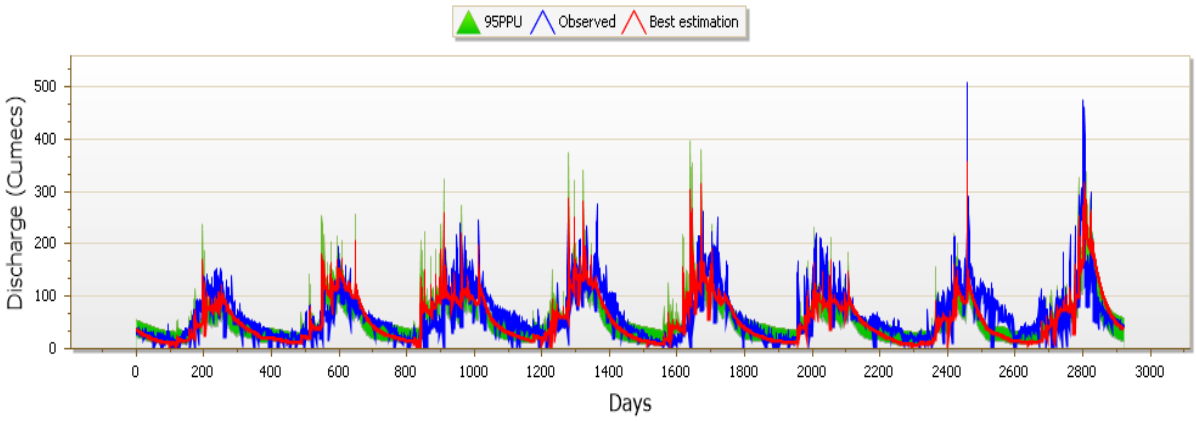

Figure 5.3 Validation of SWAT model for Umtru Basin

Table 5.2 Calibration and Validation Results for Umtru SWAT Model

	Gauging site	Model Performance on daily time scale					
		R^2	NSE	P-Bias	RSR	p-factor	r-factor
Calibration	CWC Gauge site Sonapur (1990-2007)	0.72	0.71	6.3	0.54	0.76	0.83
Validatio	CWC Gauge site Sonapur (2008-2015)	0.65	0.58	18.2	0.65	0.62	0.74

5.6.1 Effect of Kyrdemkulai Reservoir

The individual effect of Kyrdemkulai Reservoir was analyzed by comparing the streamflows before and after it came into operation. The effect on monthly flows are shown in Figure 5.4. The monthly flows are found to increase in all the months due to IBWT and reservoir. The highest discharge occurs in the month of July under Pre (1953-1979) and Post Impact (1980-2015) conditions. It is seen that the stream flow during lean period also increased. The lowest monthly average flow during pre-impact occurred in December with a mean value of 0.355 m^3/s whereas for post impact period the corresponding flow rate was 6.63 m^3/s. The maximum monthly flow rate for pre-impact period was 31.1 m^3/s for the month of September. On the other hand, the maximum flow had increased to 56.44 m^3/s during post-impact period for the same month.

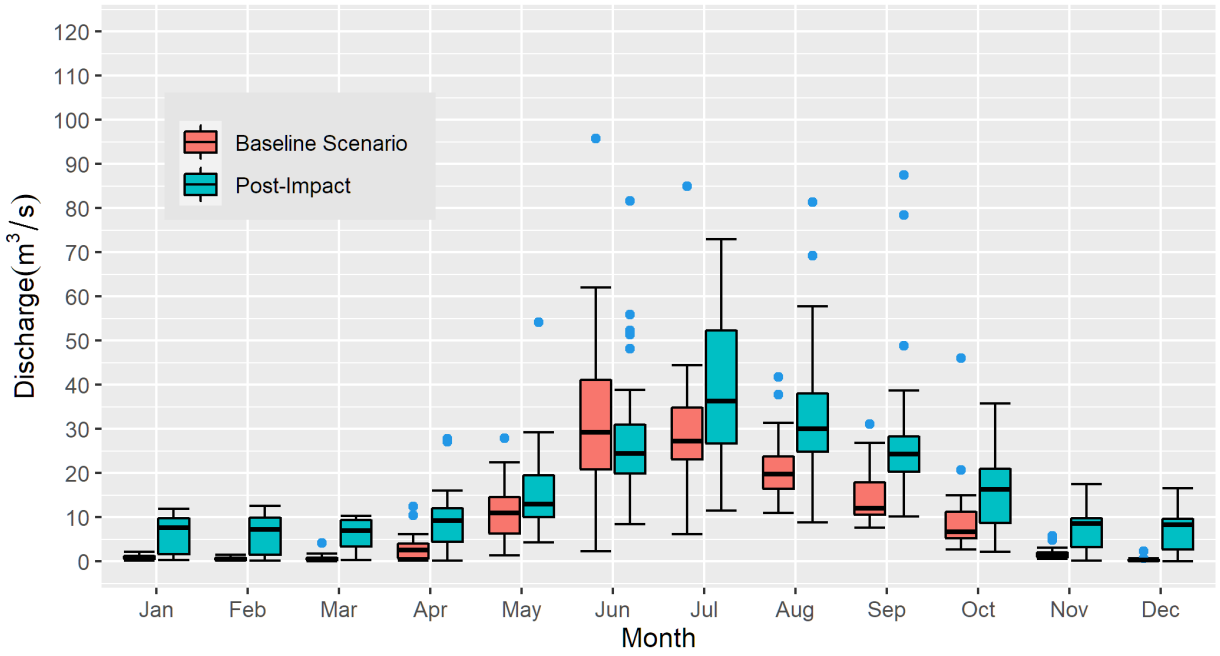

Figure 5.4 Effect of Kyrdemkulai Reservoir on monthly flows

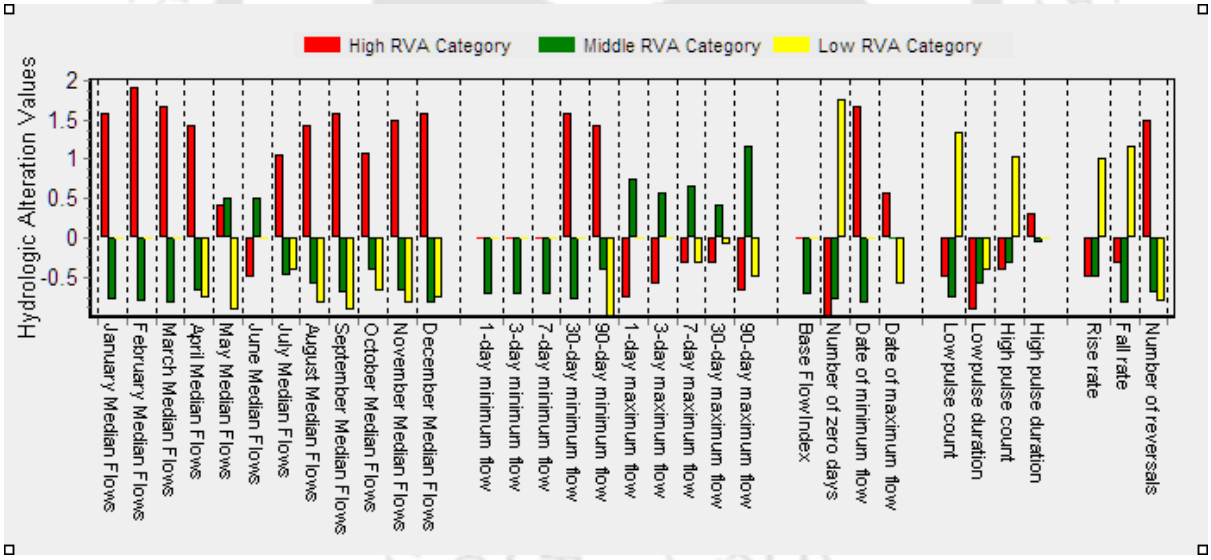

Figure 5.5 Hydrological Alteration due to Kyrdemkulai Reservoir

The hydrological alteration (HA) in High (greater than 67th percentile), Middle (34th to 67th percentiles) and Low (less than 33rd percentile) and the RVA categories are presented in Figure 5.5. The highest streamflow changes are in High RVA category. The positive changes indicate increased value during post impact period. Positive HA for low RVA category was seen in number of zero days, low pulse count, rise rate and number of reversals were increased.

5.6.2 Effect of Nongmahir Reservoir

Figure 5.6 represents the monthly flows when the Nongmahir Reservoir is in operating condition. Monthly flows are higher during the post impact period except for the month of June where the peak flow decreased from 95.79 m^3/s to 85.39 m^3/s. The maximum flow occurred in July with the flow rate of 162 m^3/s and 218 m^3/s for pre (1953-1979) and post-impact (1980-2015) period. The hydrologic alteration due to Nongmahir Reservoir is presented in Figure 5.7. The HA is positive in monthly flows for high RVA category except June where it is slightly negative. Positive HA is seen in Low RVA category for low pulse count, high pulse count, rise rate and fall rate.

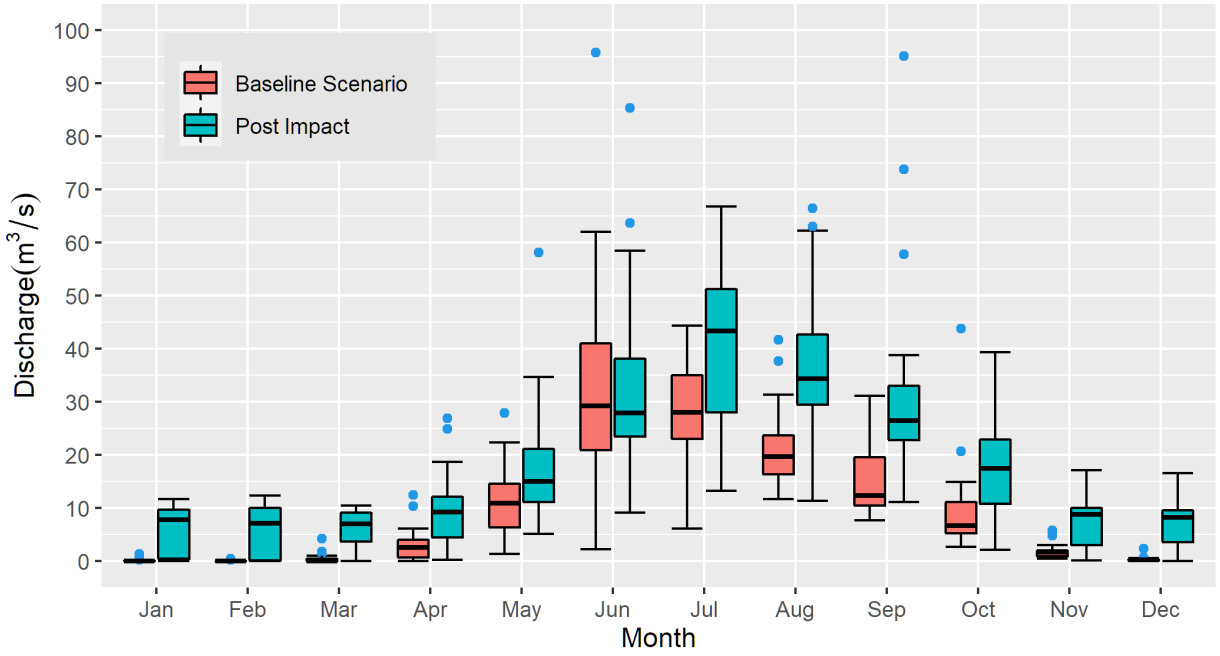

Figure 5.6 Effect of Nongmahir Reservoir on monthly flows

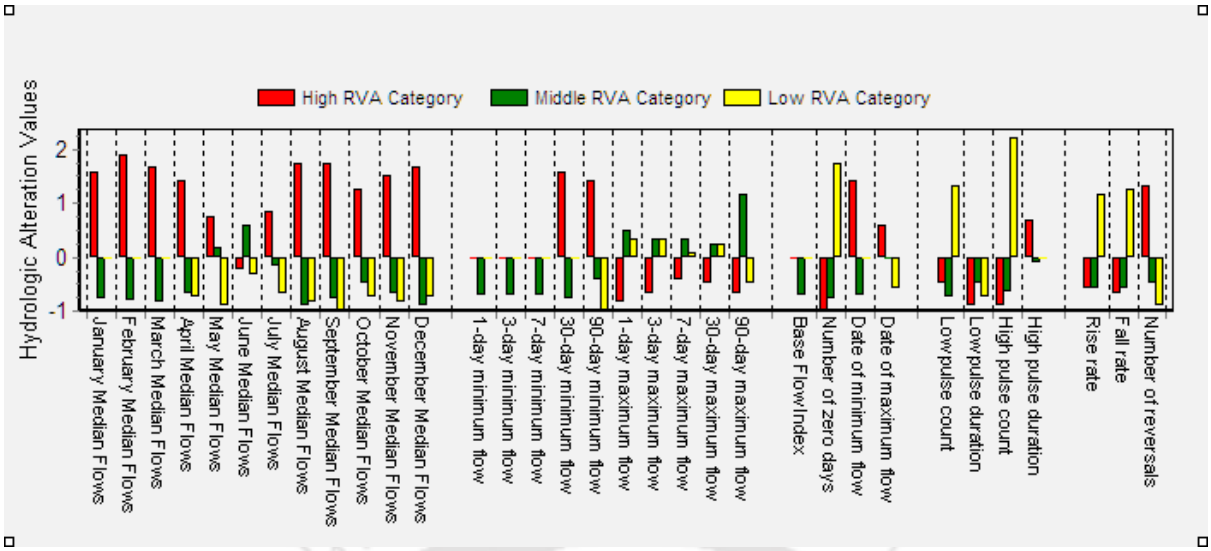

Figure 5.7 Hydrological Alteration due to Nongmahir Reservoir

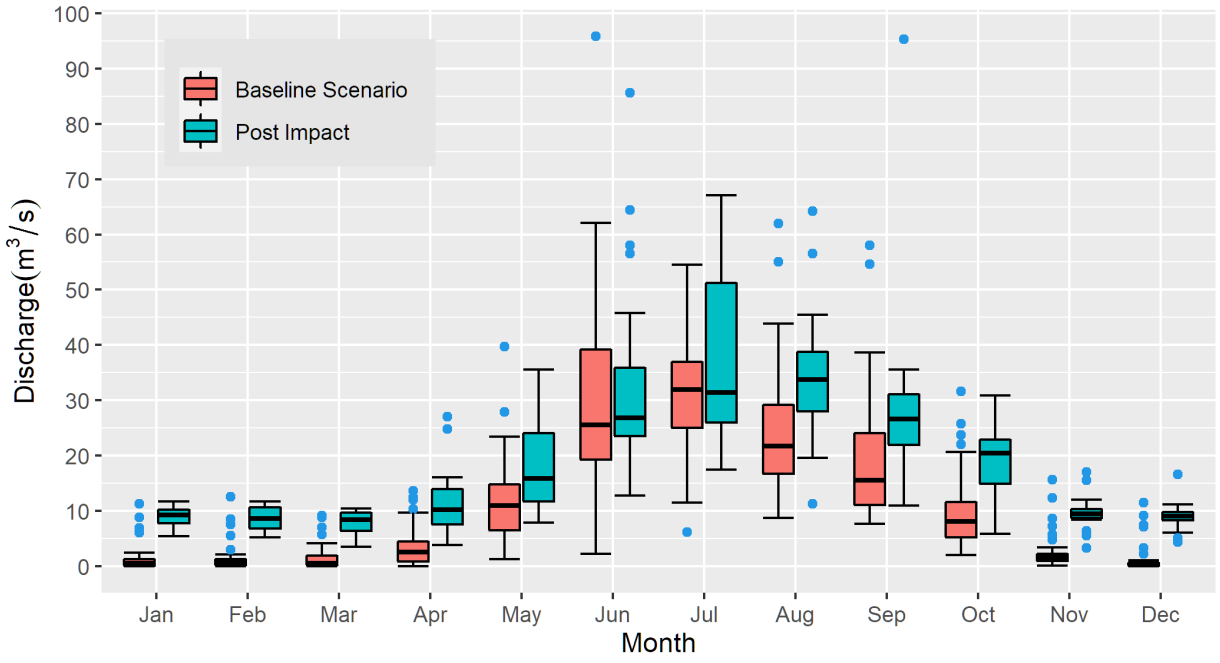

Figure 5.8 Effect of Stage-IV Reservoir on monthly flows

5.6.3 Effect of Stage-IV Reservoir

The effect of Stage-IV Reservoir on monthly flows is shown in Figure 5.8. The highest flow for pre-impact period (1953-1993) is 58.04 m^3/s, while for post-impact period (1994-2015) it is 95.24 m^3/s. It can be seen that flow magnitude increased in the winter months from November to March. The mean flow rate in January increased from 1.4232 m^3/s to 8.908 m^3/s. There was not much variation in median values of discharge for the month of June (Pre-Impact = 25.6 m^3/s and Post-

Impact = 26.85 m^3/s) and July (Pre-Impact = 31.9 m^3/s and Post-Impact = 31.45 m^3/s) but there was a lot of variation in maximum flows as seen in Figure 5.8. The highest hydrological alteration values are seen in 1-day, 3-day, 7-day minimum flow and baseflow index (Figure 5.9) in the high RVA category while there is negative alteration in middle RVA category.

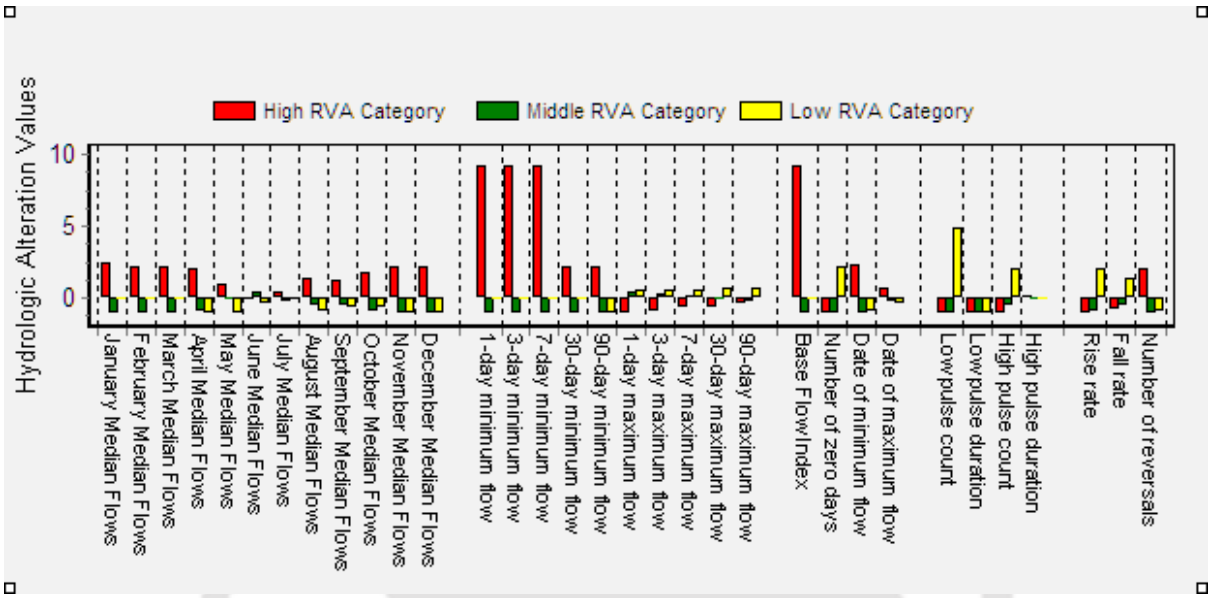

Figure 5.9 Hydrological Alteration due to Stage-IV Reservoir

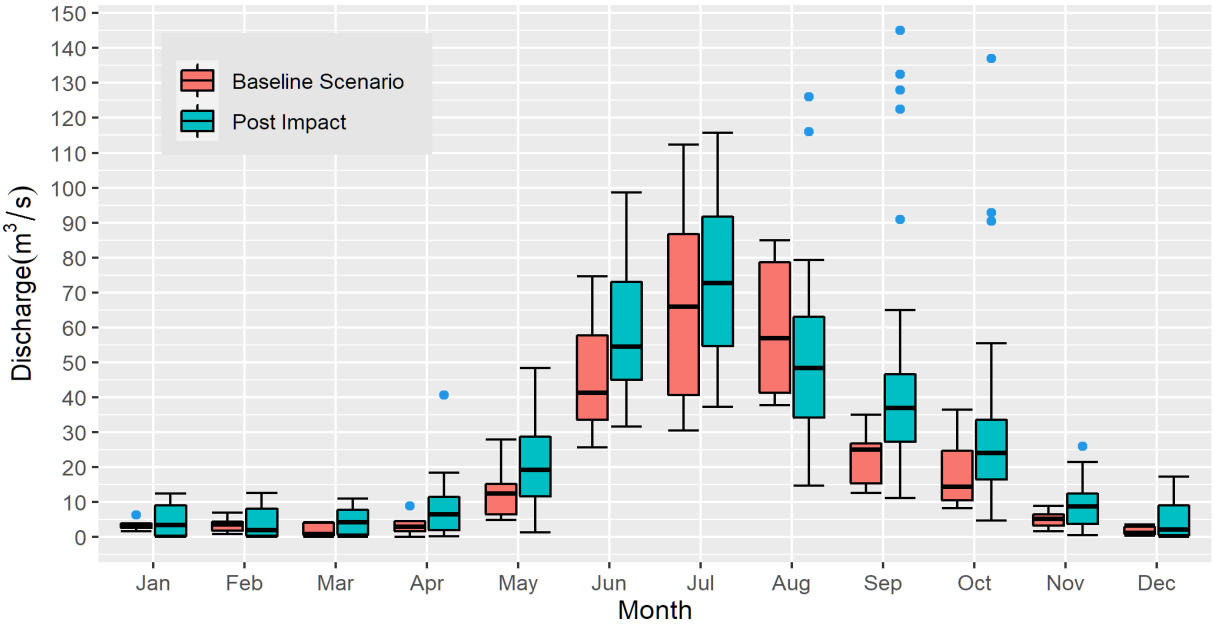

Figure 5.10 Effect of Umtru Reservoir on monthly flows

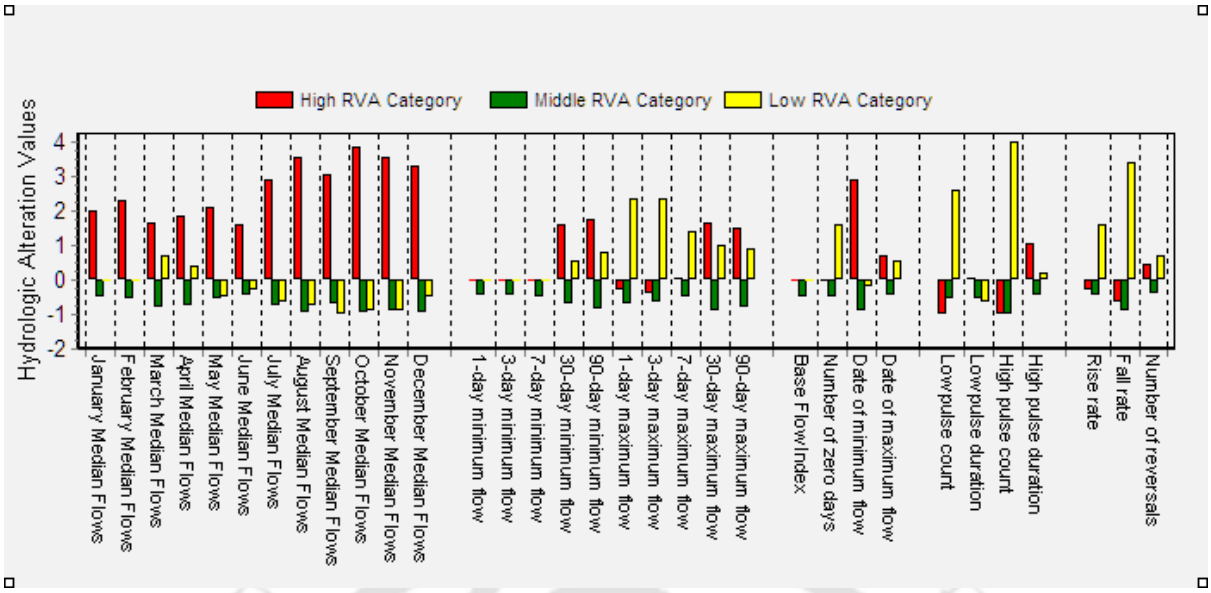

Figure 5.11 Hydrological Alteration due to Umtru Reservoir

5.6.1 Effect of Umtru Reservoir

The effect of Umtru Reservoir was analyzed considering 1953-1957 as pre-impact period and 1958-2015 as post impact period. Similar to the other scenarios, the highest flow rate is reached in the month of July. The median flow rate of pre-impact in July is 65.87 m^3/s while for post impact period it is 72.64 m^3/s. The highest difference in maximum flow rate occurs in September where the maximum pre-impact discharge was 35 m^3/s and post-impact discharge was 145 m^3/s. The overall increase in discharge may be due to the larger drainage area covered by Umtru Reservoir as compared to the other reservoirs discussed above which are located upstream.

The high RVA category in monthly flows shows positive hydrologic alteration as the monthly flows increased in magnitude due to IBWT and Umtru Reservoir (Figure 5.11). Negative hydrologic alteration is seen in middle RVA category for monthly flows and minimum and maximum flows.

5.6.2 Effect of all dams

The effect of all dams and IBWT was analyzed by comparing the SWAT simulation under different scenarios. In the first scenario (All Dams), all the reservoirs are considered to be active including the water transfer from the Umiam Reservoir and thus represents the present condition. The second scenario (IBWT-No dams) considers IBWT from the Umiam Dam but do not consider any dams in the Umtru Watershed. It is to be noted that IBWT from Umiam Dam is considered as inflow series from outside of the watershed and Umiam Dam is not depicted in the current Umtru model. The third scenario (No IBWT-No Dams) does not consider IBWT as well as dams, thus representing unaltered flow. All three scenarios were simulated from 1990 to 2015.

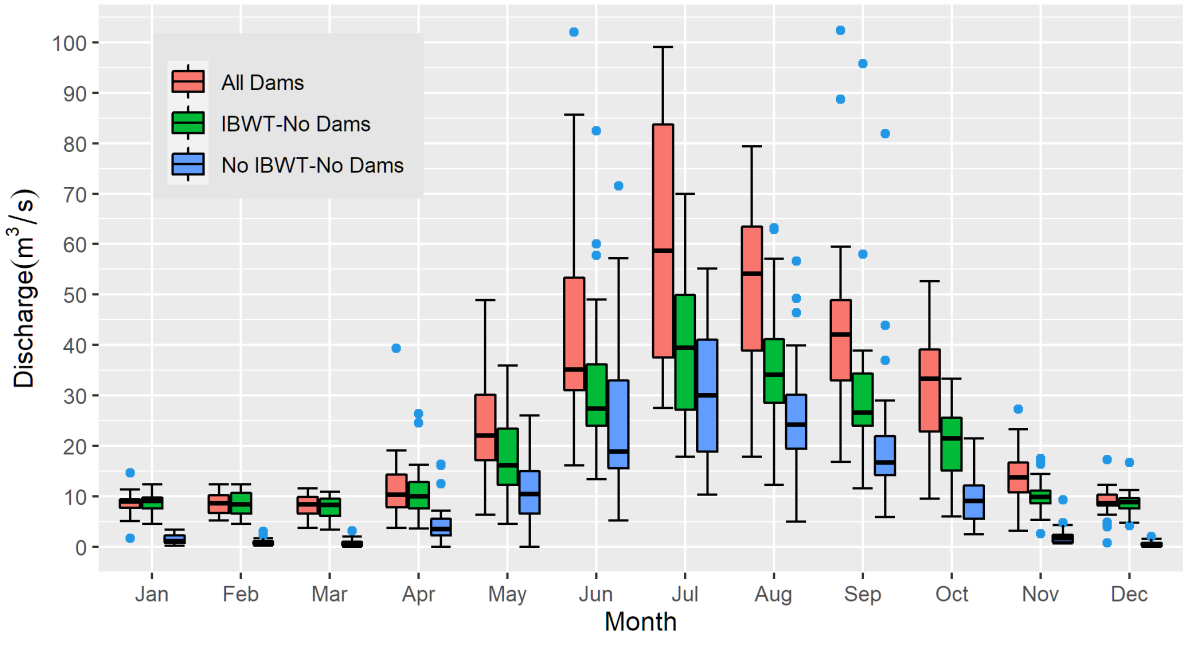

Figure 5.12 Effect of cascading reservoirs under different scenarios

The monthly flows under the three scenarios described above are shown in Figure 5.12. The median of discharges for the month of January differed only by 0.12 m^3/s when All dams scenario (8.979 m^3/s) and IBWT-No dams scenarios (9.099 m^3/s) were compared while No IBWT-No Dams scenario had median value of 1.23 m^3/s. Similarly, for the month of February to April the difference in median flow rates between the first two scenarios does not reach 1 m^3/s. The variation in flow increases from May onwards. Highest median flow occurs in July which are 58.69 m^3/s for All dams, 39.49 m^3/s for IBWT-No dams and 30.02 m^3/s for No IBWT-No Dams scenario. The higher discharge in case of All dams scenario may be due to the storage of water in the reservoir.

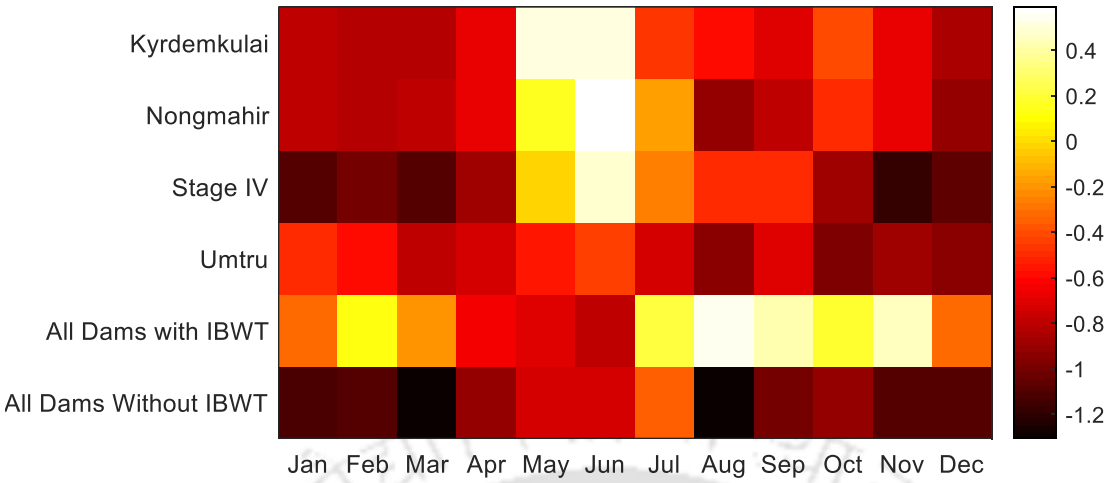

Figure 5.13 Hydrological alteration for different scenarios

Figure 5.13 shows the hydrological alterations on monthly flows calculated by IHA software. The positive alterations ranging from 0.2 to 0.4 are seen in case of Kyrdemkulai, Nongmahir and Umiam Stage IV reservoir that occurs in May and June. When all the reservoirs are considered (All Dams with IBWT) and compared with No IBWT-No Dams scenario, the positive alterations are seen in February and from July to November.

When No IBWT-No Dams was compared with All Dams without IBWT, negative alterations were highest in the month of March and August. Thus, having IBWT is beneficial in maintaining higher flow rate in the Umtru River.

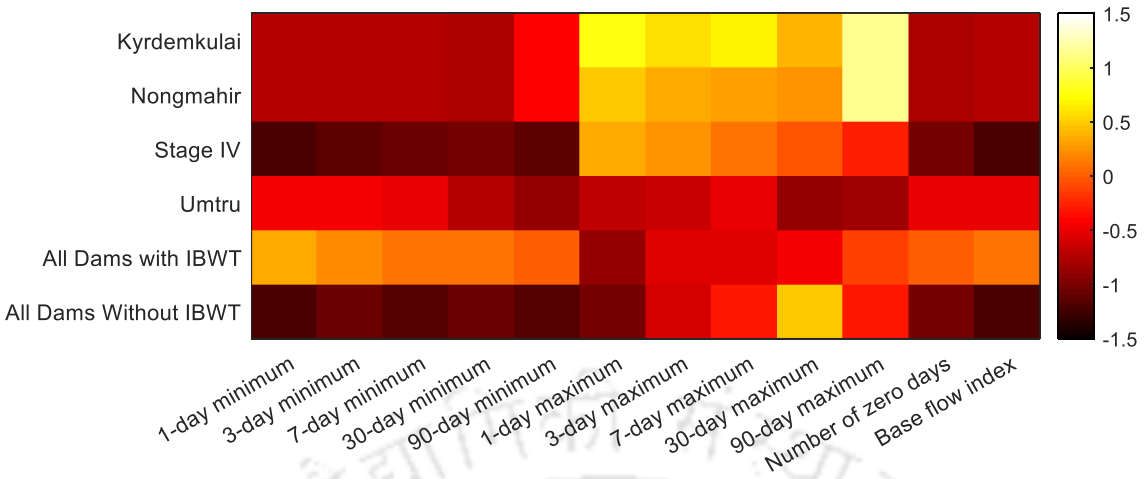

Figure 5.14 Hydrological alteration of magnitude and duration of annual extreme water conditions

The parameters related to magnitude and duration of annual extreme water conditions has significant role in structuring of river channel morphology and physical habitat conditions (Figure 5.14). The analysis revealed positive change due to Kyrdemkulai and Nongmahir dam for 1-day, 3-day, 7-day, 30-day and 90-day maximum flow. Stage IV reservoir shows negative alterations in 7 out of 12 parameters. When All Dams with IBWT is considered, the 1-day, 3-day, 7-day, 30-day and 90-day minimum flows show positive alteration ranging from 0 to 0.5. Whereas, maximum flows show negative alteration. When all dams are considered without IBWT, the hydrological alteration tends towards negativity for the minimum flows but shows positive alteration for 30-day maximum flow.

The effect of individual and cumulative effects of all reservoirs under different scenarios are presented in Figure 5.15. It is observed that Umtru Reservoir has the highest influence on yearly median flows with change percentage of 106.8%. The next highest effect is when all dams are operated without IBWT which can change yearly median flows by 95%. The effect is lowest when all dams are operating with the IBWT in place (38.49%).

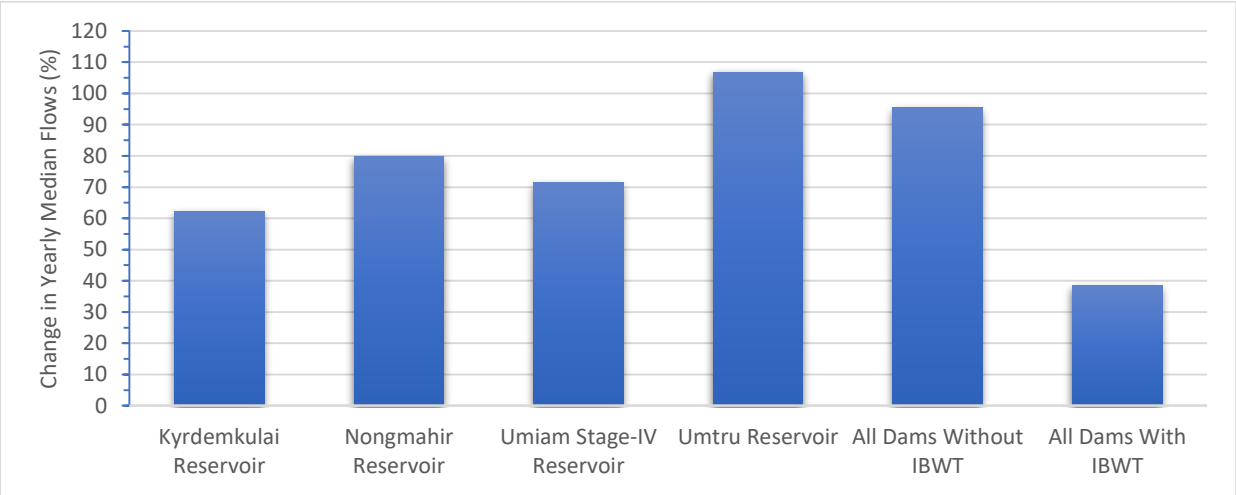

Figure 5.15 Individual and cumulative effects of reservoirs under different scenarios

5.7 **Conclusions**

The effect of individual reservoirs and IBWT was analysed in this chapter. The analysis revealed increase in monthly flows due to Kyrdemkulai, Nongmahir, Umiam Stage IV and Umtru Reservoirs. The individual effect of Umtru Reservoir was found to be highest among the four. The second highest effect was due to Nongmahir Reservoir. The cumulative effect of all reservoirs could increase the yearly median flows by 38.49% as compared to unaltered flow without IBWT and reservoirs. The change in yearly median flows were 95.43% in Umtru Basin if no water was transferred from Umiam Basin. There was increase in 1-day, 3-day, 7-day, 30-day and 90-day maximum flow due to Kyrdemkulai and Nongmahir dams.

CHAPTER 6

Trend Analysis of Spatial and Temporal Rainfall Variations

6.1 Introduction

According to the IPCC (2018), climate change in the latter half of the 21st century will have a significant impact on human lives, assets and ecosystems from extreme weather events such as heat waves, extreme precipitation, drought and associated wildfires, and coastal flooding. Among these calamities, floods and droughts are the most damaging natural phenomenon that causes loss of life, degrades the economy, nature, and property worldwide. With the consistent rise in the level of greenhouse gases, the downwelling infrared radiation gets enhanced, resulting in increased global mean temperatures. It has been observed that global mean temperatures have been increasing since the pre-industrial period and 2015-2019 recorded the warmest period since records began in 1850 (World Meteorology Organization 2019). The rise in temperature enhances evaporation and increases the moisture holding capacity of the air by 7% per 1°C rise in temperature (Trenberth 2011). Increase in atmospheric moisture can cause more intense precipitation and increases the risks of floods. For instance, Lutz et al., (2014) projected an increase in runoff over upper Ganges, Brahmaputra, Salween, Indus, and Mekong basins in Asia due to increased precipitation and ice melt. Recent analysis of rainfall trends on a global scale show an increase in the frequency of extreme events in many parts of the world (Myhre et al. 2019; Papalexiou and Montanari 2019). Increasing heavy rainfall events have been associated with increased flood occurrences in India in the past few decades (Singh and Kumar 2013). Arnell, (2004) observed that the increase in runoff due to climate change generally takes place during the high flow season and thus increase the risk of flooding. Since climate change can induce changes in the extreme meteorological events rather than the averages, the risk of droughts in addition to floods is also a major concern (Mishra and Singh 2010). In contrast to floods, all climatic zones irrespective of rainfall patterns can experience drought characterised by the

reduction in the amount of precipitation received over an extended period of time which can range from a season, a year to even a decade (Bond et al. 2008). The global increase in trends of floods and droughts have been linked to the changes in precipitation trends (Le Comte 1998; Mishra and Singh 2010; Nyaupane et al. 2018; Papalexiou and Montanari 2019). For these reasons, it is imperative to understand and identify the trends in precipitation for proper management and decision making with regards to the efficient use of water resources.

The importance of trend analysis of rainfall can be seen from the increasing number of studies all over the world (Alemu and Bawoke 2019; Caloiero et al. 2017; Rustum et al. 2017; Sonali and Nagesh Kumar 2013; Wang et al. 2020). Despite the developments in studies concerning the climatology in other parts of the world, studies on a local scale are still very limited in the North East Region (NER) of India. The NER covers an area of 0.26 million km^2 and consists of the states of Assam, Arunachal Pradesh, Manipur, Meghalaya, Mizoram, Nagaland, Sikkim, and Tripura. NER contains the northern most limit of the tropical rainforest in the world (Proctor et al. 1998) and is a major biodiversity hotspot of India (Pradhan et al. 2019). The analysis of rainfall trends is of particular importance to the Meghalaya State as it receives the heaviest rainfall in the world (Murata et al. 2007) but is also making a headway towards an increasing number of droughts (Ravindranath *et al.*, 2011). The increasing trend in droughts in the NER was also reported in another study by Sharma and Goyal (2020). Yaduvanshi et al. (2019) studied the effect of 1.5 °C and 2°C increase in global temperature compared to the pre-industrial level for all Indian states using Coupled Model Intercomparison Project 5 (CMIP5) models under the Representative Concentration Pathway (RCP) 4.5 scenario. They found that states receiving high rainfall, such as Nagaland and Meghalaya, have a more significant change in rainfall under RCP 4.5. Naidu et al., (2009) reported weakening of the Southern Oscillation and relaxation of the meridional temperature gradient over the Indian Ocean and linked it to the declining trends in summer monsoon rainfall in 19 out of 30 meteorological subdivisions in India. On subdivision and regional scale for the NER, Jain et al., (2013) detected negative trends in annual, pre-monsoon, monsoon and winter rainfall. Since the past few years, the number of studies on the precipitation trends in the NER is slowly increasing (Choudhury et al. 2012; Das et al. 2015; Duncan et al. 2013; Jain et al. 2013; Laskar et al. 2014; Murata et al. 2007; Prokop and Walanus 2003, 2015; Yadav et al. 2016).

Most of the aforementioned studies (Choudhury et al. 2012; Das et al. 2015; Duncan et al. 2013; Jain et al. 2013; Laskar et al. 2014; Murata et al. 2007; Prokop and Walanus 2003, 2015), considered few rain gauge stations and used Mann-Kendall (MK) (Kendall 1948; Mann 1945) test to detect a monotonic trend. Less attention was given to check for autocorrelation in the data series. Though MK test is widely used in trend analysis in hydrology, past studies have shown that the presence of autocorrelation can affect the detection of trends using MK and Sen's slope (Hamed and Rao 1998; Yue et al. 2002). A trend-free pre-whitening approach is adopted by some studies to remove the autocorrelation in the data series (Khattak et al. 2011; Shivam et al. 2017; Wang et al. 2020; Yue et al. 2002). However, several studies reported that pre-whitening can remove some portion of actual trend and may not be effective if serial correlation exists beyond first-order autoregressive process and if the sample size is large (Bayazit and Önöz 2007; Kumar et al. 2009; Yue and Wang 2004). In order to tackle this issue, Şen (2012) proposed a new method, known as the Innovative Trend Analysis (ITA) method, which can overcome the problem of trend detection in an autocorrelated time series data. The reliability of ITA method has been established in many studies around the world (Alashan 2018; Caloiero 2020; Güçlü et al. 2020; Romaguera et al. 2010; Şen 2014; Serencam 2019; Wang et al. 2020; Wu and Qian 2017). Therefore, the first objective of this study is to use ITA method to determine the spatial and temporal trend of long-term rainfall data on an annual and seasonal basis; secondly, to identify the trend characteristic in different rainfall categories; and thirdly, to verify the trend detected using ITA method by comparing with the MK test.

6.2 **Study area and data**

The Umiam and Umtru watersheds are located in East Khasi Hills and Ri-Bhoi Districts of Meghalaya, India (Figure 6.1). The two watersheds lie adjacent to each other and drain to the Kapili river in the neighbouring state of Assam. The spatial distribution of rainfall in Meghalaya is largely controlled by the interaction of large-scale circulation and the local topography (Prokop and Walanus 2015), where the central region of the Meghalaya plateau is above 1500 m (Sato 2013). The average annual rainfall in the area is around 1951 mm. The present study covers an area of 2963 Km^2. Out of this total area, 1553.75 Km^2 is covered by the Umtru watershed, and 1410.27 Km^2 is covered by the Umiam watershed. Umiam-Umtru system is hydrologically connected by a water transfer system for hydropower generation. These two watersheds are of significant importance as there are cascade of reservoirs that provide water for hydropower generation for meeting the power requirement in Meghalaya.

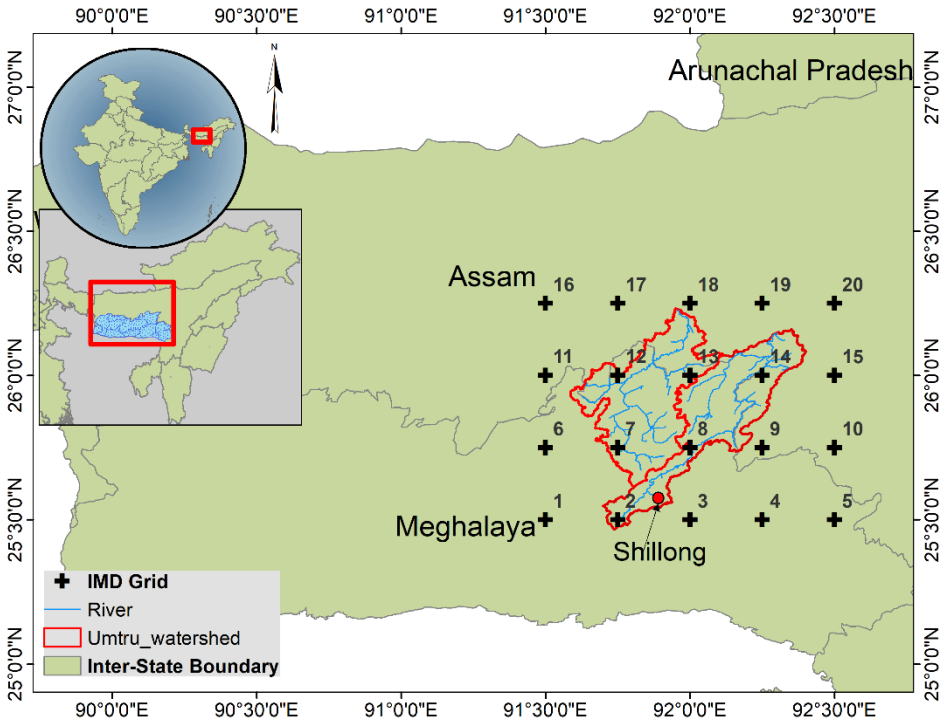

Figure 6.1 Location of the study area along with watershed boundaries and Indian Meteorological Department grid points

6.2.1 Data

In this study, the precipitation trends were examined on an annual and seasonal basis. Four seasons are considered for seasonal trend analysis by dividing the year as Winter (JF), Pre-Monsoon (MAM), Monsoon (JJAS), and Post-Monsoon (OND). The analysis in this study was carried out using the gridded rainfall data provided by the National Data Centre, India Meteorological Department (IMD), Pune. This gridded data was developed from the daily rainfall records of 6,955 rain gauge stations in India by Pai et al. (2014). Due to the variations in rain gauge density in different regions and time periods, the number of stations available for development of daily grid point data also varied. On an average about 2600 stations per year were used to generate homogeneous daily grid point data. IMD performs standard quality control checks on the data for errors right from the gauge station level. The data is checked for geographic location error, checks for coding and typographic errors, time consistency, spatial consistency and duplicates. The daily station rainfall data were interpolated into grids of 0.25° × 0.25° resolution using Shepard (1968) interpolation method. The interpolated values were computed as the weighted sum of the station data within a search radius of 1.5°. Local modification to the scheme was also applied by including the directional effects and barriers as proposed by Shepard

(1968). On comparing with four other data sets i.e. (a) 1° × 1° data set (Rajeevan et al. 2006), (b) 1° × 1° data set (Rajeevan et al. 2008) (c) 0.5° × 0.5° data set (Rajeevan and Bhatle 2009), (d) 0.25° × 0.25° data set of APHRODITE (Asian Precipitation–Highly Resolved Observational Data Integration Towards Evaluation of the Water Resources project) (Yatagai et al. 2012), the new data of 0.25° × 0.25° was found to be superior in representing the large-scale climatological features of rainfall over India (Pai et al. 2014). The original data developed by Pai et al. (2014) was till 2010 but is being updated continuously using the same methods and made available for public in the IMD web portal. For this study, the latest data till 2018 was used. The data is extensively used in many other studies thus affirming its reliability for long term trend analysis (Ali et al. 2014; Bisht et al. 2018; Dave and James 2017; Jothiprakash et al. 2017; Marak et al. 2020; Nageswararao et al. 2016). The time series plot of one of the grid points (P1) is shown in Figure 6.4Figure 6.2.

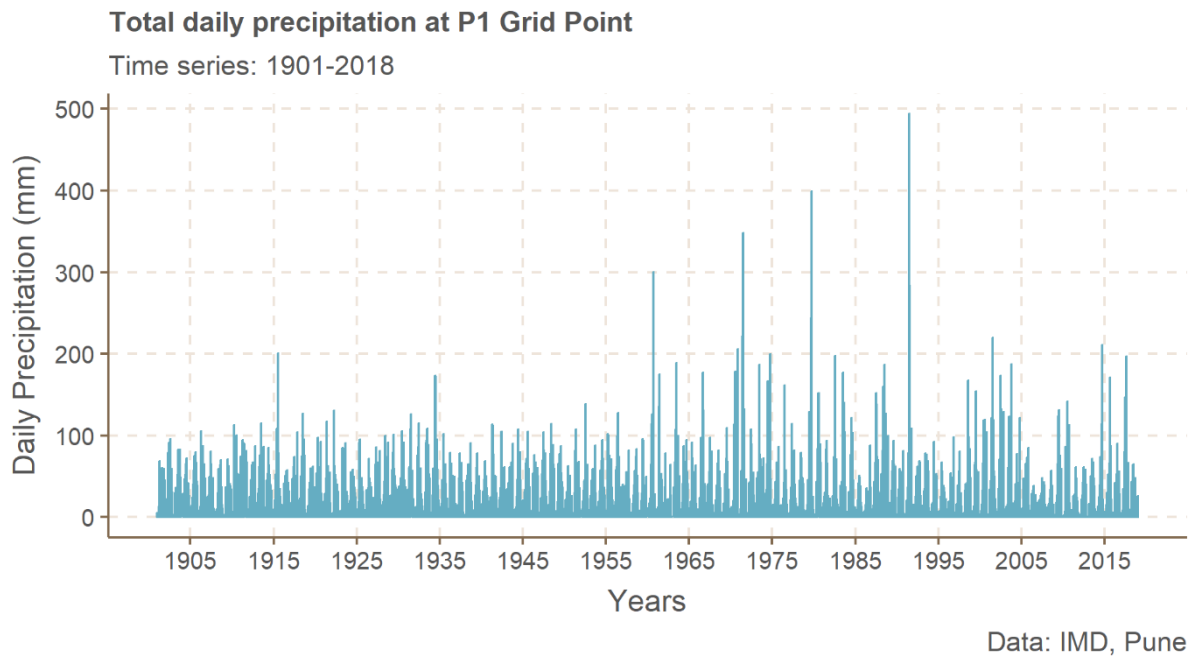

Figure 6.2 Plot of precipitation time series from 1901 to 2018 at P1 grid point.

6.3 **Methods**

6.3.1 Innovative Trend Analysis (ITA) Method

The ITA method introduced by Şen (2012) is a graphical method of trend analysis. The illustration of the ITA plot is shown in Figure 6.3 Illustration of the ITA method showing trends and rainfall

categories.Figure 6.3. Unlike the most commonly used classical methods of trend analysis like Mann-Kendal Test (Kendall 1948; Mann 1945) and Sen's slope (Sen 1968), the ITA method is free from assumptions such as serial correlation, non-normality, length of the record, etc. In the ITA, the data series is divided into two equal parts (X_i, i=1,2, 3…, n/2 and X_j, j=n/2+1, n/2+2, n/2+3…, n/2). Each series is then sorted independently in ascending order. The first half of the series (X_i) is plotted on X-axis, and the second half is plotted on Y-axis. The existence of any trend is detected with the help of a 1:1 line in the scatter plot. If all the points fall on the 1:1 line (45° line), it signifies that there is no trend in the time series. The points falling on the upper triangular area of the 1:1 line show an increasing trend in the time series, and the data falling on the lower triangular area of the 1:1 line shows a decreasing trend in the time series. In the case of a single monotonic increasing (decreasing) trend, all the points lie above (below) the 1:1 line. In such cases, it is easy to identify the trend. But when the time series has a non-monotonic trend, the scatter points may occur on upper and lower regions of the 1:1 line. In such cases, the scatter points are divided into Low, Medium, and High categories to enable more detailed analysis. Here, the rainfall intensities are divided into three categories based on the percentiles such that; low < 10%, 10% < medium < 90%, and high > 90% rainfall (Wang et al. 2020).

The slope(S) of ITA tend line can be calculated as given below (Şen 2017)

$$S = \frac{2(\overline{X}_j - \overline{X}_i)}{n} \qquad (6.1)$$

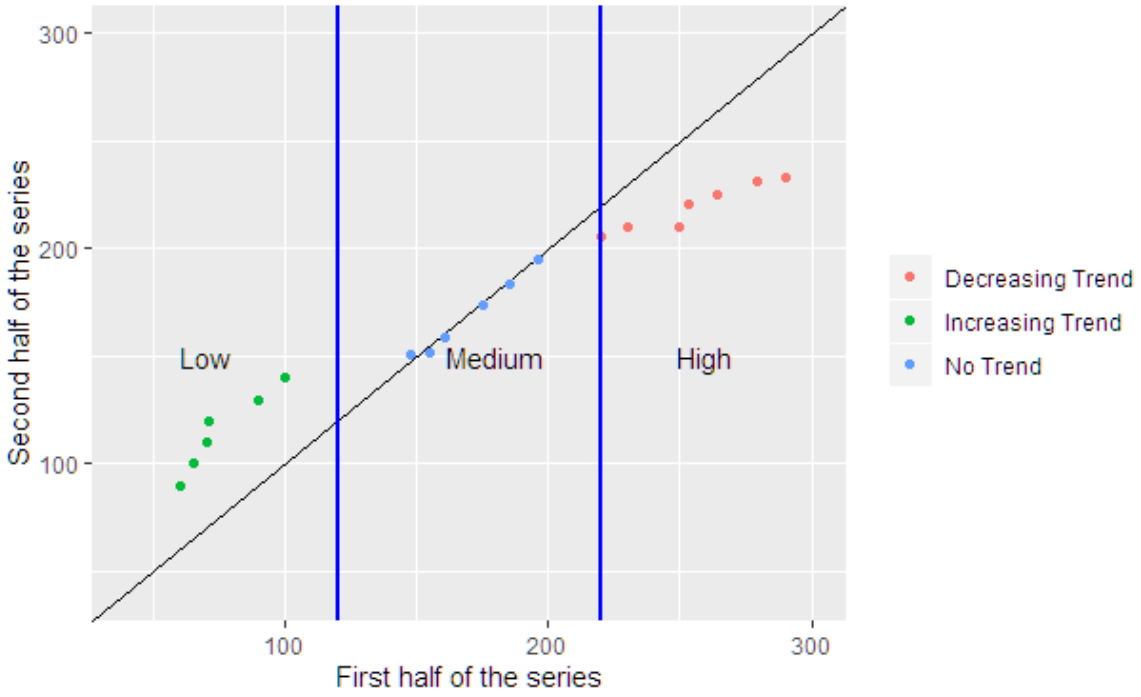

Figure 6.3 Illustration of the ITA method showing trends and rainfall categories.

where S is the ITA trend slope, n is the number of data points, $\bar{X}_i$ and $\bar{X}_j$ are the mean values of the first and second half series, respectively. Category wise trend slope (S) is calculated based on the centroid point of each category for Low, Medium, and High, according to Dabanlı et al. (2016).

To determine the significance of the trend slope S, a null hypothesis (H_0) of no significant trend and an alternative hypothesis (H_a) for the presence of a significant trend are considered. If the calculated S is less than S_{cri}, the null hypothesis (H_0) holds true, and the trend is not significant (Şen 2017). The alternative hypothesis (H_a) is true when S > S_{cri} and the trend is significant. S_{cri} denotes the confidence limits of a standard normal distribution, which has zero mean and the standard deviation σ_s. If α is the level of significance, the confidence limits (CL) of the trend slope is given by

$$CL_{(1-\alpha)} = 0 \pm S_{cri}\sigma_s \tag{6.2}$$

where α is the level of significance, and σ_s is the slope standard deviation. The value of σ_S is calculated as

$$\sigma_S = \frac{2\sqrt{2}}{n\sqrt{n}}\sigma\sqrt{1-\rho_{\bar{X}_i\bar{X}_j}} \tag{6.3}$$

In Equation (6.3, $\rho_{\bar{X}_i\bar{X}_j}$ is the cross-correlation coefficient between the means of sorted X_i and X_j series. Here a 5% level of significance is used for estimating the significance of a trend.

6.3.2 Mann-Kendall test

The Mann–Kendall (MK) is a rank-based non-parametric test that is commonly used for detecting monotonic trends in hydrometeorological data (Kendall 1938b; Mann 1945). The assumptions in MK test are that the data are independent and in random order. The MK test statistic S is given by:

$$S = \sum_{i=1}^{N-1} \sum_{j=i+1}^{N} sgn(x_j - x_i) \tag{6.4}$$

where, x_i and x_j are the sequential data points, N is the length of the data series and

$$\mathrm{sgn}(\mathrm{x_j} - \mathrm{x_i}) = \begin{bmatrix} 1 & \text{if } \mathrm{sgn}(\mathrm{x_j} - \mathrm{x_i}) > 0 \\ 0 & \text{if } \mathrm{sgn}(\mathrm{x_j} - \mathrm{x_i}) = 0 \\ -1 & \text{if } \mathrm{sgn}(\mathrm{x_j} - \mathrm{x_i}) < 0 \end{bmatrix} \tag{6.5}$$

According to (Mann 1945) and Kendall (1938), for N≥8, the statistic S is approximately normally distributed with mean and variance as given below:

$$\mathrm{E(S)} = 0 \tag{6.6}$$

$$\mathrm{V(S)} = \frac{\mathrm{N(N-1)(2N+5)} - \sum_{\mathrm{k=1}}^{\mathrm{t}} \mathrm{t_k(t_k-1)(2t_k+5)}}{18} \tag{6.7}$$

where t_k is the number of data points belonging to the k^{th} tied group and t is the number of tied groups in the dataset. The Mann- Kendall Z-statistic is computed as follows:

$$Z = \begin{bmatrix} \frac{S-1}{\sqrt{V(S)}} & if\ S > 0 \\ 0 & if\ S = 0 \\ \frac{S+1}{\sqrt{V(S)}} & if\ S < 0 \end{bmatrix} \tag{6.8}$$

where, Z is the Mann-Kendall test statistic following a standard normal distribution with zero mean and variance of one. In a two-sided trend test for significance level of alpha (α), the trend

is significant if $|Z| > Z_{\frac{\alpha}{2}}$ and the null hypothesis is rejected. A positive(negative) Z value signifies positive(negative) trend at the selected significance level (α).

In case of autocorrelated data, the probability of detecting trends is increased even if there is no trend in reality (Hamed and Rao 1998). In order to minimize the effect of autocorrelation, a pre-whitening process proposed by Yue and Wang (2004) was applied on the data series if there exists a significant (α=0.05) auto-correlation. If the auto-correlation is not significant, the MK test is applied to the original dataset.

6.3.3 Sen's slope estimator

The MK test identifies the existence of a trend in a positive or negative direction. The strength of a trend is calculated using Sen's slope (Sen 1968) as follows

$$\beta = Median\left[\frac{Y_i - Y_j}{i - j}\right] \text{ for all j } < \text{ i} \qquad (6.9)$$

where Y_i and Y_j are data values at time step i and j, respectively. The test statistic β denotes the median of all slope estimates. The positive value of β indicates an increasing trend, and negative value indicates a decreasing trend.

6.4 **Results and discussion**

6.4.1 Annual rainfall trend

The results of the ITA analysis for annual rainfall are presented in Table 6.1. Ten out of twenty grids show positive value (increasing trend) of ITA slope S (Figure 6.4), while the rest show negative (decreasing trend). The trends are found to be significant at α = 0.05 at the majority of the grids except for P3 and P19 (Figure 6.5). The increase in rainfall was maximum (minimum) at P2 (P1) which can be seen clearly in Figure 6.4, where the majority of the scatter points are above (below) the 1:1 line for P2 (P1). The percentage of grids exhibiting various trends are shown in Figure 6.6. Annual series had 45% grids each, of significantly decreasing and increasing trend, while 10 % did not show any significance at α = 0.05.

The trends in different rainfall categories of annual rainfall are highlighted in Figure 6.4 in different colours as shown in the legend (Red = Low, Blue = Medium and Green = High). These represent the average ITA slope values of each rainfall category. The trend can be identified as positive, negative, or no-trend based on the location of the scatter points above, below, or on the 1:1 line. The overall trends in different rainfall categories are summarised in (Figure 6.6) and is

discussed later in this section. In the “high” category, an increasing trend is seen for all grid points except P18 (Figure 6.4). Twelve grid points tend towards negative trend for the “medium” category, except P2, P7, P8, P12,

Table 6.1 Annual ITA results

Grid Point	Slope(S)	Standard deviation (σ)	Slope standard deviation (σ_s)	Correlation ($\rho_{\bar{X}_1\bar{X}_2}$)	Upper CL	Lower CL	Mann-Kendall (Z)	Sen's slope
P1	-10.55*	752.18	0.51	0.91	0.84	-0.84	-8.77*	-8.96
P2	16.17*	2131.38	2.22	0.78	3.65	-3.65	0.40	1.33
P3	1.56	1480.39	1.33	0.83	2.19	-2.19	-2.67*	-7.94
P4	2.07*	953.99	0.58	0.92	0.96	-0.96	-2.05*	-3.43
P5	-1.89*	312.74	0.13	0.96	0.21	-0.21	-2.83*	-2.37
P6	0.52*	561.12	0.23	0.96	0.38	-0.38	-0.22	-0.24
P7	10.17*	824.78	0.47	0.93	0.77	-0.77	2.96*	4.20
P8	12.81*	1172.48	0.93	0.87	1.52	-1.52	1.44	2.78
P9	-0.55*	328.57	0.17	0.94	0.28	-0.28	-2.33*	-1.89
P10	-0.34*	262.88	0.12	0.95	0.20	-0.20	-1.79*	-1.11
P11	-1.71*	342.34	0.12	0.97	0.20	-0.20	-0.50	-0.36
P12	1.48*	344.17	0.11	0.98	0.18	-0.18	0.04	0.03
P13	-0.38*	393.47	0.10	0.99	0.17	-0.17	-2.33*	-2.35
P14	-1.38*	454.48	0.32	0.90	0.53	-0.53	-2.75*	-2.47
P15	0.41*	346.51	0.22	0.92	0.36	-0.36	0.20	0.17
P16	1.54*	326.36	0.14	0.96	0.23	-0.23	1.91	1.10
P17	0.54*	334.57	0.08	0.99	0.13	-0.13	-1.25	-0.78
P18	-1.59*	429.49	0.10	0.99	0.16	-0.16	-2.37*	-2.40
P19	-0.58	480.03	0.40	0.85	0.66	-0.66	-2.93*	-2.71
P20	-3.86*	376.59	0.28	0.88	0.47	-0.47	-3.95*	-3.60
*Significant trend at 5% significance level (P<0.05)								

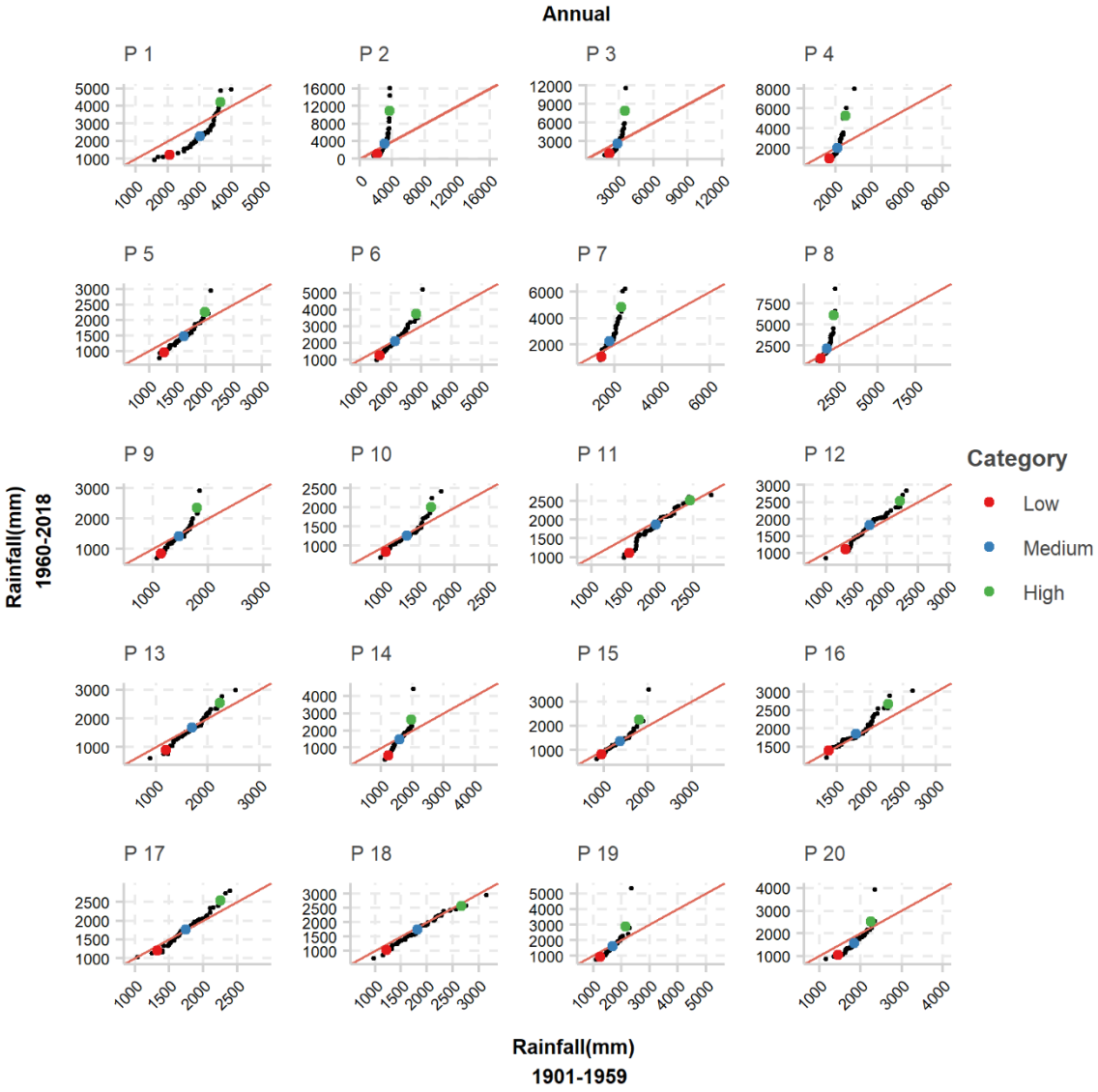

Figure 6.4 ITA plot of 20 IMD grid points for Annual rainfall

Annual

Winter

Pre-Monsoon

Monsoon

Post-Monsoon

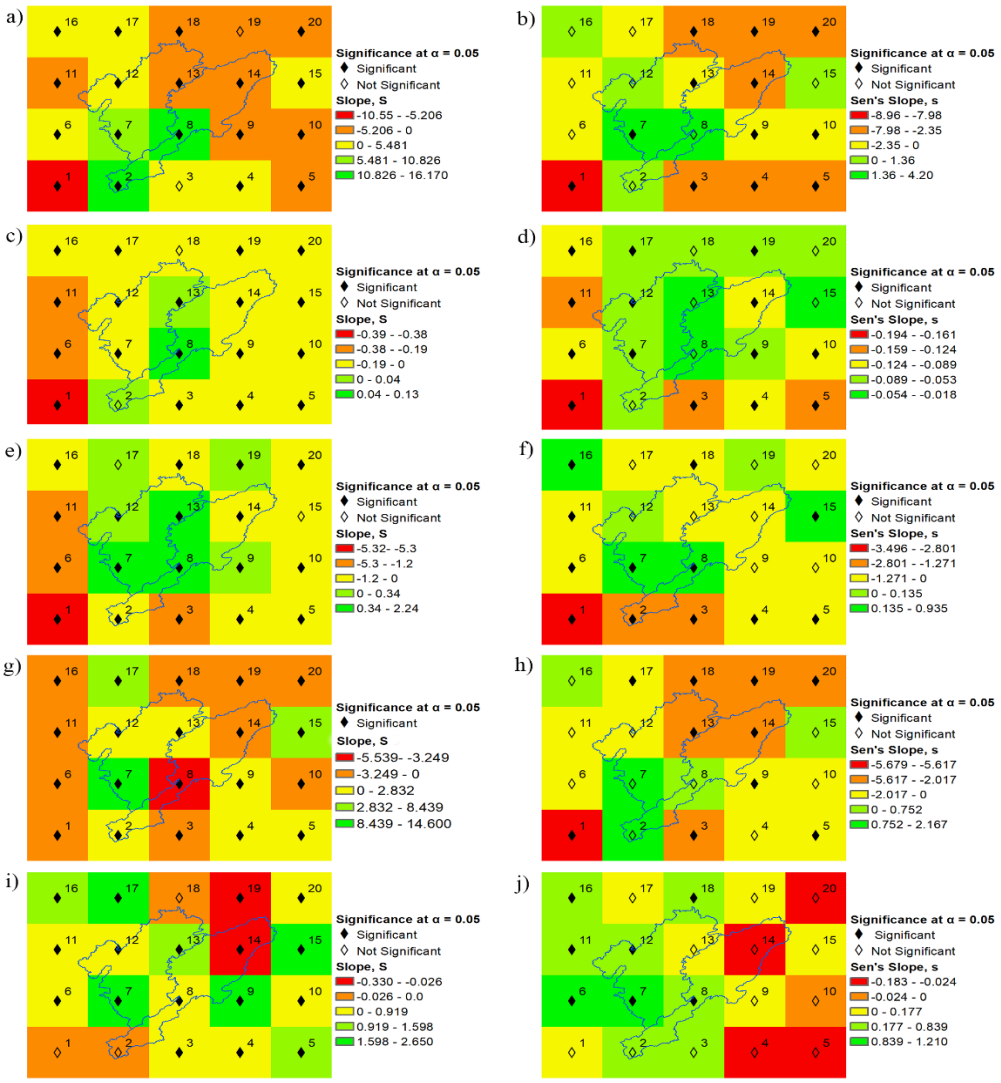

Figure 6.5 Spatial variation of ITA slope(S) (Left) and MK-Sen's slope(s) (Right). Figures a), c), e), g) and i) are ITA slope for Annual, Winter, Pre-monsoon, Monsoon and Post-Monsoon rainfall respectively. Figures b), d), f), h) and j) are MK significance with Sen's Slope values for Annual, Winter, Pre-monsoon, Monsoon and Post-Monsoon rainfall respectively.

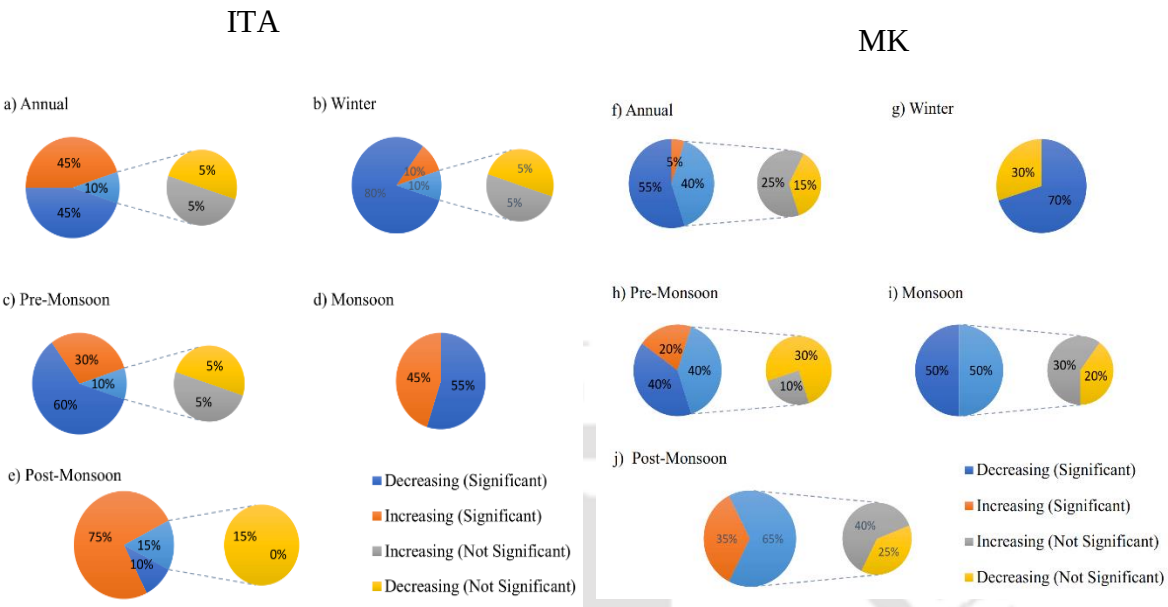

Figure 6.6 Percentage of grids showing different trends based on ITA slope (Left) and Mann Kendal test (Right) for annual and seasonal analysis.

P16, and P17. All the grid points except P16 show a decreasing trend in the "low" category rainfall. The ITA slope, S, of each category, is shown in Table 6.3.

The ITA method has proven to be effective in trend analysis even in regions of different climates. A study of rainfall in South Island of New Zealand from 1951 to 2010 period, Caloiero (2020) found increasing trend at annual scale using the ITA method for Southland area. In the same study, the positive trend was found to have been contributed by medium and high rainfall for Otago and Westland. A study by Gedefaw *et al.*, (2018) in African region of Amhara Regional State from 1980–2016 found that ITA method agrees with MK and Sen's slope. They reported decrease in rainy days and an increase in extreme events during 1980-2016. In Western Asia, Dabanli and Şen, (2018) found increasing trend in high, medium and low rainfall (1981-2010) for Akacay basin using the ITA method.

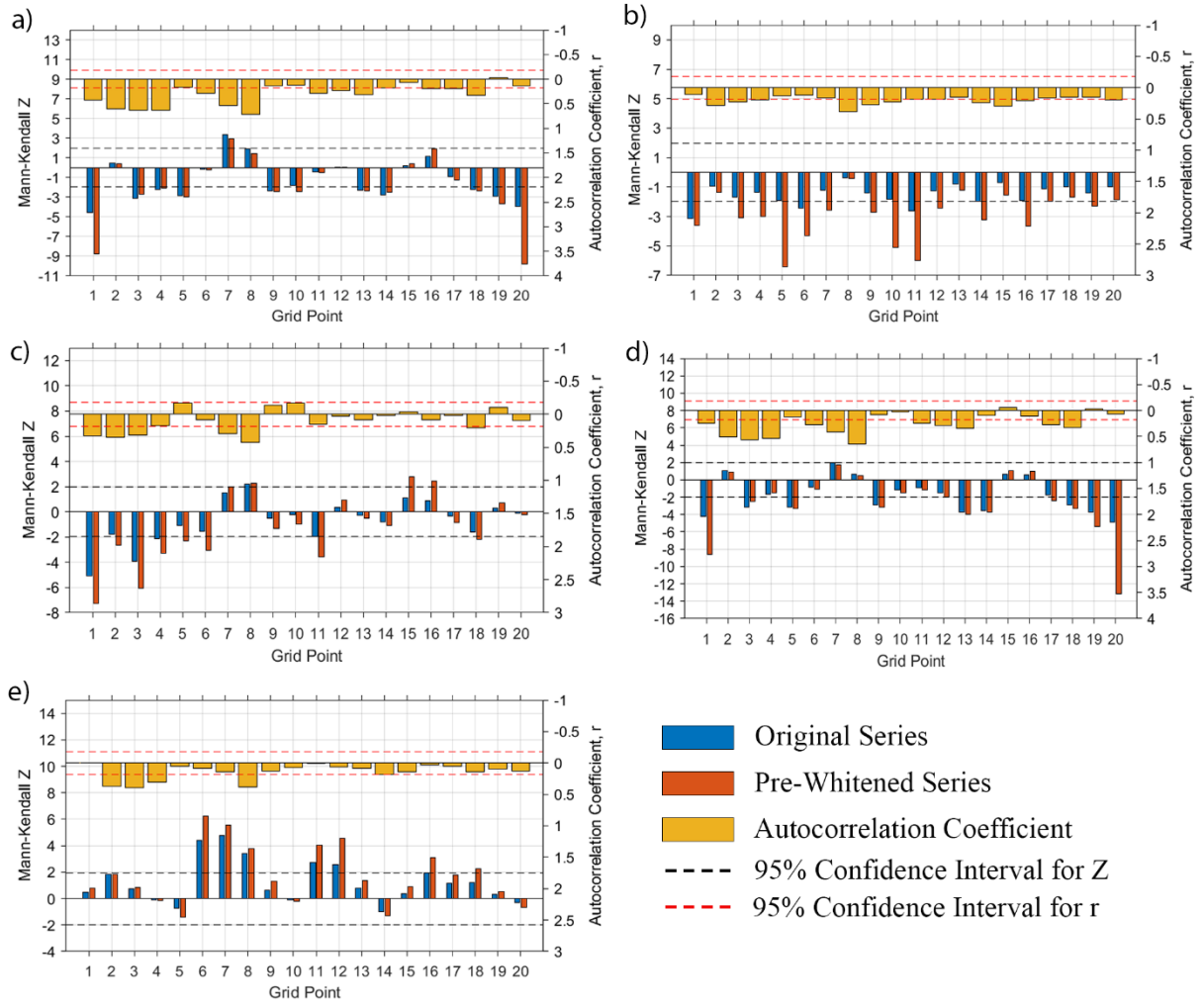

Figure 6.7 Plot of Mann-Kendall Z values for original and pre-whitened series along with autocorrelation coefficient (95% level). a) Annual, b) Winter, c) Pre-Monsoon, d) Monsoon, e) Post-Monsoon.

Figure 6.7 presents the lag-1 autocorrelation in each grid point. In the annual time scale, grids: P5, P9, P10, P14, P15, P19, and P20 were free from significant autocorrelation. The data for these grids can be used directly for trend detection using MK test. For the rest of the grids, a pre-whitening technique proposed by Yue and Wang (2004) was applied to the rainfall data using "modifiedmk" package (Patakamuri 2020) in R statistical software. This was done to minimize the effect of serial correlation in trend detection. The variation of autocorrelation can be seen across different seasons. More number of grids are found to display significant autocorrelation during winter and monsoon seasons.

After the autocorrelation check and pre-whitening of rainfall data, the widely accepted MK test was carried out to compare with the trends detected using ITA. The results of MK test show an increasing trend in 6 grids, while 14 grids were in decreasing trend with negative Z value (Table 6.2). The Z value for all the grids lies in the range -8.77 to 2.96, and the variation in its statistical significance over the study area is represented in Figure 6.5. The trends using MK test were significant only in 12 grids, whereas ITA detected significant trends in 18 grids. This shows that ITA can detect hidden trends in the data series, which are not detected by the MK test. The magnitude of the monotonic trend was determined by Sen's slope. Sen's slope magnitude was higher in the southern region with a maximum of -8.96 mm/year at P1 (Figure 6.5b). The only grid showing a significant increasing trend with a positive slope was P7. About 55% of the grids with significant trends are found to exhibit a decreasing trend (Figure 6.6f). This affirms the decreasing trend detected in ITA analysis. However, only 5% of the grids show significantly increasing trend using MK test in contrast to 45% using ITA test mentioned earlier. 25% of the grids, which show an increasing trend was not significant (α=0.05). In an earlier study, Choudhury et al. (2012) reported that the total annual rainfall trend at Umiam increased non-significantly at the rate of 3.72 mm/year. If the region specified in their paper (25°41' N, 91° 55' E), which falls under grid P2 and P3 in the present study is considered, similar increasing trends can be observed but significant at P3 (Figure 6.5b). The differences in detection of significant trend in the study area may be due to the length of data considered for the analysis because the power of MK test in its ability to detect trends increases as the sample size is increased (Sheng Yue et al. 2002). The data used by Choudhury et al. (2012) was from 1983-2010 (28 years), whereas the present study uses longer data period from 1901-2018 (118 years) which results in a much larger sample size.

6.4.2 Winter rainfall trend

The ITA plot for winter (Figure 6.9), reveals weak decreasing trends, which are significant except at P2 and P18. Most of the data points lie close to the 1:1 line. The range of ITA slope varies from -0.39 to 0.13 (Table 6.2). The high rainfall category shows a decreasing trend in P1, P6, P11, and P16, as shown by the location of the categorical average with respect to 1:1 line in Figure 6.9. A noticeable increasing trend is seen at P2 and P8. The means values of low and medium category rainfall tended to lie close to the 1:1 line and did not exhibit any discernible trend except in P1, where the medium rainfall shows a decreasing trend. The overall decreasing trend in low and medium rainfall and increasing trend in high rainfall can be observed in winter (Figure 6.8b). Our

results concord with Prokop and Walanus (2015) in which a decreasing trend was observed in light and medium rainfall around Shillong.

Table 6.2 Seasonal ITA and Mann-Kendall test results. S represents the ITA slope, Z is MK statistic, and s is Sen's Slope.

Grid Point	Winter			Pre-Monsoon			Monsoon			Post-Monsoon		
	ITA S	Z	Sen's s	ITA S	Z	Sen's s	ITA S	Z	Sen's s	ITA S	Z	Sen's s
P1	-0.39*	-3.60*	-0.19	-5.30*	-7.24*	-3.49	-5.54*	-8.58*	-5.67	0.69*	0.79	0.12
P2	0.01	-1.37	-0.08	-1.09*	-2.64*	-1.51	14.60*	0.87	2.16	2.65*	1.81	0.75
P3	-0.11*	-3.10*	-0.12	-2.68*	-6.04*	-2.79	2.82*	-2.51*	-5.59	1.53*	0.82	0.25
P4	-0.08*	-2.99*	-0.12	-1.13*	-3.27*	-1.26	2.75*	-1.51	-2.01	0.52*	-0.13	-0.02
P5	-0.11*	-6.39*	-0.12	-0.27*	-2.31*	-0.44	-1.18*	-3.32*	-1.56	-0.33*	-1.43	-0.14
P6	-0.21*	-4.32*	-0.11	-1.43*	-3.06*	-0.79	0.56*	-1.07	-0.82	1.60*	6.21*	1.07
P7	-0.05*	-2.59*	-0.05	1.45*	1.97*	0.63	6.58*	1.76	1.76	2.19*	5.56*	1.21
P8	0.13*	-0.41	-0.01	2.24*	2.28*	0.93	8.43*	0.49	0.73	2.01*	3.79*	0.83
P9	-0.03*	-2.73*	-0.06	0.06*	-1.29	-0.14	-0.86*	-3.14*	-1.72	0.26*	1.31	0.12
P10	-0.10*	-5.08*	-0.09	-0.11*	-0.99	-0.06	-0.02	-1.46	-0.58	-0.11*	-0.20	-0.02
P11	-0.22*	-5.98*	-0.15	-1.59*	-3.56*	-0.73	-0.83*	-1.18	-0.56	0.93*	4.05*	0.53
P12	-0.05*	-2.41*	-0.07	0.31*	0.96	0.12	0.28*	-1.95	-1.02	0.93*	4.57*	0.52

P13	0.04*	-1.23	-0.03	0.35*	-0.50	-0.08	-1.18*	-4.00*	-2.75	0.42*	1.35	0.15
P14	-0.05*	-3.21*	-0.09	-0.20*	-1.06	-0.21	-1.11*	-3.69*	-2.36	-0.02	-1.31	-0.18
P15	-0.04*	-1.55	-0.03	-0.01	2.78*	0.33	0.48*	1.06	0.31	-0.02	0.86	0.08
P16	-0.19*	-3.63*	-0.11	-0.22*	2.43*	0.33	1.31*	0.95	0.44	0.65*	3.10*	0.36
P17	-0.03*	-1.97*	-0.06	0.04	-0.82	-0.09	-0.05	-2.41*	-1.22	0.58*	1.78	0.17
P18	-0.01	-1.67	-0.06	-0.76*	-2.17*	-0.55	-1.29*	-3.34*	-2.33	0.48*	2.23*	0.24
P19	-0.04*	-2.30*	-0.07	0.10*	0.72	0.07	-0.85*	-5.38*	-2.75	0.21*	0.50	0.06
P20	-0.07*	-1.86	-0.05	-0.53*	-0.20	-0.03	-3.23*	-13.18*	-3.48	-0.02	-0.65	-0.04
*Significant trend at 5% significance level (P<0.05)												

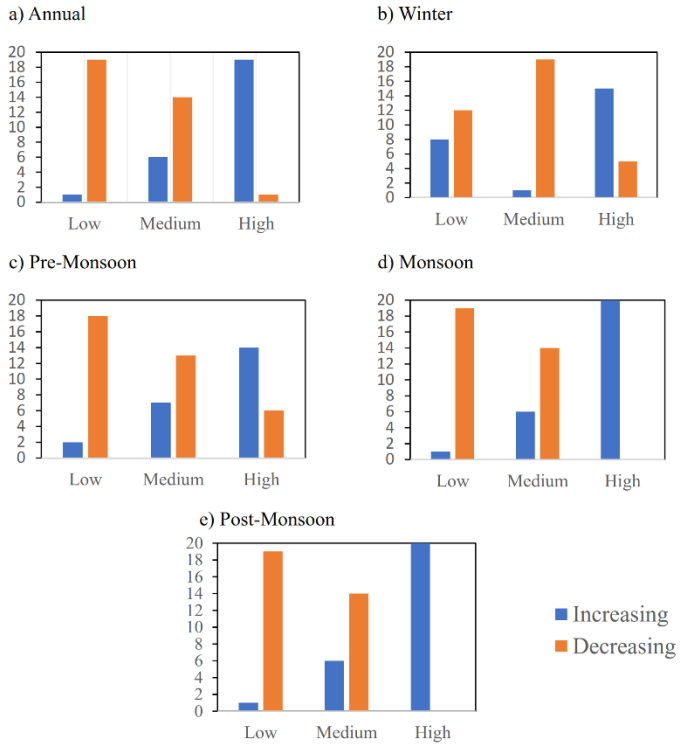

Figure 6.8 Trends in different rainfall categories on annual and seasonal basis. The bar chart shows number of grids under increasing or decreasing trend.

The difference between their study and the present study is that Prokop and Walanus (2015) used single rain gauge station data, whereas the present study uses 20 IMD gridded data. Out of 20 grids, 80% shows a significantly decreasing trend in winter (Figure 6.6b). 10% comprised of grids showing significantly increasing trend whereas the rest 10% was equally divided between non-significantly increasing and decreasing trends.

On MK test, the winter rainfall trend tends to decrease at all the grids (Figure 6.5d), out of which 70% were significant, and 30% were not significant (Figure 6.6g). The magnitude of trend given by Sen slope varies from -0.194 to -0.018 mm/year. The sharpest decrease was seen at P1 in both the tests (Table 6.2). Laskar et al. (2014) did not find any significant trend for seasonal rainfall in the Shillong region, which falls under P2 and P3 grids in this study. However, both the ITA and MK tests show significantly decreasing trends for the winter season in this study.

6.4.3 Pre-Monsoon rainfall trend

Table 6.2 presents the ITA results for the pre-monsoon rainfall trend, and the ITA plots are shown in Figure 6.10. The scatter points in the majority of the grids lie below the 1:1 line. The categorical

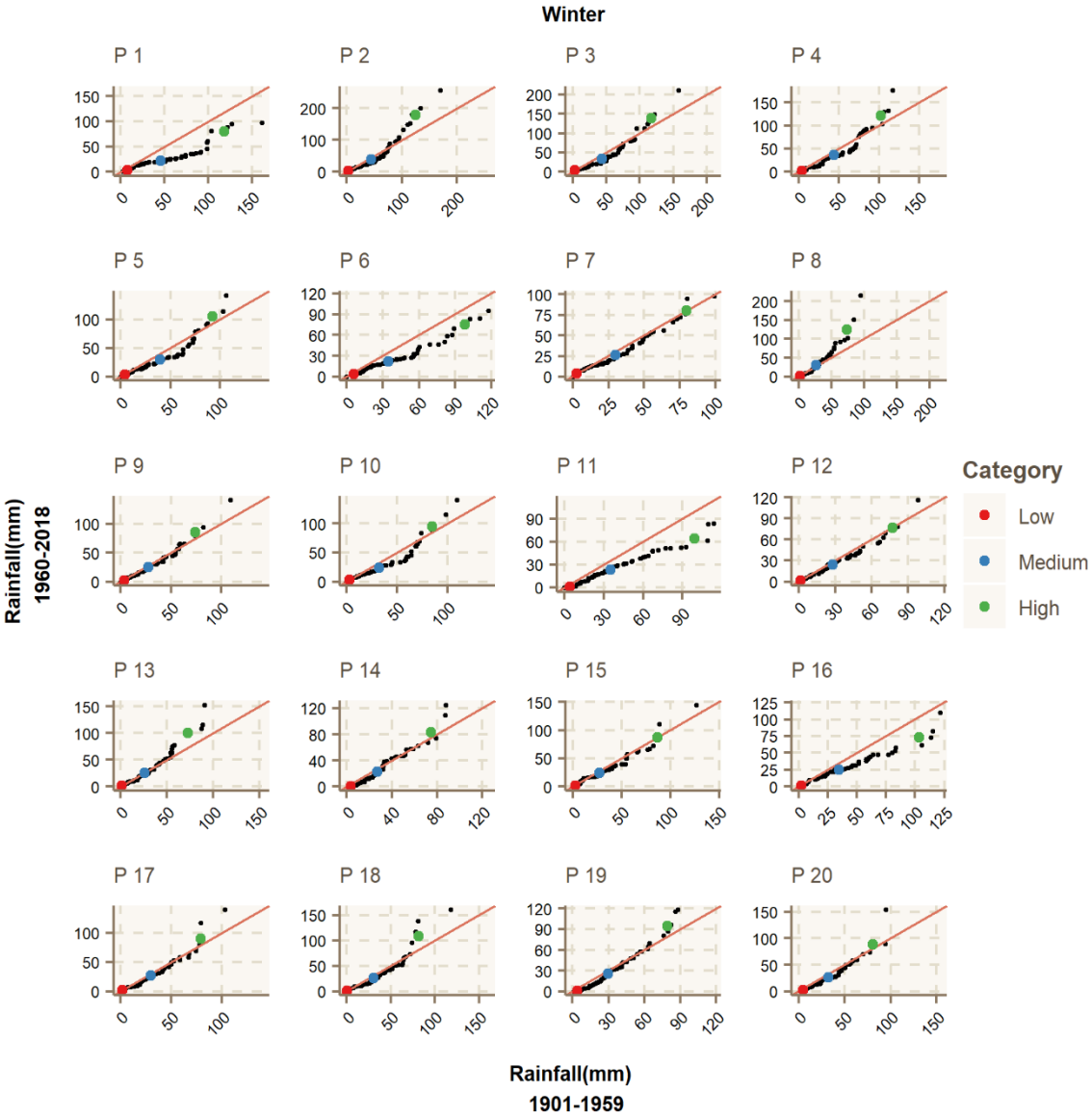

Figure 6.9 ITA plot of 20 IMD grid points for Winter rainfall.

mean of high rainfall in Figure 6.10 are located above the 1:1 line in the majority of the grids, indicating an increasing trend in high rainfall. In Figure 6.5e, the significance, and variation of ITA slope are shown. It can be seen that the negative value of ITA slope are in the majority, and most of them are significant except P15 and P17. The high rainfall category shows an increasing trend in P2, P3, P4, P5, P7, and P8. The maximum decreasing trend was seen at P1 while the maximum increasing trend was at P8 for the high category. The low and medium rainfall exhibit a decreasing trend in the majority of the grids (Figure 6.8). In general, 60% of the grids show a significantly decreasing trend, 30% showed significantly increasing trend, and from the rest 20%, non-significant and significant occupies 10% each (Figure 6.6c).

The MK test Z values for pre-monsoon are given in Table 6.2. 20% of the grids are found to show an increasing trend (Figure 6.6h) out of which P7, P8, P15, and P16 are significant (Figure 6.5f). A significant decreasing trend was detected at 40% of the grids. Again, the number of non-significant trends reported by MK test was 40%, while ITA test reported only 10%. Figure 6.5f also shows the variation of Sen's slope in different grids. The value of Sen's slope ranges from -3.496 to 0.935. The maximum changes are seen at grid P1 in both ITA and MK test and both indicate a negative trend.

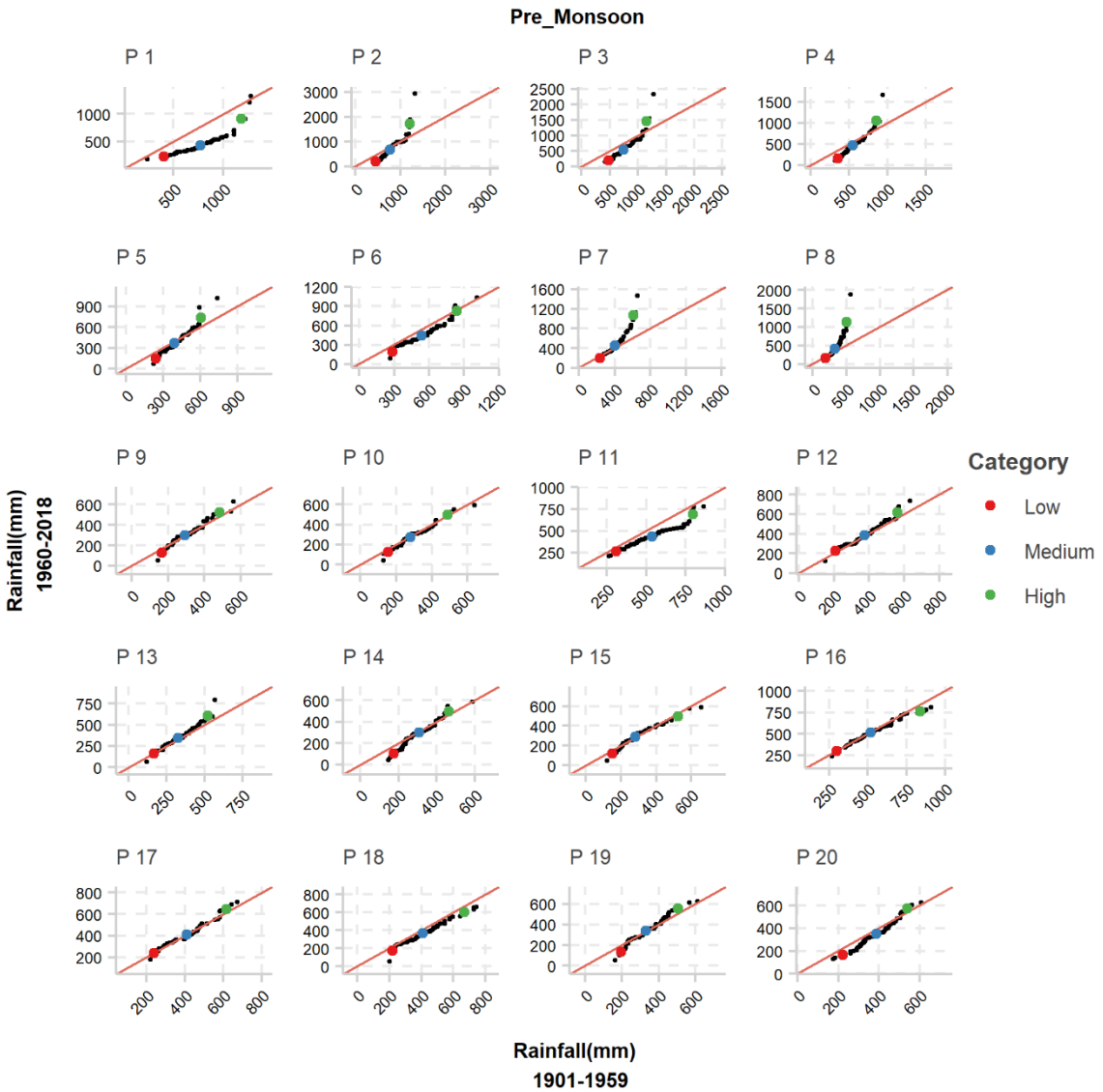

Figure 6.10 ITA plot of 20 IMD grid points for Pre-Monsoon rainfall.

6.4.4 Monsoon rainfall trend

The ITA representation of the monsoon rainfall trend is presented in Figure 6.11. The value of ITA slope for monsoon rainfall ranges from -5.539 to 14.6. An increasing trend is seen at 9 grids, while 11 grids show a decreasing trend. The trends are found to be significant at all the grids except P10 and P17 (Figure 6.5i). Overall, the trends in monsoon were all significant, with 45% of the grids showing an increasing trend and 55% showing a decreasing trend (Figure 6.6d).

The high rainfall category is found to exhibit an increasing trend in all of the grids (Figure 6.11). The low rainfall category exhibits a decreasing trend in almost all the grids except P16 and P17. The medium category rainfall shows a decreasing trend at P1 and P20. The overall distribution of trends in different categories is given in Figure 6.8.

On MK test, the number of grids showing increasing trend reduces to 5 (Figure 6.5) (as compared to 9 with ITA test), none of them being significant. A decreasing trend was significant at 50% of the grids, including significant and non-significant. A non-significant increasing trend was seen at 30% of the grids, whereas 20% had a non-significant decreasing trend (Figure 6.6). The magnitude of Sen's slope varies from -5.679 to 2.167 mm/year. The values of the statistics for each grid is presented in Table 6.2.

6.4.5 Post-monsoon rainfall trend

The post-monsoon rainfall ITA test result for each grid point is presented in Table 6.2 and the ITA plot is shown in Figure 6.12. The ITA test reveal that the post-monsoon rainfall is dominated by a significant positive trend. The ITA slope values of P14, P15, and P20 are found to be the same, i.e., -0.02, which shows that there is a weak non-significant decreasing trend. Figure 6.5 shows the plot of the ITA slope over the area along with their significance. The decrease in rainfall trends tends to cluster on the eastern region for post-monsoon rainfall. Most of the high rainfall category average except P5, P10, and P15, tend to show an increasing trend. A similar increasing trend is found for medium category rainfall, but P5, P14, and P20 exhibit a slightly decreasing trend. Low category rainfall tends towards a positive trend in few grids, of which the major ones are P6, P7, P8, and P11. While the rest show, a trivial decreasing trend, P2, P3, and P18 has no trend which is also be evident in Table 6.3. The overall trend is summarised in Figure 6.6e. 75% of the grids show a significantly increasing trend, and 25% show a decreasing trend, out of which 15% were not significant. This shows an increasing trend in post-monsoon seasonal rainfall. High-intensity rainfall shows an increasing trend at all

Table 6.3 Mean ITA slopes for each rainfall category.

Grid Point	Annual			Winter			Pre-Monsoon			Monsoon			Post-Monsoon		
	L	M	H	L	M	H	L	M	H	L	M	H	L	M	H
P1	-14.26	-12.59	9.22	-0.07	-0.40	-0.65	-3.02	-5.70	-4.51	-9.80	-7.25	12.07	-0.14	0.33	4.34
P2	-18.25	6.76	124.25	0.00	-0.11	0.92	-4.40	-1.92	8.71	-10.95	6.98	99.87	0.02	1.55	13.90
P3	-18.78	-5.19	74.86	0.00	-0.18	0.37	-4.84	-3.40	5.15	-10.62	-2.42	57.37	0.09	0.63	9.98
P4	-11.84	-1.66	45.23	-0.03	-0.14	0.33	-3.24	-1.42	3.32	-7.20	-0.43	37.61	-0.24	0.13	4.37
P5	-5.24	-2.26	4.37	-0.02	-0.17	0.21	-1.60	-0.41	2.17	-2.93	-1.49	3.03	-0.12	-0.20	-1.59
P6	-6.37	-0.44	14.94	-0.05	-0.21	-0.39	-1.51	-1.57	-0.21	-5.62	-0.24	12.99	0.37	1.46	4.00
P7	-6.32	8.04	43.33	0.02	-0.06	0.01	-0.61	0.91	7.73	-4.08	4.79	31.29	0.47	1.78	7.10
P8	-5.50	8.20	67.25	-0.01	0.06	0.87	-0.52	1.52	10.65	-3.65	5.09	46.69	0.34	1.41	8.38
P9	-5.27	-1.17	9.02	-0.02	-0.05	0.18	-0.61	0.07	0.67	-3.69	-1.27	5.21	0.14	0.27	0.36
P10	-2.82	-0.80	5.75	0.00	-0.15	0.16	-0.50	-0.10	0.13	-1.24	-0.40	4.15	-0.26	0.01	-0.82
P11	-7.57	-1.32	1.12	-0.06	-0.20	-0.59	-0.80	-1.67	-1.73	-4.72	-0.71	2.13	0.26	0.70	3.46
P12	-3.73	1.63	5.42	0.00	-0.06	-0.01	0.31	0.23	0.99	-2.06	0.30	2.42	0.23	0.79	2.76
P13	-5.09	-0.49	5.20	0.00	-0.02	0.47	-0.11	0.27	1.42	-3.38	-1.27	1.68	0.14	0.31	1.56
P14	-11.24	-1.78	11.67	-0.05	-0.07	0.14	-1.20	-0.18	0.60	-8.07	-1.56	9.40	-0.11	-0.08	0.58
P15	-2.06	-0.20	7.66	-0.02	-0.05	0.01	-0.54	0.12	-0.50	-1.12	0.09	5.15	-0.20	0.09	-0.75
P16	0.34	1.03	6.67	-0.02	-0.17	-0.52	0.00	-0.12	-1.27	1.18	0.89	4.68	0.21	0.41	2.96
P17	-2.19	0.34	4.81	0.01	-0.06	0.19	-0.03	-0.01	0.56	-0.56	-0.18	1.43	0.01	0.34	2.97
P18	-3.30	-1.36	-1.64	0.01	-0.08	0.46	-0.85	-0.71	-1.08	-1.48	-1.47	0.35	0.00	0.52	0.62
P19	-5.28	-1.61	12.30	-0.05	-0.08	0.26	-1.04	0.14	0.89	-4.40	-1.74	9.73	-0.21	0.21	0.61

L= Low

M= Medium

H=High

P20	-6.97	-4.56	4.84	-0.05	-0.10	0.14	-0.98	-0.62	0.58	-3.99	-3.89	2.67	-0.26	-0.03	0.32

the grids. The rainfall intensities falling towards low and medium categories are dominated by a decreasing trend (Figure 6.8e). The increasing rainfall trend in post-monsoon season might have a significant impact on the soil, which are left barren after

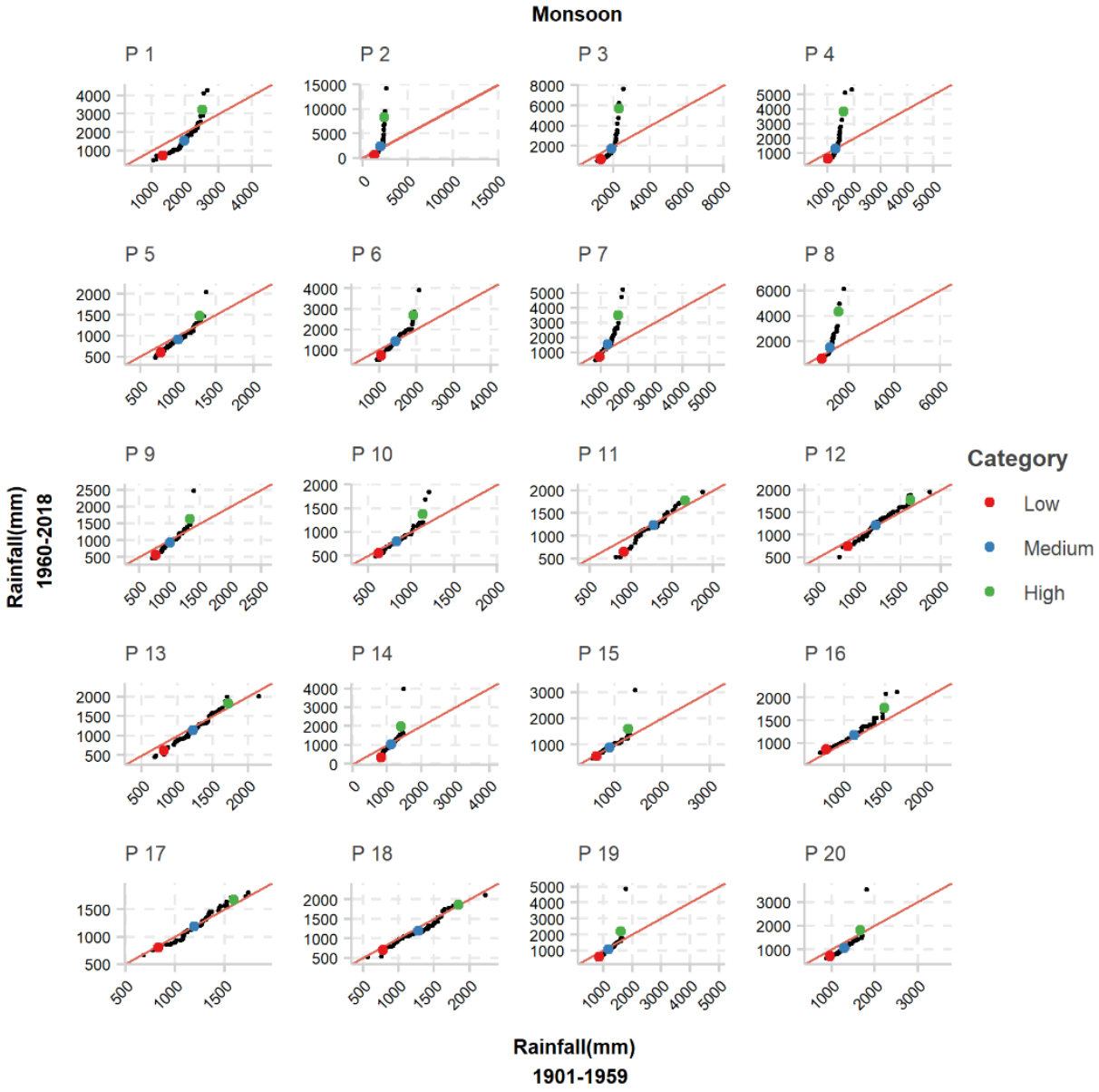

Figure 6.11 ITA plot of 20 IMD grid points for Monsoon rainfall.

slash and burn cultivation practiced widely in Meghalaya. The increase in high-intensity rainfall can also affect harvesting operations and increase soil loss after harvest.

Figure 6.5j presents the significance of MK test and also the Sen's slope for post-monsoon rainfall. Significant increasing trend ranging from 0.177 to 1.21 mm/year is found at 35% of the grids

(Figure 6.6j). Non-significant decreasing trends are found at grids P4, P5, P10, P14, and P20. Similar decreasing trends were observed on the ITA test for P5 and P10 but with significant values. Significant trends detected by the ITA were at 17 grids, whereas by MK test, it was only at 7 grids, once again showing the superiority of the ITA test in detecting hidden trends.

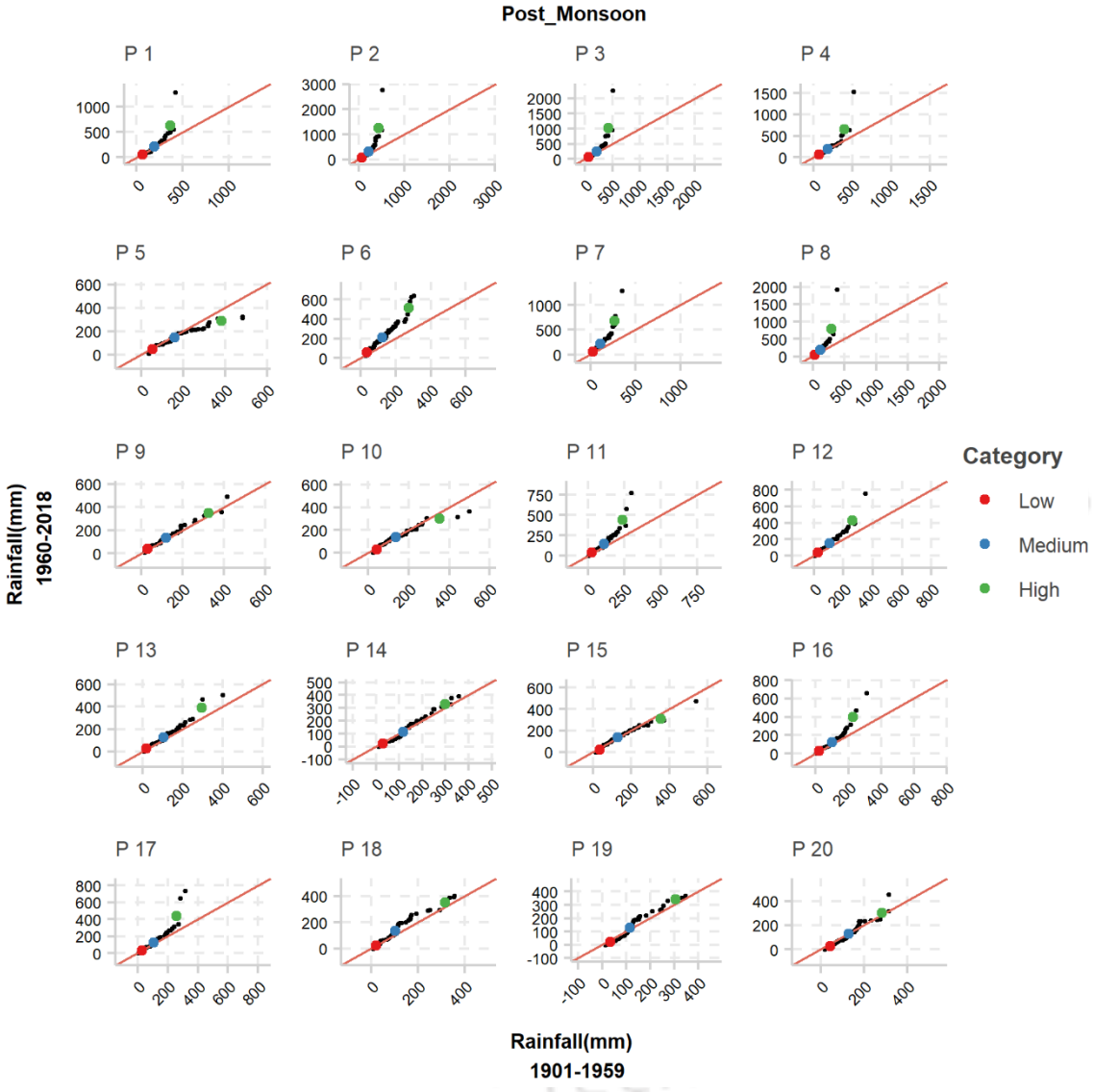

Figure 6.12 Post-Monsoon rainfall trend

6.5 Comparison with other studies

Trend analysis of rainfall in the study area is very limited. However, the results of the present study is compared with available existing literature. Choudhury et al. (2012) analysed the rainfall data of a single gauge in Umiam for the period 1983-2010. The study reported decreasing trend in monsoon rainfall, while non-significant increase in pre-monsoon and post-monsoon rainfall was found. Increasing trend in extreme rainfall was also reported in their study. The results of the present study is in agreement with Choudhury et al. (2012) for monsoon and post-monsoon rainfall trends. However, a decreasing trend for pre-monsoon rainfall was found in this study. Decreasing trend in monsoon rainfall was also reported by Jain et al. (2013) for Assam and Meghalaya region in their analysis for 1871-2008 period. Prokop and Walanus (2015), reported declining trend in low and moderate rainfall events during winter for Shillong and Cherrapunjee which is located approximately 50 Km from the present study area. Increase in heavy rains in pre-monsoon and monsoon season reported in their study is also consistent with the findings in the present study. Likewise, an increasing trend in annual rainfall was also reported by Prokop and Walanus (2003) for Cherrapunjee, Shillong and Mawplhang. Laskar et al. (2014) carried out the analysis of rainfall and temperature trends during 1913-2012 for the whole NER of India. The study reported no significant trend in all seasons for Shillong and Cherrapunjee whereas, Subash and Sikka (2013) reported decreasing trend in annual rainfall for Assam and Meghalaya region.

It was found that grid points lying towards the southern region (25° 30’ 00” N) which are at higher elevations of Shillong plateau, show increasing trends for both ITA and MK test (for eg. P2, P7, P8). Whereas, majority of the grid points show a decreasing trend towards the northern region at lower elevation, bordering Assam. Previous study by Sato (2013) on the mechanism of orographic precipitation in Meghalaya reported that the high convective systems develop over the southern slope. This may be the reason why heavy precipitation is mostly concentrated in the southern slope of Meghalaya (Murata et al. 2007). Another reason for orographic precipitation in the southern region of Meghalaya was moisture rich southwesterly wind. The higher elevation in the Shillong plateau may act as a barrier and induce a rain shadow effect on the lee side of the plateau (Sato 2013). Thus, the precipitation trends in regions where orography plays a major role may slightly differ when compared on a larger scale with its surroundings.

On comparing the results obtained using the ITA and Mann-Kendall test, it is observed that ITA is more robust in detecting trends, which is in agreement with other studies (Dabanlı et al. 2016; Öztopal and Şen 2017; Wu and Qian 2017; Zhou et al. 2018).

6.6 **Conclusions**

In this chapter, the variation of annual and seasonal rainfall in Umiam and Umtru watersheds were analyzed using the ITA and MK-test. The graphical nature of the ITA test enables the easier perception of even the non-monotonic trends. Since ITA method is relatively new, the authenticity of ITA method was verified using a widely used method, the MK test. The ITA method was used to find the trend on an annual and seasonal basis and also to find the trends in different rainfall categories. The results obtained from the two methods generally concur, supporting the capability of the ITA method. The ITA test is relatively simple to use and easy to understand. Its non-dependability on data distribution, autocorrelation, and length of data is an added advantage to its applications in hydrology. Moreover, the ITA method presents certain advantages in detecting trends in different clusters of data, which enables in-depth insight into extreme values. A consensus is observed with regards to trends in extreme rainfall values across annual and seasonal scales. There has been an increasing trend in high rainfall. Low and medium rainfall seems to have decreased during the 1901 to 2018 period. It is found that ITA is more sensitive in detecting hidden trends missed out by the MK test. For example, in the case of annual rainfall, significant trends were detected in 60% of the grids in the MK test, whereas the ITA method detected 90%. From the results obtained using the two methods, it can be concluded that annual, winter, pre-monsoon, and monsoon rainfall is decreasing, whereas, the post-monsoon rainfall is increasing in Umiam and Umtru watershed. The outcomes of this study may be helpful in planning and management of water resources projects and in planning of mitigation measures to alleviate the effects of climate change under extreme rainfall conditions.

CHAPTER 7

Impact of projected climate change and human activities on streamflow

7.1 Bias correction of the Coordinated Regional Downscaling Experiment (CORDEX).

CORDEX is a program sponsored by World Climate Research Program (WCRP) to develop an improved framework for generating regional-scale climate projections for impact assessment and adaptation studies worldwide using improved downscaling techniques, both statistical and dynamical.

Table 7.1 CORDEX data used

CORDEX RCM	Driving AOGCM	Institute
IITM_RegCM4	CCCma-CanESM2	Canadian Centre for Climate Modelling and Analysis (CCCma), Canada
SMHI-RCA4	CSIRO-Mk3-6-0	CSIRO, Australia
MPI-CSC-REMO2009	MPI-M-MPI-ESM-LR	MPI-M, Germany

Bias correction of the CORDEX output was done using linear scaling method (Lenderink et al. 2007)

$$P_{cor,m,d} = \ = P_{raw,m,d} \times \frac{\mu(P_{obs,m})}{\mu(P_{raw,m})} \quad (7.1)$$

Where, μ represents monthly mean value of observed precipitation, $P_{obs,m}$ and uncorrected model precipitation, $P_{raw,m}$.

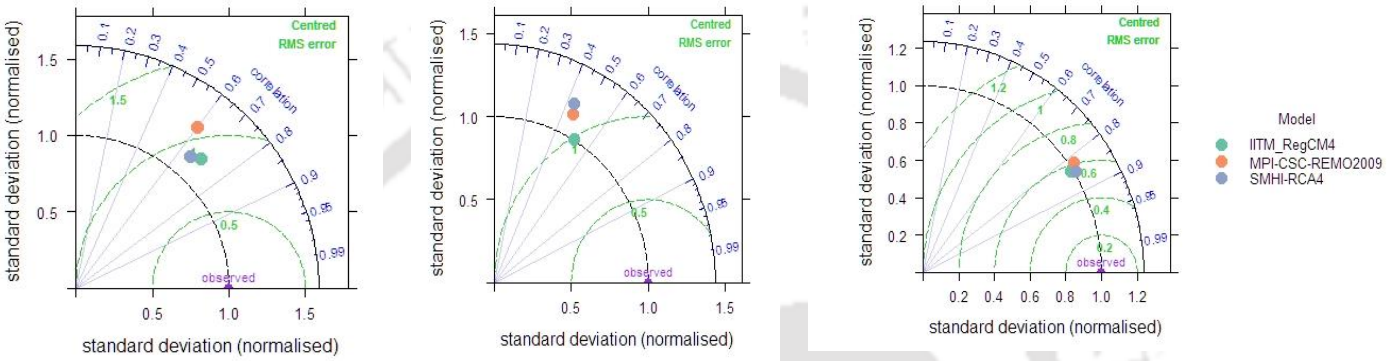

a. PCP b.TMAX c.TMIN

Figure 7.1 Taylor diagrams showing performance of RCM outputs against observed data

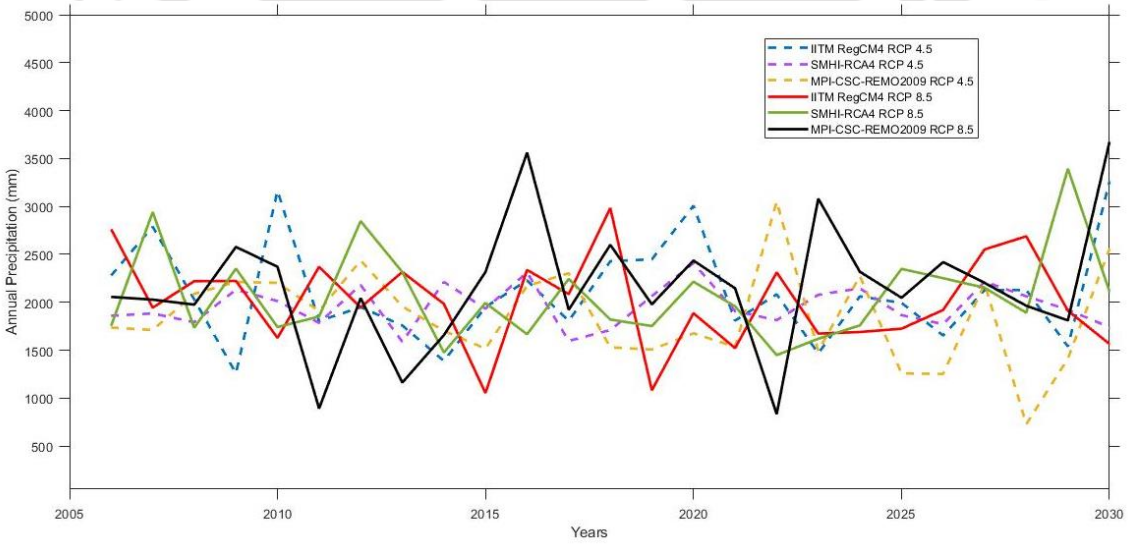

Figure 7.2 Comparison of precipitation generated by different RCM models under RCP scenarios.

Figure 7.2 Shows the precipitation generated by different RCM models. It is observed that precipitation tends to be intensified under RCP 8.5. From RCP 4.5 scenarios, the IITM_RegCM4 predicts higher precipitation in several years whereas from RCP 8.5 scenario the MPI-CSC-REMO2009 predicts higher precipitation.

7.2 **Projection of landuse changes using ANN and Cellular Automata**

Landuse/landcover (LULC) map for 2005, 2010 from National Remote Sensing Centre, was used to project LULC of 2015 based on the CA-ANN model using MOLUSCE (Modules of Land Use Change Evaluation) software. This software has been found to be reliable in other studies (Alam et al. 2021; Hakim et al. 2019). Two types of variables were considered as the input variables while performing the prediction for this study; the dependent variable and the independent variable. The historical change pattern of the LULC maps of 2005 and 2010 were considered as the dependent variable, and the independent variables was the elevation (DEM). Seven landuse classes were defined in the landuse maps.

The scenarios with different LULC and Climate data combinations are given in Table 7.3. From this table, the effect of LULC and Climate can be worked out as:

$$\text{Effect of LULC} = S2 - S1 \quad (7.2)$$

$$\text{Effect of Climate} = S3 - S1 \quad (7.3)$$

$$\text{Effect of LULC} + \text{Climate} = S4 - S1 \quad (7.4)$$

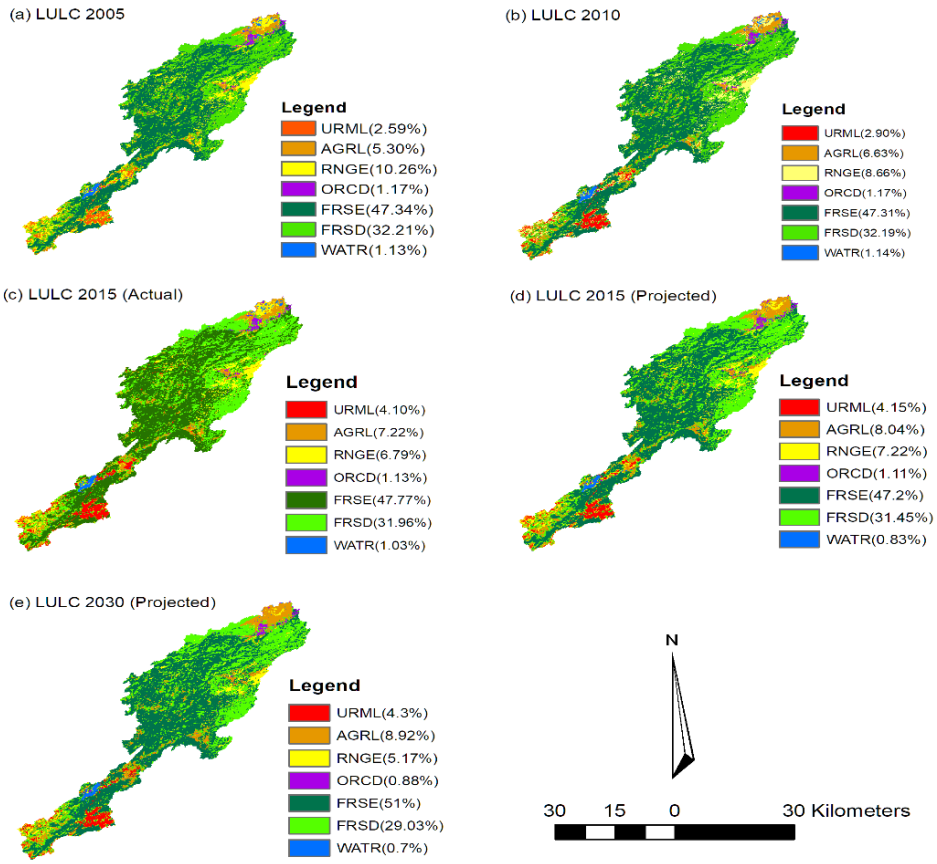

Figure 7.3 LULC change prediction

Table 7.2 Transition matrix of LULC classes (2005-2010)

	URML	AGRL	RNGE	ORCD	FRSE	FRSD	WATR
URML	0.855662	0.025692	0.057885	0.000459	0.017909	0.040556	0.001837
AGRL	0.008301	0.764566	0.087495	0.011615	0.023855	0.095101	0.009068
RNGE	0.044719	0.163409	0.610917	0.003432	0.067905	0.101132	0.008487
ORCD	0.003633	0.034938	0.044661	0.78642	0.022971	0.089054	0.018324
FRSE	0.001193	0.002208	0.014738	0.000493	0.921852	0.059056	0.000461
FRSD	0.003708	0.019222	0.030056	0.003389	0.086146	0.855792	0.001687
WATR	0.002321	0.057247	0.050229	0.015914	0.020224	0.055424	0.798641

Table 7.3 Model configuration under different scenarios.

	LULC	Climate	CORDEX RCM	Driving AOGCM	Institute	RCP	Simulation Numbering
S1	2010	2006-2015 (IMD)	None	None	None	None	S1
S2	2025	2006-2015 (IMD)	None	None	None	None	S2
S3	2010	2021-2030 (CORDEX)	IITM_RegCM4	CCCma-CanESM2	Canadian Centre for Climate Modelling and Analysis (CCCma), Canada	RCP4.5	S3.1(a)
						RCP8.5	S3.1(b)
			SMHI-RCA4	CSIRO-Mk3-6-0	CSIRO, Australia	RCP4.5	S3.2(a)
						RCP8.5	S3.2(b)
			MPI-CSC-REMO2009	MPI-M-MPI-ESM-LR	MPI-M, Germany	RCP4.5	S3.3(a)
						RCP8.5	S3.3(b)
S4	2025	2021-2030 (CORDEX)	IITM_RegCM4	CCCma-CanESM2	Canadian Centre for Climate Modelling and Analysis (CCCma), Canada	RCP4.5	S4.1(a)
						RCP8.5	S4.1(b)
			SMHI-RCA4	CSIRO-QCCCE-	CSIRO, Australia	RCP4.5	S4.2(a)
						RCP8.5	S4.2(b)

		CSIRO-Mk3-6-0			
	MPI-CSC-REMO2009	MPI-M-MPI-ESM-LR	MPI-M, Germany	RCP4.5 RCP8.5	S4.3(a) S4.3(b)

7.3 **Results and discussion**

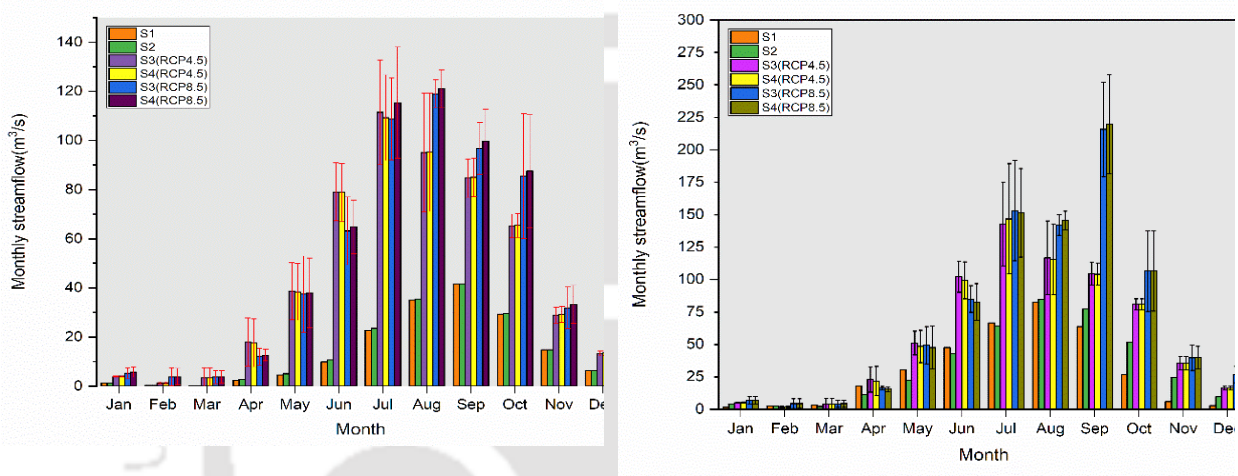

With Umiam Dam Umiam Undammed

Figure 7.4 Mean value of monthly flow for different RCMs. The error bars represent range of standard deviation.

IITM_RegCM4 and SMHI-RCA4 gives the best result in simulating precipitation among 3 CORDEX models with the lesser value of normalized standard deviation and higher R^2. In contrast, the SMHI-RCA4 gives less accurate results in simulating maximum temperature as seen in Taylor diagrams (Figure 7.4). All three RCMs simulated minimum temperature (TMIN) more accurately than precipitation (PCP) and maximum temperature (TMAX).

Under dammed condition, highest flow in January to March occurs in S3 and S4 (RCP 8.5). In April, June highest flow occurs in S3 and S4 (RCP 4.5). In the rest of the months, the highest flow occurs in S3 and S4 under RCP 8.5. Under undammed scenario, the timing of highest flow shifts to September for S3 and S4 scenarios under RCP 8.5(Figure 7.4). The simulations with and without the reservoir, show huge differences in streamflow rate under all scenarios. The maximum flow

under dammed condition was 121 while the minimum flow was 0.155 m^3/s whereas under undammed condition, the maximum flow was 219 m^3/s and minimum flow was 1.45 m^3/s.

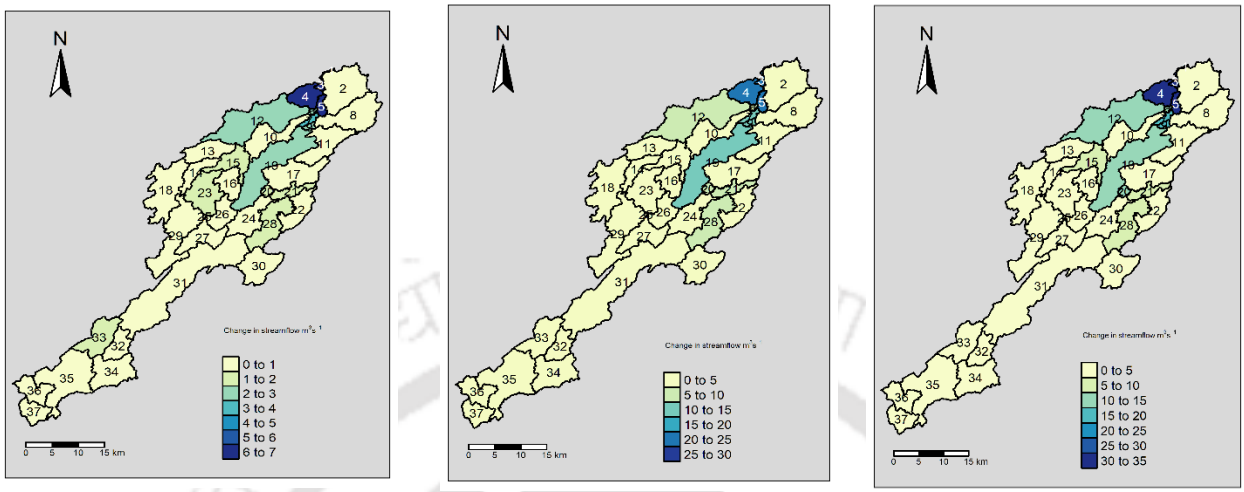

S2-S1 S3.1a-S1 S3.1b-S1

Figure 7.5 Spatial variation of changes in streamflow under different climate scenarios

Spatial variation of changes in streamflow due to LULC change is shown in Figure 7.5. This value is obtained by subtracting the streamflow in S1 from that of S2. The range of streamflow change reaches up to 7 m^3/s. The value of streamflow obtained by operation S3-S1 represents the changes in streamflow due to climate only as the LULC was constant. The changes were more pronounced in sub-basin 1,3,4,5 and 19 under both RCPs and different RCMs as shown from Figure 7.5 to Figure 7.8. Indicating that these sub-basins are more vulnerable to climate change.

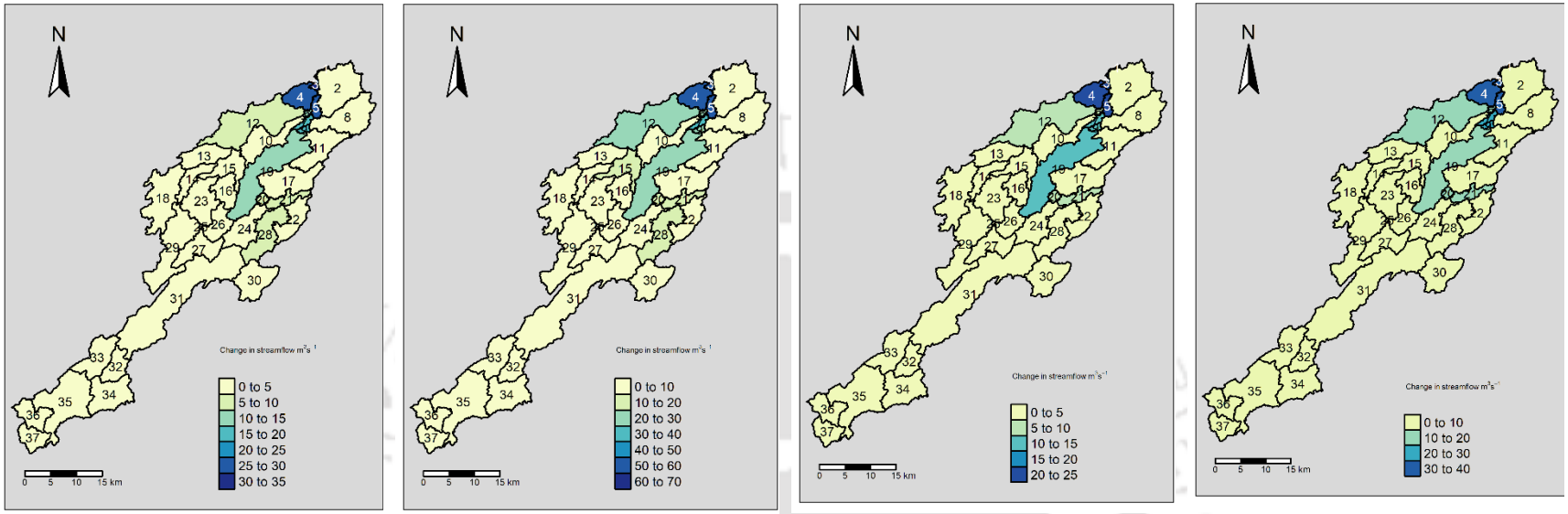

S3.2a-S1 S3.2b-S1 S3.3a-S1 S3.3b-S1

Figure 7.6 Spatial variation of changes in streamflow under different climate scenarios

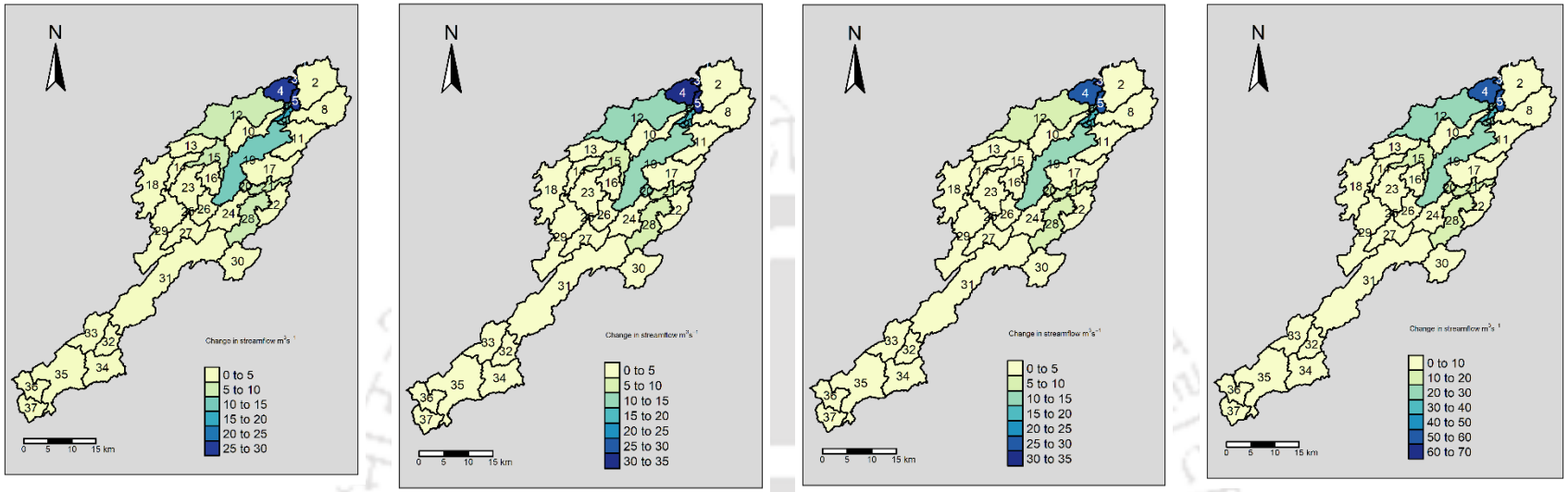

S4.1a-S1 S4.1b-S1 S4.2a-S1 4.2b-S1

Figure 7.7 Spatial variation of changes in streamflow due to climate and landuse change

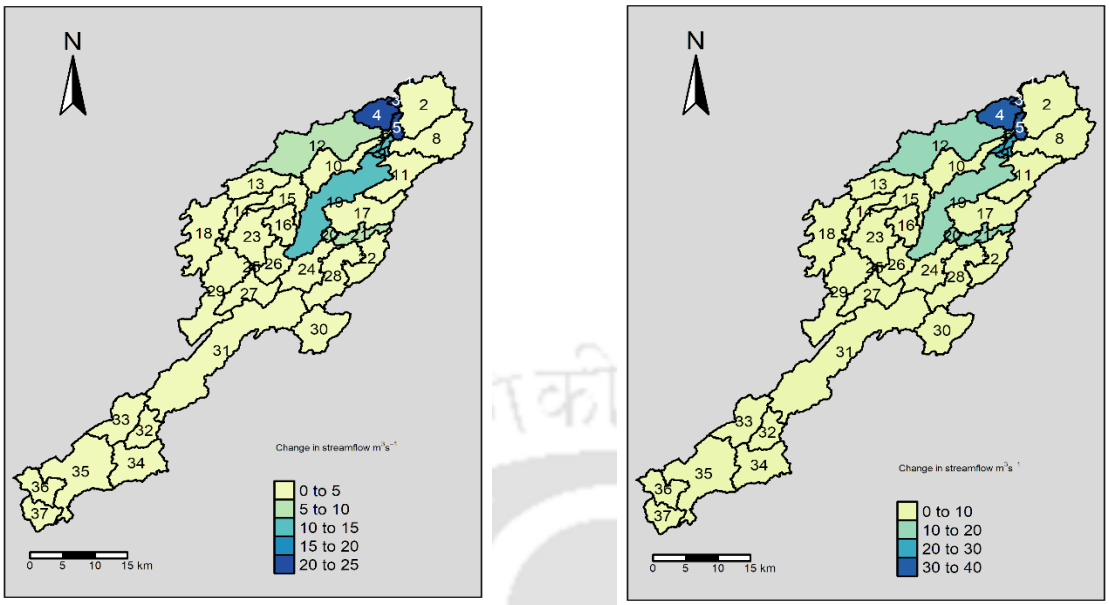

S4.3a-S1 S4.3b-S1

Figure 7.8 Spatial variation of changes in streamflow due to climate and landuse change for (S4.3a-S1) and (S4.3b-S1)

Similarly, under undammed condition the changes in streamflow under all the above climate change scenarios were also calculated. The streamflow for S2-S1 under undammed condition has lower variation than with the dam (Figure 7.9) indicating that effect of lulc change is lesser. The highest change due to LULC is found in sub-basin 4.

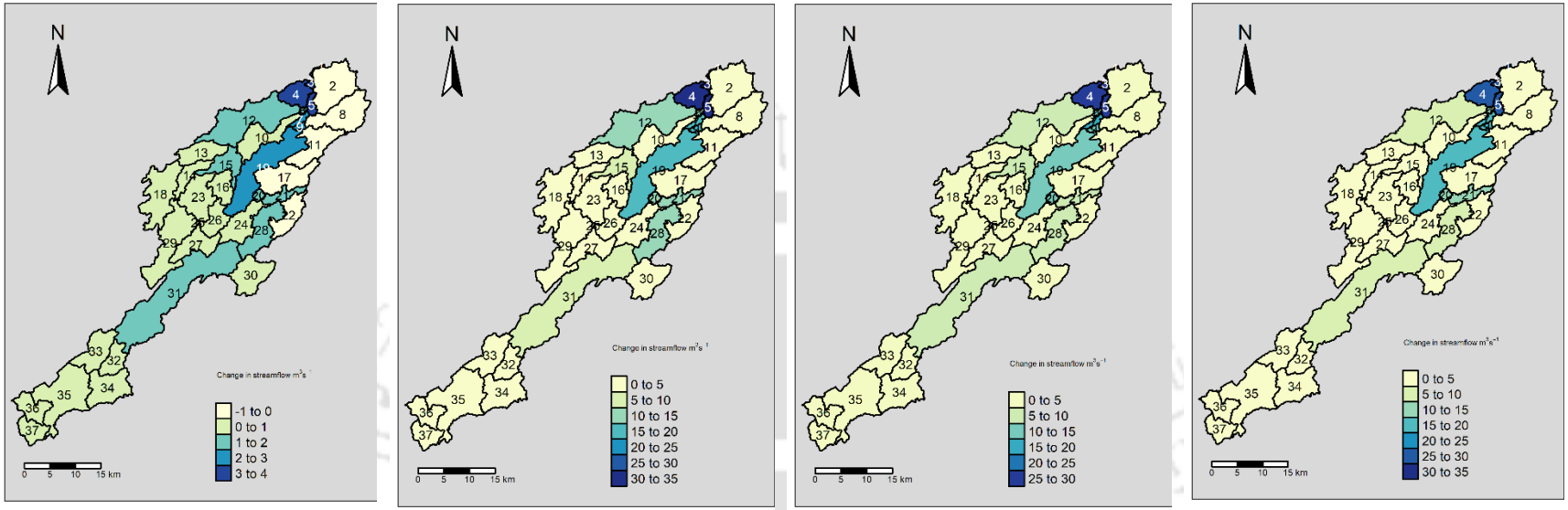

S2-S1 S3.1a-S1 S3.1b-S1 S3.2a-S1

Figure 7.9 Spatial variation of changes in streamflow due to climate and landuse change under no reservoir condition (S2-S1) to (S3.2a-S1).

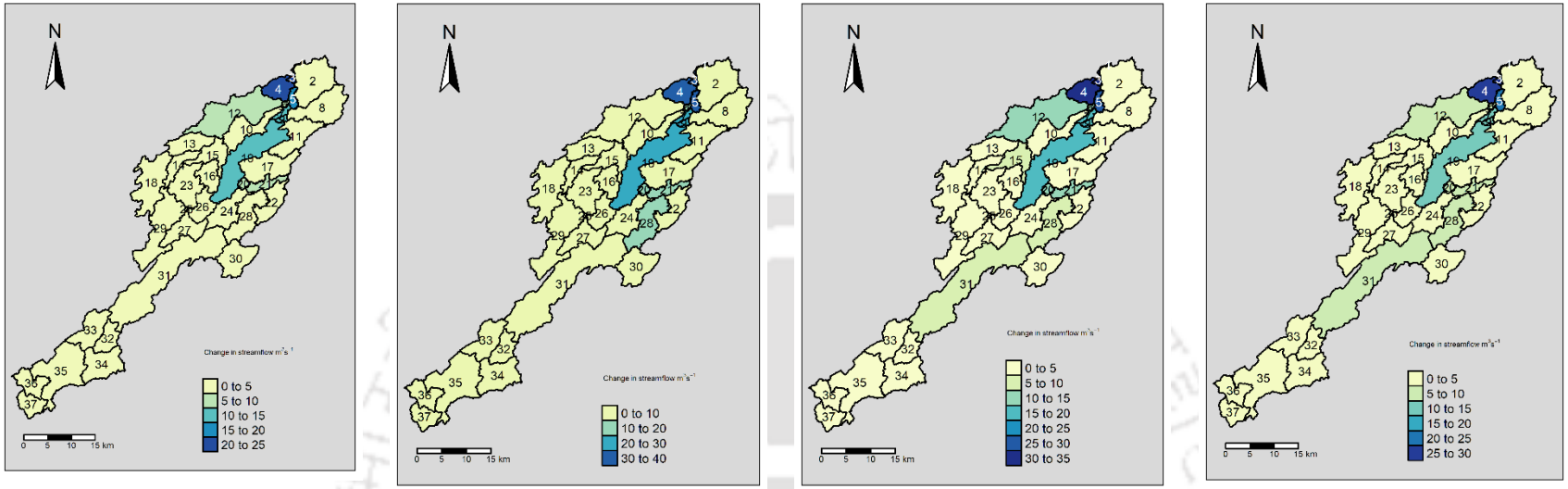

S3.2b-S1 S3.3a-S1 S3.3b-S1 S4.1a-S1

Figure 7.10 Spatial variation of changes in streamflow due to climate and landuse change under no reservoir condition (S3.2b-S1) to (S4.1a-S1).

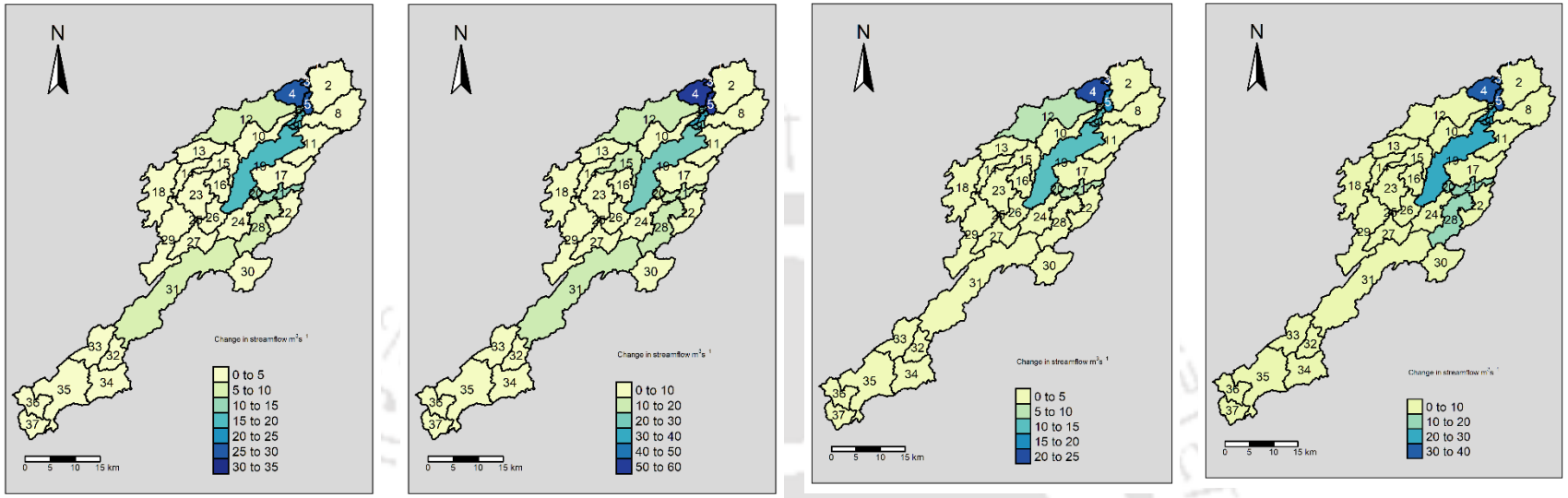

S4.1b-S1 S4.2a-S1 S4.2b-S1 S4.3a-S1

Figure 7.11 Spatial variation of changes in streamflow due to climate and landuse change under no reservoir condition (S4.1b-S1) to (S4.3a-S1).

7.4 **Conclusions**

The effect of climate change and landuse change was analyzed using SWAT model and CORDEX climate model outputs. Three CORDEX models were considered in this study, IITM_RegCM4, MPI-CSC-REMO2009 and SMHI-RCA4. IITM_RegCM4 and SMHI-RCA4 gives the best result in simulating precipitation among 3 CORDEX models with the lesser value of normalized standard deviation and higher R^2. Under dammed condition, highest flow in January to March occurs in S3 and S4 (RCP 8.5). In April, June highest flow occurs in S3 and S4 (RCP 4.5). Under undammed scenario, the timing of highest flow shifts to September for S3 and S4 scenarios under RCP 8.5. In all the scenarios, sub-basin 4 is found to have the highest change in flow due to climate and landuse change.

CHAPTER 8

Summary and conclusion

8.1 Introduction

The chapters presented in this thesis dealt with different objectives exclusively, but there exists an intrinsic relationship among these objectives that are essential in understanding the hydrological behavior of the watersheds. This chapter presents the overall conclusions that were obtained from this research work.

8.2 Summary and Conclusions

The review of literature provided an overview of the impacts of changing climate on hydrological response. Studies conducted in different regions of the world were explored and most of them projected increasing temperature and precipitation extremes in near future. While there have been many studies done by different researchers in India, studies on climate change impacts on watersheds with regulated flows and Inter-Basin Water Transfer were very limited especially in the North Easter region of India. This led the author to take up Umiam and Umtru watersheds in Meghalaya for analyzing the impacts of IBWT and also to assess the effect of climate change on its hydrology.

The Umiam Reservoir is the first reservoir in the Umiam River. The main purpose of the Umiam Reservoir is to transfer water from Umiam Basin to Umtru Basin for hydropower generation. The diverted water then joins Umtru River and runs through a cascade of reservoirs comprising of Kyrdemkulai Reservoir, Nongmahir Reservoir, Umiam Stage-IV Reservoir and Umtru Reservoir. In order to analyze the effects of these reservoirs a hydrological model was set up using SWAT and was run under designed scenarios. The SWAT model was also run under different landuse and climate scenarios.

The effect of IBWT from Umiam Basin was analyzed by creating two flow scenarios i.e. natural flow and altered flow. The analysis was carried out for 32 parameters based on Range of Variability Approach applied through the Indicators of Hydrologic Alteration (IHA) software. The results indicated reduced flow during the lean period. At 50% exceedance probability for flow, the flow rates decreased by 32.5% and 1-day maximum flows was decreased by 54%. The analysis found an overall alteration of 71.82%.

After analysis of changes in flow in Umiam Basin due to IBWT Reservoir, the impacts on the recipient Umtru Watershed was analysed using the similar methods. The analysis revealed that Inter-Basin Water Transfer and cascading reservoirs have increased the flow rate in Umtru Basin. It was also found out that the negative hydrological alterations would have been higher if the dams are constructed without IBWT being done. Among all the reservoirs, the highest impact comes from Umtru Reservoir which can alter yearly median flows by up to 106.8%. When all dams are operated without IBWT yearly median flows change by 95%. The effect is lowest when all dams are operating with the IBWT in place (38.49%).

After the hydrological analysis, the rainfall trend in the study area was analysed which is one of the most important factors affecting streamflow. The trend analysis was performed on gridded rainfall data of Indian Meteorological Department using the Innovative Trend Analysis (ITA) method and Mann-Kendall Test. The trend analysis of rainfall indicates an increasing trend in high-intensity rainfall and a decreasing trend in low and medium-intensity rainfall on an annual and seasonal scale in the Umiam and Umtru watershed.

The assessment of the impacts of climate change and landuse change was also attempted using CORDEX data with 3 RCMs i.e., IITM_RegCM4, SMHI-RCA4, MPI-CSC-REMO2009. The analysis revealed that changes in landuse and climate increases the streamflow in the Umiam Basin. The hydrological model simulation was done with and without the dam. It was found that the occurrence of high flows under climate change is less when dam is present.

8.3 **Scope for future work:**

- The study considered only hydrological aspects of the watershed. Future studies may explore hydraulic and flood inundation studies for future climate scenarios.
- Although reservoir was considered, optimization algorithms were not incorporated, therefore there is a scope to incorporate optimization of reservoir operation.

- Hydrologic alteration can affect the habitat suitability of aquatic species. In this study, the hydrological alterations were studied but there is a scope to include habitat suitability of different aquatic species.
- The model can be coupled with outputs from Weather Research and Forecasting (WRF) data for flood prediction and advance reservoir operating rules.

Bibliography

Abbaspour, K. C. (2015). *SWAT-CUP: SWAT Calibration and Uncertainty Programs—A User Manual*. *Swiss Federal Institute of Aquatic Science and Technology*, Dubendorf, Switzerland.

Abbaspour, K. C., Rouholahnejad, E., Vaghefi, S., Srinivasan, R., Yang, H., and Kløve, B. (2015). "A continental-scale hydrology and water quality model for Europe: Calibration and uncertainty of a high-resolution large-scale SWAT model." *Journal of Hydrology*, Elsevier B.V., 524, 733–752.

Abbaspour, K., Vaghefi, S., and Srinivasan, R. (2017). "A Guideline for Successful Calibration and Uncertainty Analysis for Soil and Water Assessment: A Review of Papers from the 2016 International SWAT Conference." *Water*, 10(1), 6.

Adam, J. C., Haddeland, I., Su, F., and Lettenmaier, D. P. (2007). "Simulation of reservoir influences on annual and seasonal streamflow changes for the Lena, Yenisei, and Ob' rivers." *Journal of Geophysical Research Atmospheres*, 112(24), 1–22.

Ahmadaali, J., Barani, G.-A., Qaderi, K., and Hessari, B. (2018). "Analysis of the Effects of Water Management Strategies and Climate Change on the Environmental and Agricultural Sustainability of Urmia Lake Basin, Iran." *Water*, 10(2), 160.

Alam, N., Saha, S., Gupta, S., and Chakraborty, S. (2021). "Prediction modelling of riverine landscape dynamics in the context of sustainable management of floodplain: a Geospatial approach." *Annals of GIS*, Taylor & Francis, 00(00), 1–16.

Alashan, S. (2018). "An improved version of innovative trend analyses." *Arabian Journal of Geosciences*, 11(3).

Alcamo, J., Flörke, M., and Märker, M. (2007). "Future long-term changes in global water resources driven by socio-economic and climatic changes." *Hydrological Sciences Journal*, 52(2), 247–275.

Alcamo, J., and Henrichs, T. (2002). "Critical regions: A model-based estimation of world water resources sensitive to global changes." *Aquatic Sciences*, Birkhäuser Verlag, 352–362.

Alemu, M. M., and Bawoke, G. T. (2019). "Analysis of spatial variability and temporal trends of

rainfall in Amhara region, Ethiopia." *Journal of Water and Climate Change*, 1–16.

Ali, H., Mishra, V., and Pai, D. S. (2014). "Observed and projected urban extreme rainfall events in India." *Journal of Geophysical Research: Atmospheres*, John Wiley & Sons, Ltd, 119(22), 12,612-621,641.

Arnell, N. W. (2004). "Climate change and global water resources: SRES emissions and socio-economic scenarios." *Global Environmental Change*, Pergamon, 14(1), 31–52.

Arnold, J. G., and Fohrer, N. (2005). "SWAT2000: Current capabilities and research opportunities in applied watershed modelling." *Hydrological Processes*, 19(3), 563–572.

Arnold, J. G., Moriasi, D. N., Gassman, P. W., Abbaspour, K. C., White, M. J., Srinivasan, R., Santhi, C., Harmel, R. D., Griensven, a. Van, VanLiew, M. W., Kannan, N., and Jha, M. K. (2012). "Swat: Model Use, Calibration, and Validation." *Asabe*, 55(4), 1491–1508.

Arnold, J. G., Srinivasan, R., Muttiah, R. S., and Williams, J. R. (1998). "LARGE AREA HYDROLOGIC MODELING AND ASSESSMENT PART I: MODEL DEVELOPMENT1." *JAWRA Journal of the American Water Resources Association*, John Wiley & Sons, Ltd (10.1111), 34(1), 73–89.

Arthington, A., Bunn, S., Poff, L., and Naiman, R. (2006). "The Challenge of Providing Environmental Flow Rules To Sustain River Ecosystems." *Ecological Applications*, 16(4), 1311–1318.

Asefa, T., Clayton, J., Adams, A., and Anderson, D. (2014). "Performance evaluation of a water resources system under varying climatic conditions: Reliability, Resilience, Vulnerability and beyond." *Journal of Hydrology*, Elsevier B.V., 508, 53–65.

Atkinson, H. D. E., Johal, P., Falworth, M. S., Ranawat, V. S., Dala-Ali, B., and Martin, D. K. (2010). "Adductor tenotomy: Its role in the management of sports-related chronic groin pain." *Archives of Orthopaedic and Trauma Surgery*, 130(8), 965–970.

Bal, P. K., Ramachandran, A., Palanivelu, K., Thirumurugan, P., Geetha, R., and Bhaskaran, B. (2016). "Climate change projections over India by a downscaling approach using PRECIS." *Asia-Pacific Journal of Atmospheric Sciences*, 52(4), 353–369.

Bates, B. C., Kundzewicz, Z. W., Wu, S., and Palutikof, J. P. (2008). *Climate Change and Water*. *Climate change and water*.

Bayazit, M., and Önöz, B. (2007). “To prewhiten or not to prewhiten in trend analysis?” *Hydrological Sciences Journal*, 52(4), 611–624.

Bekele, E. G., and Knapp, H. V. (2010). “Watershed Modeling to Assessing Impacts of Potential Climate Change on Water Supply Availability.” *Water Resources Management*, 24(13), 3299–3320.

Biemans, H., Haddeland, I., Kabat, P., Ludwig, F., Hutjes, R. W. A., Heinke, J., Von Bloh, W., and Gerten, D. (2011). “Impact of reservoirs on river discharge and irrigation water supply during the 20th century.” *Water Resour. Res*, 47.

Bisht, D. S., Chatterjee, C., Raghuwanshi, N. S., and Sridhar, V. (2018). “Spatio-temporal trends of rainfall across Indian river basins.” *Theoretical and Applied Climatology*, Theoretical and Applied Climatology, 132(1–2), 419–436.

Bond, N. R., Lake, P. S., and Arthington, A. H. (2008). “The impacts of drought on freshwater ecosystems: An Australian perspective.” *Hydrobiologia*.

Brunner, M. I., Björnsen Gurung, A., Zappa, M., Zekollari, H., Farinotti, D., and Stähli, M. (2019). “Present and future water scarcity in Switzerland: Potential for alleviation through reservoirs and lakes.” *Science of The Total Environment*, Elsevier, 666, 1033–1047.

Caloiero, T. (2020). “Evaluation of rainfall trends in the South Island of New Zealand through the innovative trend analysis (ITA).” *Theoretical and Applied Climatology*, Theoretical and Applied Climatology, 139(1–2), 493–504.

Caloiero, T., Coscarelli, R., and Ferrari, E. (2017). “Analysis of rainfall trend in southern Italy through the application of the ITA technique.” *European Water*, 59(2014), 199–206.

Carvalho-Santos, C., Monteiro, A. T., Azevedo, J. C., Honrado, J. P., and Nunes, J. P. (2017). “Climate Change Impacts on Water Resources and Reservoir Management: Uncertainty and Adaptation for a Mountain Catchment in Northeast Portugal.” *Water Resources Management*, Water Resources Management, 31(11), 3355–3370.

Choudhury, B. U., Das, A., Ngachan, S. V, Slong, A., Bordoloi, L. J., and Chowdhury, P. (2012). “Trend Analysis of Long Term Weather Variables in Mid Altitude Meghalaya , North-East India.” *Journal of Agricultural Physics*, 12(1), 12–22.

Christensen, N., and Lettenmaier, D. P. (2007). “A multimodel ensemble approach to assessment

of climate change impacts on the hydrology and water resources of the Colorado River Basin." *Hydrology and Earth System Sciences Discussions*, 3, 3727–3770.

Le Comte, D. (1998). "Weather Highlights: Around the World." *Weatherwise*, Routledge, 51(2), 26–31.

Dabanli, I., and Şen, Z. (2018). "Classical and innovative-Şen trend assessment under climate change perspective." *International Journal of Global Warming*, 15(1), 19–37.

Dabanlı, İ., Şen, Z., Yeleğen, M. Ö., Şişman, E., Selek, B., and Güçlü, Y. S. (2016). "Trend Assessment by the Innovative-Şen Method." *Water Resources Management*, 30(14), 5193–5203.

Das, A., Ghosh, P. ., Choudhury, B. ., Patel, D. ., Munda, G. ., Ngachan, S. ., and Chowdhury, P. (2009). "Climate Change in Northeast India: Recent Facts and Events –Worry for Agricultural Management." *ISPRS Archives XXXVIII-8/W3 Workshop Proceedings: Impact of Climate Change on Agriculture*, 1–6.

Das, S., Tomar, C. S., Saha, D., Shaw, S. O., and Singh, C. (2015). "Trends in Rainfall Patterns over North-East India during 1961-2010 ." *International Journal of Earth and Atmospheric Science*, 2(2), 37–48.

Dave, H., and James, M. E. (2017). "Characteristics of intense rainfall over Gujarat State (India) based on percentile criteria." *Hydrological Sciences Journal*, Taylor & Francis, 62(12), 2035–2048.

Dimri, A. P., Kumar, D., Choudhary, A., and Maharana, P. (2018). "Future changes over the Himalayas: Mean temperature." *Global and Planetary Change*, Elsevier, 162(November 2017), 235–251.

Duncan, J. M. A., Dash, J., and Atkinson, P. M. (2013). "Analysing temporal trends in the Indian Summer Monsoon and its variability at a fine spatial resolution." *Climatic Change*, 117(1–2), 119–131.

Fowler, H. J., Blenkinsop, S., and Tebaldi, C. (2007). "Linking climate change modelling to impacts studies: recent advances in downscaling techniques for hydrological modelling." *International Journal of Climatology*, Wiley-Blackwell, 27(12), 1547–1578.

Frederick, K. D., and Major, D. C. (1997). "Climate change and water resources." *Climatic*

Change.

Gao, B., Li, J., and Wang, X. (2018). "Analyzing changes in the flow regime of the Yangtze River using the eco-flow metrics and IHA metrics." *Water (Switzerland)*, 10(11).

Gedefaw, M., Yan, D., Wang, H., Qin, T., Girma, A., Abiyu, A., and Batsuren, D. (2018). "Innovative trend analysis of annual and seasonal rainfall variability in Amhara Regional State, Ethiopia." *Atmosphere*, 9(9).

Güçlü, Y. S., Şişman, E., and Dabanlı, İ. (2020). "Innovative triangular trend analysis." *Arabian Journal of Geosciences*, 13(2).

Gul, Gulay Onusluel, Rosbjerg, Dan, Gul, Ali, Ondracek, Maria, Dikgola, K. (2010). "Ecohydrology Bearing - Invited Commentary Transformation ecosystem change and ecohydology: ushering in a new era for watershed management." *Ecohydrology*, 130(February), 126–130.

Hakim, A. M. Y., Baja, S., Rampisela, D. A., and Arif, S. (2019). "Spatial dynamic prediction of landuse / landcover change (case study: Tamalanrea sub-district, makassar city)." *IOP Conference Series: Earth and Environmental Science*, 280(1).

Hamed, K. H., and Rao, A. R. (1998). "A modified Mann-Kendall trend test for autocorrelated data." *Journal of Hydrology*, 204(1), 182–196.

Hamlet, A. F., and Lettenmaier, D. P. (2000). "JOURNAL OF THE AMERICAN WATER RESOURCES ASSOCIATION EFFECTS OF CLIMATE CHANGE ON HYDROLOGY AND WATER RESOURCES IN THE COLUMBIA RiVER BASIN1 natural and managed water resources of the Pacific Northwest . The basin covers portions of seven west- ern states ." 35(6), 1597–1623.

Hussen, B., Mekonnen, A., and Pingale, S. M. (2018). "Integrated water resources management under climate change scenarios in the sub-basin of Abaya-Chamo, Ethiopia." *Modeling Earth Systems and Environment*, Springer International Publishing, 4(1), 221–240.

"Indicators of Hydrologic Alteration, Version 7.1, User's Manual." (2009). *The Nature Conservancy*.

IPCC. (2018). "Summary for Policymakers. In: Global warming of 1.5°C. An IPCC Special Report on the impacts of global warming of 1.5°C above pre-industrial levels and related

global greenhouse gas emission pathways, in the context of strengthening the global response to." *World Meteorological Organization, Geneva, Switzerland.*

Jain, S. K., Kumar, V., and Saharia, M. (2013). "Analysis of rainfall and temperature trends in northeast India." *International Journal of Climatology*, 33(4), 968–978.

Jothiprakash, V., Praveenkumar, C., and Manasa, M. (2017). "Daily runoff estimation in Musi river basin , India , from gridded rainfall using SWAT model." *European Water*, 57, 63–69.

Kendall, M. G. (1938a). *Rank correlation. Nature*, Griffin, Oxford, England.

Kendall, M. G. (1938b). "A New Measure of Rank Correlation." *Biometrika*, 30(1–2), 81–93.

Kendall, M. G. (1948). *Rank correlation methods.* Charles Griffin & Co. Ltd., London.

Khan, M. L., Menon, S., and Bawa, K. S. (1997). "Effectiveness of the protected area network in biodiversity conservation: a case-study of Meghalaya state." *Biodiversity and Conservation*, Kluwer Academic Publishers, 6(6), 853–868.

Khattak, M. S., Babel, M. S., and Sharif, M. (2011). "Hydro-meteorological trends in the upper Indus River basin in Pakistan." *Climate Research*, 46(2), 103–119.

Kulshreshtha, S. N. (1998). "A Global Outlook for Water Resources to the Year 2025." *Water Resources Management*, 12(3), 167–184.

Kumar, D., and Dimri, A. P. (2017). "Regional climate projections for Northeast India: an appraisal from CORDEX South Asia experiment." *Theoretical and Applied Climatology*, Theoretical and Applied Climatology, 1–17.

Kumar, S., Merwade, V., Kam, J., and Thurner, K. (2009). "Streamflow trends in Indiana: Effects of long term persistence, precipitation and subsurface drains." *Journal of Hydrology*, Elsevier B.V., 374(1–2), 171–183.

Kundzewicz, Z. W., and Döll, P. (2009). "Will groundwater ease freshwater stress under climate change?" *Hydrological Sciences Journal*, 54(4), 665–675.

Lajoie, F., Assani, A. A., Roy, A. G., and Mesfioui, M. (2007). "Impacts of dams on monthly flow characteristics. The influence of watershed size and seasons." *Journal of Hydrology*, 334(3), 423–439.

Laskar, S. I., Kotal, S. D., and Bhowmik, S. K. R. (2014). "Analysis of rainfall and temperature

trends of selected stations over North East India during last century." *Mausam*, 65(4), 497–508.

Leavesley, G. H. (1994). "Modeling the effects of climate change on water resources - a review." *Climatic Change*, Kluwer Academic Publishers, 28(1–2), 159–177.

Lenderink, G., van Ulden, A., van den Hurk, B., and Keller, F. (2007). "A study on combining global and regional climate model results for generating climate scenarios of temperature and precipitation for the Netherlands." *Climate Dynamics*, 29(2–3), 157–176.

Liew, M. W. V. A. N. (2004). "Impact of flood retarding structures on simulated streamflow for various sized watersheds under varying climatic conditions." *Proceedings of ICGRHWE*, IAHS, 33–40.

Liu, Y., Yang, W., Yu, Z., Lung, I., Yarotski, J., Elliott, J., and Tiessen, K. (2014). "Assessing Effects of Small Dams on Stream Flow and Water Quality in an Agricultural Watershed." *Journal of Hydrologic Engineering*, 19(10), 05014015.

Lu, X. X., Li, S., Kummu, M., Padawangi, R., and Wang, J. J. (2014). "Observed changes in the water flow at Chiang Saen in the lower Mekong: Impacts of Chinese dams?" *Quaternary International*, 336, 145–157.

Lutz, A. F., Immerzeel, W. W., Shrestha, A. B., and Bierkens, M. F. P. (2014). "Consistent increase in High Asia's runoff due to increasing glacier melt and precipitation." *Nature Climate Change*, 4(7), 587–592.

Mann, H. B. (1945). "Nonparametric Tests Against Trend." *Econometrica*, [Wiley, Econometric Society], 13(3), 245–259.

Marak, J. D. K., Sarma, A. K., and Bhattacharjya, R. K. (2020). "Assessing the Impacts of Interbasin Water Transfer Reservoir on Streamflow." 25(2019), 1–13.

McCully, P. (1996). *The Ecology and Politics of Large Dams*. *Zed Books*, Zed Books.

Middelkoop, H., Daamen, K., Gellens, D., Grabs, W., Kwadijk, J. C. J., Lang, H., Parmet, B. W. A. H., Schädler, B., Schulla, J., and Wilke, K. (2001). "Impact of climate change on hydrological regimes and water resources management in the Rhine basin." *Climatic Change*, 49(1–2), 105–128.

Mishra, A. K., and Singh, V. P. (2010). "A review of drought concepts." *Journal of Hydrology*,

Elsevier, 391(1–2), 202–216.

Moriasi, D. N., Arnold, J. G., Van Liew, M. W., Bingner, R. L., Harmel, R. D., and Veith, T. L. (2007). "Model evaluation guidelines for systematic quantification of accuracy in watershed simulations." *American Society of Agricultural and Biological Engineers*, 50(3), 885–900.

Murata, F., Hayashi, T., Matsumoto, J., and Asada, H. (2007). "Rainfall on the Meghalaya plateau in northeastern India-one of the rainiest places in the world." *Natural Hazards*, 42(2), 391–399.

Myhre, G., Alterskjær, K., Stjern, C. W., Hodnebrog, Marelle, L., Samset, B. H., Sillmann, J., Schaller, N., Fischer, E., Schulz, M., and Stohl, A. (2019). "Frequency of extreme precipitation increases extensively with event rareness under global warming." *Scientific Reports*, 9(1), 1–10.

Nageswararao, M. M., Mohanty, U. C., Ramakrishna, S. S. V. S., Nair, A., and Prasad, S. K. (2016). "Characteristics of winter precipitation over Northwest India using high-resolution gridded dataset (1901–2013)." *Global and Planetary Change*, Elsevier B.V., 147, 67–85.

Naidu, C. V., Durgalakshmi, K., Krishna, K. M., Rao, S. R., Satyanarayana, G. C., Lakshminarayana, P., and Rao, L. M. (2009). "Is summer monsoon rainfall decreasing over India in the global warming era?" *Journal of Geophysical Research Atmospheres*, 114(24), 1–16.

Neitsch, S. ., Arnold, J. ., Kiniry, J. ., and Williams, J. . (2011). "Soil & Water Assessment Tool Theoretical Documentation Version 2009." *Texas Water Resources Institute*, 1–647.

Nohara, D., Kitoh, A., Hosaka, M., and Oki, T. (2006). "Impact of Climate Change on River Discharge Projected by Multimodel Ensemble." *Journal of Hydrometeorology*, 7(5), 1076–1089.

Nyaupane, N., Thakur, B., Kalra, A., and Ahmad, S. (2018). "Evaluating future flood scenarios using CMIP5 climate projections." *Water (Switzerland)*, 10(12), 1–18.

Ouyang, W., Hao, F., Song, K., and Zhang, X. (2011). "Cascade Dam-Induced Hydrological Disturbance and Environmental Impact in the Upper Stream of the Yellow River." *Water Resources Management*, Springer Netherlands, 25(3), 913–927.

Öztopal, A., and Şen, Z. (2017). "Innovative Trend Methodology Applications to Precipitation

Records in Turkey." *Water Resources Management*, 31(3), 727–737.

Pai, D. S., Sridhar, L., Rajeevan, M., Sreejith, O. P., Satbhai, N. S., and Mukhopadyay, B. (2014). "Development of a new high spatial resolution (0 . 25 ° × 0 . 25 °) Long Period (1901-2010) daily gridded rainfall data set over India and its comparison with existing data sets over the region data sets of different spatial resolutions and time period." *Mausam*, 1(January), 1–18.

Pai, D., Sridhar, L., Rajeevan, M., Sreejith, O., and Satbhai, N. S. and Mukhopadhyay, B. (2015). "Development of a new high spatial resolution (0.25× 0.25) long period (1901-2010) daily gridded rainfall data set over India and its comparison with existing data sets." *Metnet.Imd.Gov.in*, 1(January), 0–18.

Palmer, M. A., Reidy Liermann, C. A., Nilsson, C., Flörke, M., Alcamo, J., Lake, P. S., and Bond, N. (2008). "Climate change and the world's river basins: Anticipating management options." *Frontiers in Ecology and the Environment*, 6(2), 81–89.

Papalexiou, S. M., and Montanari, A. (2019). "Global and Regional Increase of Precipitation Extremes Under Global Warming." *Water Resources Research*, John Wiley & Sons, Ltd, 55(6), 4901–4914.

Patakamuri, S. K. (2020). "modifiedmk: Modified Versions of Mann Kendall and Spearman's Rho Trend Tests." *CRAN*, CRAN.

Pfeiffer, M., and Ionita, M. (2017). "Assessment of hydrologic alterations in Elbe and Rhine Rivers, Germany." *Water (Switzerland)*, 9(9).

Poméon, T., Diekkrüger, B., Springer, A., Kusche, J., and Eicker, A. (2018). "Multi-objective validation of SWAT for sparsely-gaugedWest African river basins - A remote sensing approach." *Water (Switzerland)*, 10(4).

Pradhan, R., Singh, N., and Singh, R. P. (2019). "Onset of summer monsoon in Northeast India is preceded by enhanced transpiration." *Scientific Reports*, Springer US, 9(1), 1–11.

Priyadarshini, S. (2018). "India ' s north east gets attention from climate change scientists." <http://www.natureasia.com/en/nindia/article/10.1038/nindia.2013.41> (May 16, 2018).

Proctor, J., Haridasan, K., and Smith, G. W. (1998). "How far north does lowland evergreen tropical rain forest go?" *Global Ecology and Biogeography Letters*, 7(2), 141–146.

Prokop, P., and Walanus, A. (2003). “Trend and periodicity in the longest instrumental rainfall series for the area of most extreme rainfall in the world, northeast India.” *Geographia Polonica*, 76(2), 25–35.

Prokop, P., and Walanus, A. (2015). “Variation in the orographic extreme rain events over the Meghalaya Hills in northeast India in the two halves of the twentieth century.” *Theoretical and Applied Climatology*, 121(1–2), 389–399.

Prudhomme, C., Reynard, N., and Crooks, S. (2002). “Downscaling of global climate models for flood frequency analysis: where are we now?” *Hydrological Processes*, 16(6), 1137–1150.

Rahbeh, M., Chanasyk, D., and Miller, J. (2011). “Two-Way Calibration-Validation of SWAT Model for a Small Prairie Watershed with Short Observed Record.” *Canadian Water Resources Journal / Revue canadienne des ressources hydriques*, 36(3), 247–270.

Rahmstorf, S., Foster, G., and Cahill, N. (2017). “Global temperature evolution: recent trends and some pitfalls.” *Environmental Research Letters*, 12, 7.

Rajeevan, M., Bhate, J., and Jaswal, A. K. (2008). “Analysis of variability and trends of extreme rainfall events over India using 104 years of gridded daily rainfall data.” *Geophysical Research Letters*, 35(18), 1–6.

Rajeevan, M., Bhate, J., Kale, J. D., and Lal, B. (2006). “High resolution daily gridded rainfall data for the Indian region: Analysis of break and active monsoon spells.” *Current Science*, 91(3), 296–306.

Rajeevan, M., and Bhatle, J. (2009). “A high resolution daily gridded rainfall dataset (1971 – 2005) for mesoscale meteorological studies Author (s): M . Rajeevan and Jyoti Bhate Published by : Current Science Association Stable URL : http://www.jstor.com/stable/24105470 A high resolution.” *Current Science*, 96(4), 558–562.

Ravindranath, N. H., Rao, S., Sharma, N., Nair, M., Gopalakrishnan, R., Rao, A. S., Malaviya, S., Tiwari, R., Sagadevan, A., Munsi, M., Krishna, N., and Bala, G. (2011a). “Climate change vulnerability profiles for North East India.” *Current Science*, 101(3), 384–394.

Ravindranath, N. H., Rao, S., Sharma, N., Nair, M., Gopalakrishnan, R., Rao, A. S., Malaviya, S., Tiwari, R., Sagadevan, A., Munsi, M., Krishna, N., Bala, G., Ravindranath, A. N. H., Rao, S., Sharma, N., Nair, M., Rao, A. S., Malaviya, S., Tiwari, R., Sagadevan, A., Munsi, M., Krishna, N., Bala, G., Ravindranath, N. H., Rao, S., Sharma, N., Nair, M., Sagadevan,

A., Munsi, M., and Krishna, N. (2011b). “Climate change vulnerability profiles for North East India.” *Current Science*, 101(3), 384–394.

Richter, B. D., Baumgartner, J. V., Braun, D. P., and Powell, J. (1998). “A spatial assessment of hydrologic alteration within a river network.” *Regulated Rivers: Research & Management*, John Wiley & Sons, Ltd, 14(4), 329–340.

Richter, B. D., Baumgartner, J. V., Powell, J., And, and Braun., D. P. (1996). “A Method for Assessing Hydrologic Alteration within Ecosystems.” *Conservation Biology*, 10(4), 1163–1174.

Richter, B. D., Baumgartner, J. V., Wigington, R., and Braun, D. P. (1997). “How much water does a river need?” *Freshwater Biology*, Wiley/Blackwell (10.1111).

Romaguera, M., Hoekstra, A. Y., Su, Z., Krol, M. S., and Salama, M. S. (2010). “Potential of using remote sensing techniques for global assessment of water footprint of crops.” *Remote Sensing*, 2(4), 1177–1196.

Rustum, R., Adeloye, A. J., and Mwale, F. (2017). “Spatial and temporal Trend Analysis of Long Term rainfall records in data-poor catchments with missing data , a case study of Lower Shire floodplain in Malawi for the Period 1953-2010.” (November).

Saikia, H. (2012). “Political economy of big Dam in North East India.” *Journal of Social & political Science*, 1(September), 1–11.

Sato, T. (2013). “Mechanism of orographic precipitation around the meghalaya plateau associated with intraseasonal oscillation and the diurnal cycle.” *Monthly Weather Review*, 141(7), 2451–2466.

Schuol, J., Abbaspour, K. C., Srinivasan, R., and Yang, H. (2008). “Estimation of freshwater availability in the West African sub-continent using the SWAT hydrologic model.” *Journal of Hydrology*, 352(1–2), 30–49.

Sen, P. K. (1968). “Estimates of the Regression Coefficient Based on Kendall’s Tau.” *Journal of the American Statistical Association*, Taylor & Francis, 63(324), 1379–1389.

Şen, Z. (2012). “Innovative trend analysis methodology.” *Journal of Hydrologic Engineering*, 17(9), 1042–1046.

Şen, Z. (2014). “Trend identification simulation and application.” *Journal of Hydrologic*

Engineering, 19(3), 635–642.

Şen, Z. (2017). "Innovative trend significance test and applications." *Theoretical and Applied Climatology*, 127(3–4), 939–947.

Serencam, U. (2019). "Innovative trend analysis of total annual rainfall and temperature variability case study: Yesilirmak region, Turkey." *Arabian Journal of Geosciences*, 12(23), 1–9.

Sharma, A., and Goyal, M. K. (2020). "Assessment of drought trend and variability in India using wavelet transform." *Hydrological Sciences Journal*, Taylor & Francis, 65(9), 1539–1554.

Sharma, C. K. (2018). "Dam, 'Development' and Popular Resistance in Northeast India." *Sociological Bulletin*, 67(3), 317–333.

Sheffield, J., Goteti, G., and Wood, E. F. (2006). "Development of a 50-Year High-Resolution Global Dataset of Meteorological Forcings for Land Surface Modeling." *Journal of Climate*, American Meteorological Society, 19(13), 3088–3111.

Sheng Yue, Paul Pilon, and George Cavadias. (2002). "Power of the Mann±Kendall and Spearman's rho tests for detecting monotonic trends in hydrological series." *Journal of Hydrology* , 259, 254±271.

Shiau, J. T., and Wu, F. C. (2004). "Assessment of hydrologic alterations caused by chi-chi diversion weir in Chou-Shui Creek, Taiwan: Opportunities for restoring natural flow conditions." *River Research and Applications*, 20(4), 401–412.

Shivam, Goyal, M. K., and Sarma, A. K. (2017). "Analysis of the change in temperature trends in Subansiri River basin for RCP scenarios using CMIP5 datasets." *Theoretical and Applied Climatology*, 129(3), 1175–1187.

Shrestha, M. K., Recknagel, F., Frizenschaf, J., and Meyer, W. (2016). "Assessing SWAT models based on single and multi-site calibration for the simulation of flow and nutrient loads in the semi-arid Onkaparinga catchment in South Australia." *Agricultural Water Management*, Elsevier, 175, 61–71.

Singh, O., and Kumar, M. (2013). "Flood events, fatalities and damages in India from 1978 to 2006." *Natural Hazards*, 69(3), 1815–1834.

Sinha, P., Rollason, E., Bracken, L. J., Wainwright, J., and Reaney, S. M. (2020). "A new

framework for integrated, holistic, and transparent evaluation of inter-basin water transfer schemes." *Science of the Total Environment*, Elsevier B.V., 721, 137646.

Sonali, P., and Nagesh Kumar, D. (2013). "Review of trend detection methods and their application to detect temperature changes in India." *Journal of Hydrology*, Elsevier B.V., 476, 212–227.

Subash, N., and Sikka, A. K. (2013). "Trend analysis of rainfall and temperature and its relationship over India." (1974).

Teutschbein, C., and Seibert, J. (2010). "Regional Climate Models for Hydrological Impact Studies at the Catchment Scale : A Review of Recent Modeling Strategies." 7, 834–860.

Tien Bui, Talebpour Asl, Ghanavati, Al-Ansari, Khezri, Chapi, Amini, and Thai Pham. (2020). "Effects of Inter-Basin Water Transfer on Water Flow Condition of Destination Basin." *Sustainability*, 12(1), 338.

Todini, E. (1988). "Rainfall-runoff modeling — Past, present and future." *Journal of Hydrology*, Elsevier, 100(1–3), 341–352.

Trenberth, K. E. (2011). "Changes in precipitation with climate change." *Climate Research*, 47(1–2), 123–138.

Vogel, R., and Fennessey, N. (1994). "Flow-Duration Curves. I: New Interpretation and Confidence Intervals." *Journal of Water Resources Planning and Management*, American Society of Civil Engineers, 120(4), 485–504.

Vörösmarty, C. J., Green, P., Salisbury, J., and Lammers, R. B. (2000). "Global water resources: vulnerability from climate change and population growth." *Science (New York, N.Y.)*, American Association for the Advancement of Science, 289(5477), 284–8.

Wang, G., and Xia, J. (2010). "Improvement of SWAT2000 modelling to assess the impact of dams and sluices on streamflow in the Huai River basin of China." *Hydrological Processes*, 24(11), 1455–1471.

Wang, Y., Xu, Y., Tabari, H., Wang, J., Wang, Q., Song, S., and Hu, Z. (2020). "Innovative trend analysis of annual and seasonal rainfall in the Yangtze River Delta, eastern China." *Atmospheric Research*, Elsevier, 231(37), 104673.

Werner, P., and Gerstengarbe, F. (1997). "Proposal for the development of climate scenarios."

Climate Research, 8(October), 171–182.

Wilby, R. L., Wigley, T. M. L., Conway, D., Jones, P. D., Hewitson, B. C., Main, J., and Wilks, D. S. (1998). "Statistical downscaling of general circulation model output: A comparison of methods." *Water Resour. Res.*, Wiley-Blackwell, 34(11), 2995–3008.

World Meteorology Organization. (2019). *WORLD METEOROLOGICAL ORGANIZATION Global Annual to Decadal Climate Update*. *World Meteorological Organization, Geneva, Switzerland.*

Wu, H., and Qian, H. (2017). "Innovative trend analysis of annual and seasonal rainfall and extreme values in Shaanxi, China, since the 1950s." *International Journal of Climatology*, 37(5), 2582–2592.

Wu, X., Xiang, X., Chen, X., Zhang, X., and Hua, W. (2018). "Effects of cascade reservoir dams on the streamflow and sediment transport in the Wujiang River basin of the Yangtze River, China." *Inland Waters*.

Xu, C. (1999a). "Operational testing of a water balance model for predicting climate change impacts." *Agricultural and Forest Meteorology*, 98–99, 295–304.

Xu, C. (1999b). "Climate Change and Hydrologic Models: A Review of Existing Gaps and Recent Research Developments." *Water Resources Management*, Kluwer Academic Publishers, 13(5), 369–382.

Xu, C. (2000). "Modelling the Effects of Climate Change on Water Resources in Central Sweden." *Water Resources Management*, 14(3), 177–189.

Xu, C., Widén, E., and Halldin, S. (2005). "Modelling hydrological consequences of climate change—Progress and challenges." *Advances in Atmospheric Sciences*, Science Press, 22(6), 789–797.

Xue, L., Zhang, H., Yang, C., Zhang, L., and Sun, C. (2017). "Quantitative Assessment of Hydrological Alteration Caused by Irrigation Projects in the Tarim River basin, China." *Scientific Reports*, Springer US, 7(1), 1–13.

Yadav, S., Deb, P., Kumar, S., Pandey, V., and Pandey, P. K. (2016). "Trends in major and minor meteorological variables and their influence on reference evapotranspiration for mid Himalayan region at east Sikkim, India." *Journal of Mountain Science*, 13(2), 302–315.

Yaduvanshi, A., Zaroug, M., Bendapudi, R., and New, M. (2019). "Impacts of 1.5 °C and 2 °C global warming on regional rainfall and temperature change across India." *Environmental Research Communications*, IOP Publishing, 1(12), 125002.

Yang, T., Zhang, Q., Chen, Y. D., Tao, X., Xu, C., and Chen, X. (2012). "A spatial assessment of hydrologic alteration caused by dam construction in the middle and lower Yellow River, China." *Hydrological Processes*, John Wiley & Sons, Ltd, 26(March), 1–16.

Yatagai, A., Kamiguchi, K., Arakawa, O., Hamada, A., Yasutomi, N., and Kitoh, A. (2012). "Aphrodite constructing a long-term daily gridded precipitation dataset for Asia based on a dense network of rain gauges." *Bulletin of the American Meteorological Society*, 93(9), 1401–1415.

Yue, S., Pilon, P., Phinney, B., and Cavadias, G. (2002). "The influence of autocorrelation on the ability to detect trend in hydrological series." *Hydrological Processes*, 16(9), 1807–1829.

Yue, S., and Wang, C. Y. (2004). "The Mann-Kendall test modified by effective sample size to detect trend in serially correlated hydrological series." *Water Resources Management*, 18(3), 201–218.

Zhang, J., Sun, M., Deng, Z., Lu, J., Wang, D., Chen, L., and Liu, X. (2017). "Runoff and Sediment Response to Cascade Hydropower Exploitation in the Middle and Lower Han River, China." *Mathematical Problems in Engineering*, Hindawi, 2017, 1–15.

Zhang, X., Srinivasan, R., and Van Liew, M. (2008). "Multi-site calibration of the SWAT model for hydrologic modeling." *Transactions of the ASABE*.

Zhang, Y., Xia, J., Liang, T., and Shao, Q. (2010). "Impact of water projects on river flow regimes and water quality in Huai River Basin." *Water Resources Management*, 24(5), 889–908.

Zhou, Z., Wang, L., Lin, A., Zhang, M., and Niu, Z. (2018). "Innovative trend analysis of solar radiation in China during 1962 e 2015." *Renewable Energy*, Elsevier Ltd, 119, 675–689.

Zhuang, W. (2016). "Eco-environmental impact of inter-basin water transfer projects: a review." *Environmental Science and Pollution Research*, Springer Verlag, 23(13), 12867–12879.

Publications

1. Marak, J. D. K, Sarma, A. K, and Bhattacharjya, R. K. (2020), "Innovative trend analysis of spatial and temporal rainfall variations in Umiam and Umtru watersheds in Meghalaya, India", Theoretical and Applied Climatology, (https://doi.org/10.1007/s00704-020-03383-1).
2. Marak, J. D. K, Sarma, A. K, and Bhattacharjya, R. K. (2020), "Assessing the Impacts of Inter-Basin Water Transfer Reservoir on Streamflow", Journal of Hydrologic Engineering, ASCE (https://doi.org/10.1061/(ASCE)HE.1943-5584.0001984).
3. Marak, J. D. K, Sarma, A. K, and Bhattacharjya, R. K. (2019). "Calibration, Validation and Uncertainty Analysis of SWAT Model for predicting reservoir inflow in Umiam Watershed, Meghalaya". THA 2019, International Conference on Water Management and Climate Change towards Asia's Water-Energy-Food Nexus and SDGs, Bangkok, Thailand.